ASSESSMENT OF RESERVOIR ROCK AND FLUID DATA FOR BLACK OIL SIMULATION – A CASE STUDY

A THESIS SUBMITTED TO
THE GRADUATE SCHOOL OF NATURAL AND APPLIED SCIENCES
OF
MIDDLE EAST TECHNICAL UNIVERSITY

BY

ONUR SUSUZ

IN PARTIAL FULFILLMENT OF THE REQUIREMENTS FOR THE DEGREE
OF
MASTER OF SCIENCE
IN
PETROLEUM AND NATURAL GAS ENGINEERING
DEPARTMENT

DECEMBER 2009

ASSESSMENT OF RESERVOIR ROCK AND FLUID DATA FOR BLACK OIL SIMULATION – CASE STUDY

submitted by **ONUR SUSUZ** in partial fulfillment of the requirements for the degree of **Master of Science in Petroleum and Natural Gas Engineering Department, Middle East Technical University** by,

Prof Dr. Canan Özgen _____
Dean, Graduate School of **Natural and Applied Sciences**

Prof. Dr. Mahmut Parlaktuna _____
Head of Department, **Petroleum and Natural Gas Engineering Dept.**

Prof. Dr. Mahmut Parlaktuna _____
Supervisor, **Petroleum and Natural Gas Engineering Dept., METU**

Prof. Dr. Serhat Akın _____
Co-Supervisor, **Petroleum and Natural Gas Engineering Dept., METU**

Examining Committee Members:

Prof. Dr. Nurkan Karahanoğlu _____
Geological Engineering Dept., METU

Prof. Dr. Mahmut Parlaktuna _____
Petroleum and Natural Gas Engineering Dept., METU

Prof. Dr. Serhat Akın _____
Petroleum and Natural Gas Engineering Dept., METU

Uğur Karabakal, M.Sc. _____
Petroleum and Natural Gas Engineer., TPAO

Hüseyin Ali Doğan, M.Sc. _____
Petroleum and Natural Gas Engineer, TPAO

Date:

I hereby declare that all information in this document has been obtained and presented in accordance with academic rules and ethical conduct. I also declare that, as required by these rules and conduct, I have fully cited and referenced all material and results that are not original to this work.

Name, Last name : Onur SUSUZ

Signature :

ABSTRACT

ASSESSMENT OF RESERVOIR ROCK AND FLUID DATA

FOR BLACK OIL SIMULATION – A CASE STUDY

Susuz, Onur

M.Sc., Department of Petroleum and Natural Gas Engineering

Supervisor : Prof. Dr. Mahmut Parlaktuna

Co-Supervisor : Prof. Dr. Serhat Akın

December 2009, 169 pages

Reservoir simulation studies are one of the key tools in an integrated reservoir management study. A successful reservoir simulation application requires representative input data for reservoir rock and fluid properties. This study aims to develop a road map from laboratory measurements to the input data file of reservoir simulation and to make a probabilistic approach for the estimation of unknown parameters. Raw data of reservoir rock and fluid properties of a selected oil field of Turkey will be interpreted and prepared in a way that they will be used as input data of a simulator.

Keywords : Core Analysis, PVT Analysis, Black Oil Simulation

ÖZ

"BLACK OIL" SİMÜLASYONU İÇİN REZERVUAR KAYA VE AKIŞKAN VERİLERİNİN DEĞERLENDİRİLMESİ – BİR ÖRNEK ÇALIŞMA

Susuz, Onur

Yüksek Lisans, Petrol ve Doğal Gaz Mühendisliği Bölümü

Tez Yöneticisi : Prof. Dr. Mahmut Parlaktuna

Ortak Tez Yöneticisi : Prof. Dr. Serhat Akın

Aralık 2009, 169 sayfa

Rezervuar simülasyonu çalışmaları entegre bir rezervuar yönetimi çalışmasındaki temel araçlardan bir tanesidir. Başarılı bir rezervuar simulasyonu uygulaması için rezervuar kayaç ve akışkan özelliklerini temsili veriler gereklidir. Bu çalışma laboratuar ölçümlerinden rezervuar simülasyonu veri dosyasına kadar bir yol haritası ortaya koymayı ve bilinmeyen parametrelerin tahminine yönelik olasılıklı bir yaklaşım getirmeyi hedeflemektedir. Türkiye'de seçilmiş bir petrol sahasına ait rezervuar kaya ve akışkan özellikleri simülatör için girdi veri olarak kullanılacak şekilde hazırlanacak ve yorumlanacaktır.

Anahtar Kelimeler : Karot Analizleri, PVT Analizleri, Black Oil Simülasyonu

ACKNOWLEDGEMENTS

The author wishes to thank his thesis supervisor Prof. Dr. Mahmut Parlaktuna and co-supervisor Prof. Dr. Serhat Akın for their guidance, advice and encouragements throughout the research.

The author would also like to thank directors of TPAO Research Center for their permissions and supports and specifically to Mr. Uğur Karabakal for his encouragements.

His parents are also acknowledged for their patience and his precious Selen Günel is gratefully acknowledged for her endoursements and encouragements.

TABLE OF CONTENTS

LIST OF TABLES

LIST OF FIGURES

CHAPTER 1

INTRODUCTION

Reservoir simulation studies are one of the key tools in an integrated reservoir management study. The major goal of these studies is to predict future performance of the reservoir. Classical methods of reservoir simulation studies include analytical, experimental and mathematical methods. The analytical methods use features of mature reservoirs to estimate the reservoir performance. The experimental methods measure physical properties of reservoir rock and fluids then scale them up to the whole field. Mathematical models use the model equations. *This study is mainly focused on experimental methods.* (Fig.1.1)

A petroleum reservoir is the porous medium that contains hydrocarbons. So, studying reservoir rock and fluid properties becomes important. Reservoir simulations can be classified into two by the type of reservoir fluids. Black oil simulation is used in cases where recovery processes are not sensitive to compositional changes in the hydrocarbons. Compositional studies are applied when recovery processes are sensitive to compositional changes.

In a black oil system, the oil, water and gas phases coexist in equilibrium under isothermal conditions. The oil component forms the bulk of the oil phase. The solution-gas component dissolves in it and the remaining gas forms the gas phase. Oil and water are immiscible and both do not dissolve in the gas phase. Therefore, the black-oil system consists of the water component, the oil component and the gas component.

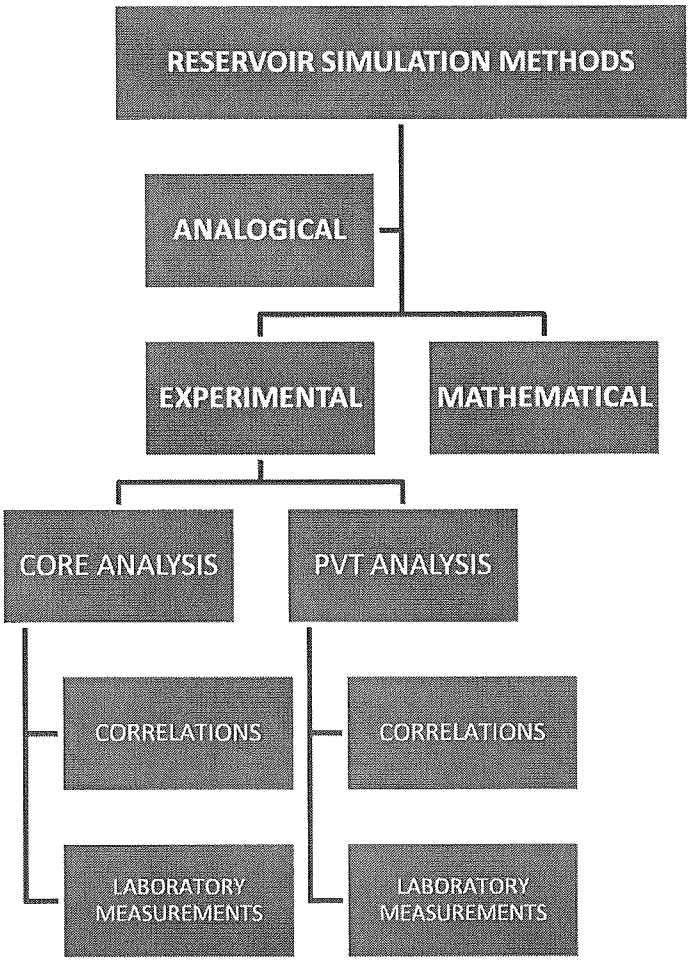

Fig.1.1. Classification of reservoir simulation methods.

Core analysis and PVT analysis are essential parts of successful reservoir characterization studies. Modeling the core and PVT laboratory measurement data are necessary to use in the experimental simulation studies. Fig. 1.2 is important to see the place of petrophysical studies in reservoir simulation. In order to evaluate a reservoir, petrophysical data such as rock and pore types are used to characterize capillarity and flow properties [1].

Core analysis section involves the test methods of laboratory measurements, results of the core analysis and modelling of the measured parameters. Besides, in order to average the measured data various estimations are tested. Porosity, permeability, relative permeability and capillary pressure properties of the reservoir rock are tested with the help of the laboratory equipments.

Phase behaviour models can be used to evaluate the measured PVT data, or to generate such data as input in black oil reservoir simulation. The main application of phase behaviour models, based on determining the critical properties of components in both phases by EOS, is however in compositional reservoir simulation. [2]

Hydrocarbon phase is represented by two groups; liquid hydrocarbons and gaseous hydrocarbons. Oil formation volume factor, bubble point pressure, gas-oil ratio, viscosity and density properties of the reservoir oil is known from previous studes. PVT analysis section consists of correlations to use in the lack of laboratory data, C_{7+} characterization and equations of state calculations. First, many correlations are tested to use due to the lack of reservoir oil and water properties. Then, knowing that a compositional model is generally necessary to estimate recovery by injection of CO_2, equations of state are applied with the oil and gas compositional analysis due to the probability of any CO_2 injection process. Thus, in order to make accurate equations of state calculations, characterizing C_{7+} properties of the oil sample becomes indispensible.

Finally, results of the measured and calculated properties of reservoir rock and fluid of the X-field are discussed in the experimental results and discussion chapter.

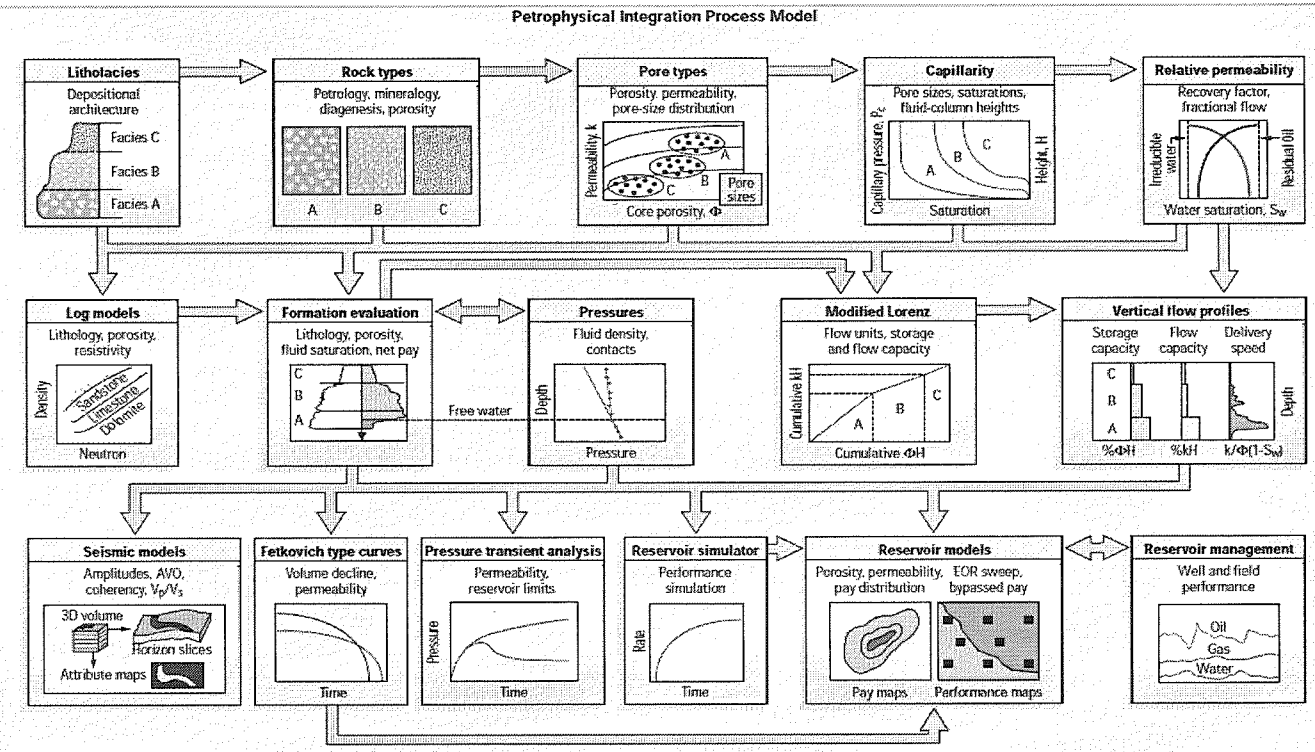

> A systematic approach to petrophysics problems. The Petrophysical Integration Process Model, or PIPM, provides a methodology to evaluate a reservoir. Cores provide data on the rock and pore types, which are used to characterize capillarity and flow. Addition of log and well data determines flow units and storage and flow capacity. With this basic picture of the reservoir, seismic data, well data and reservoir flow simulation provide a model of the reservoir. The ultimate goal is improved reservoir management.

Fig. 1.2. Petrophysical Integration Process Model [1]

CHAPTER 2

LITERATURE REVIEW

2.1. CORE ANALYSIS

The main objective of core analysis is to understand the petro-physical properties and to estimate the storage and flow capacities of reservoir rocks. In order to make reservoir characterization of any field, basic core analysis data, i.e. porosity, permeability, capillary pressure and relative permeability, should be determined by the help of core analysis to enhance the knowledge of subsurface geology from a hydrocarbon resource potential perspective. There are some other techniques to evaluate the petro-physical properties of core samples such as well logs, pressure drawdown tests. However, laboratory measurement of cores allows visual examination of the formation and direct measurements of some important properties of the rock.

Core analysis can be divided as conventional core analysis and special core analysis. Conventional core analysis includes the routine analysis of core samples, that are porosity, permeability and grain density. Special core analysis give more detailed rock properties. However, it requires longer time than conventional core analysis. Capillary pressure, relative permeability, resistivity and wettability measurements can be thought under the title of special core analysis.

2.1.1. Porosity

Porosity is defined as the ratio of the pore volume in a reservoir rock to the bulk volume. It is the storage capacity of reservoir rocks. So, porosity is one of the most important reservoir rock properties.

$$\Phi = \frac{V_{pore}}{V_{bulk}} \qquad (2\text{-}1/1)$$

There are two types of porosity; one is effective and the other one is total porosity. Total porosity is the ratio of total pore volume to bulk volume. On the other hand, effective porosity, which is more important for reservoir engineering calculations, is the ratio of the volume of interconnected pore volume to the bulk volume.

Moreover, porosity can be classified as primary porosity and secondary porosity. Primary porosity is native porosity developed during the deposition of the rock, whereas secondary porosity is developed by geological process that follows the deposition. Fractures and vugs can be regarded as examples of secondary porosity. The importance of this classification is that reservoir rocks with primary porosity can be thought as more homogenic in porosity and permeability.

Grain size, grain shape, sorting, clay content, compaction and cementation affect the porosity of reservoir rocks. Porosity values often vary between 10 to 40 percent in sandstones and 5 to 25 percent in dolomites and limestones [3].

Determination of porosity requires pore volume, bulk volume and grain volume measurements. Pore volumes can be measured on a cleaned core plug by resaturation of the core plug sample. Resaturating the core plug with Helium gas gives the best pore volume results because of its small molecule size that allows rapid penetration to small pores and its inertness. Bulk volume can be determined by calipering the length and diameter of the core plug sample and applying the mathematical formulas after determining the pore volumes by helium injection method. Grain volume of samples is usually calculated from dry sample weight and grain density.

Helium gas expansion porosimeter is used to determine porosity of the core samples. It is based upon the Mariotte-Boyle law. Boyle's law method of measuring porosity is a gas transfer technique that involves the compression of gas into the pores of a clean and dry sample. Helium is used as the test gas because, the small helium molecule will penetrate the small capillaries associated with reservoir rock. This method is also useful at being rapid in most cases and yielding core samples can be used for other measurements.

From the Fig. 2.1, it is seen that the system includes a chamber in which the sample is placed. In the reference volume, V_1, at a pressure P_1, helium expands into matrix cup with an unknown volume, V_2, and initial pressure, P_2. The system can be brought to equilibrium when the core holder valve is opened. By measuring the final equilibrium pressure the unknown volume, V_2 can be determined. When the core holder valve is opened, the volume of the system will be the equilibrium volume V, which is the sum of the volumes V_1 and V_2.

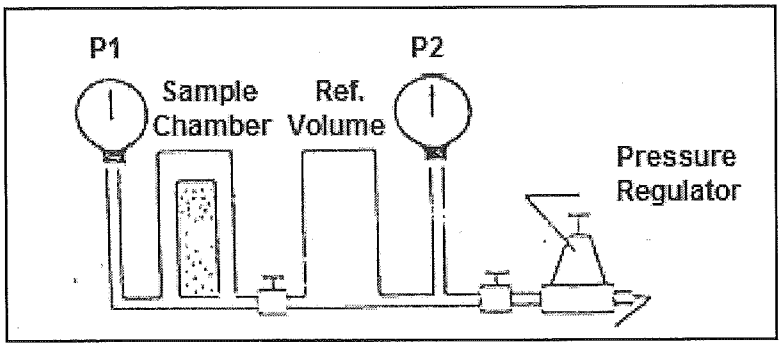

Figure 2.1. Schematic diagram of a helium porosimeter.

2.1.2. Permeability

In the previous section, porosity is defined as the storage capacity of the reservoir rock. On the other hand, permeability is defined as the specific flow capacity of reservoir rock. It is a measure of the capacity of transmitting fluids.

Based on the experimental studies Henry Darcy stated that the volumetric flow rate through the core plug can be calculated with the Equation (2-1/2).

$$- \quad Q = -\frac{k}{\mu} A \frac{dP}{dL} \qquad (2\text{-}1/2)$$

It should be noted that this equation is valid if flow is laminar, core plug samples are 100 % saturated with flowing fluids, flowing fluids is incompressible and there should be no reaction between rock and flowing fluid.

Permeability values can be found from well tests, pressure drawdown tests, well logs and core analysis. Routine core analysis are usually made by dry air and calculated with a modified Darcy equation for gas flows;

$$k_{air} = \frac{2L\mu_{air}Q_{air}}{A} - \frac{P_a}{\left(P_1^2 - P_2^2\right)} \qquad (2\text{-}1/3)$$

Gas permeameter is used in order to determine the absolute air permeability of the core samples. Hassler type core holder uses compressed air or nitrogen in order to squeeze the core sample in a rubber sleeve. Inside the rubber sleeve core sample is enclosed except its two opposite faces. 250 psi of air is applied over the sleeve to prevent inlet air from flowing between the sample and the sleeve. In order to remove or insert the core sample a vacuum is usually applied to expand the sleeve. The airflow path through the permeameter is shown in Figure 2.2. The air flows through the core sample and orifice in proportion to the applied differential air pressure. The differential pressure across the calibrated orifice is used to determine the air flow rate.

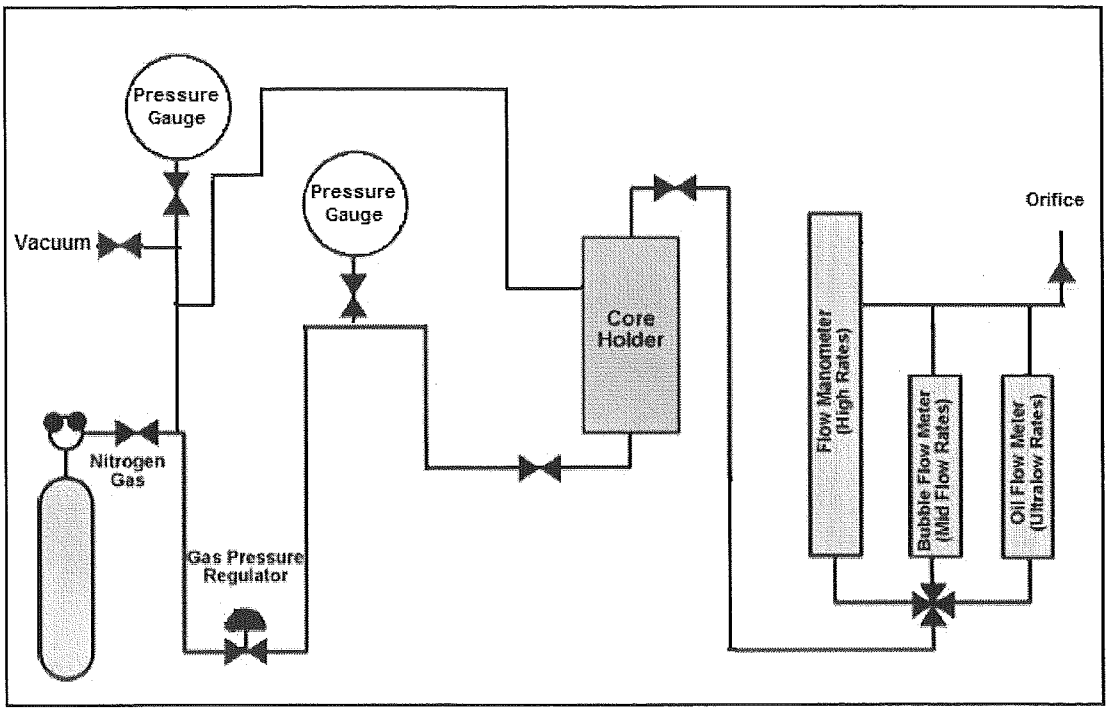

Figure 2.2. Schematic view of a gas permeameter

The gauge "C" values which are read from the gas permeameter can be used to simplify the modified Darcy equation.

$$C = \frac{(1000)(2)(\mu_a)P_a}{(P_1 + P_a)(P_1 - P_a)} \qquad (2\text{-}1/4)$$

By replacing C parameter, equation becomes as shown below;

$$k_a = \frac{CQ_aL}{A} \qquad (2\text{-}1/5)$$

where,

$$Q_a = \frac{(Q_{Orifice})(H_W)}{200} \qquad (2\text{-}1/6)$$

- H_w : height of the liquid inside manometer, mm
- $Q_{orifice}$: orifice constant

With the help of the measured data and the equations given above, air permeability values can be calculated. Then, these air permeability results have to be adjusted with a Klinkenberg correction factor to obtain the absolute permeability of reservoir rock. According to the kinetic theory of gases, the gas molecules can be considered as tiny spheres and that spheres move at high speeds and collide in a random manner. At low pressures, these collisions take place between the molecules and against the wall. This fact increases the internal friction due to collision of the molecules and affect the permeability measurement results. The difference between the liquid flow and gas flow is the slippage of gas molecules at the walls [4]. In order to find the corrected value of permeability, Klinkenberg develops the formula given in Equation (2-1/7) [5].

$$k_g = k_\infty \left(1 + \frac{b}{P_M}\right), \qquad (2\text{-}1/7)$$

where,

k_g : Gas permeability

k_∞ : Klinkenberg permeability

b : Klinkenberg slippage factor

P_M : Average pressure.

2.1.3 Porosity and Permeability Measurements Under Overburden Pressure

A change in the internal stress in the formation takes place over the reservoir rock, causing the rocks to be subjected an increased and variable overburden load, with the depletion of the fluids from the reservoir. Knowing that the net overburden pressure is the difference between the formation pressure on top of the reservoir rock and the hydrostatic pressure. This pressure change over the reservoir rock results in the compaction of the rock structure. With the change in pressure on the reservoir rock, porosity and permeability properties are changed.

CMS-300 test system is used to develop porosity and permeability curves with increasing overburden pressure. Test system uses an integrated form of the combined Darcy, Klinkenberg and Forchheimer equations to accurately determine permeability.

Porosity and permeability change under net overburden pressure graphs are used to correlate the relationship between pressure and porosity and permeability. With the slopes of these graphs following equations and their coefficients a, b, c and d are determined:

- $$\phi_{NOP} = \phi_{800} \left\{ a \times [NOP]^{b} \right\},$$ (2-1/9)

- $$k_{L\,NOP} = k_{L800} \left\{ c \times [NOP]^{d} \right\},$$ (2-1/10)

where,

ϕ_{NOP} = porosity under net overburden pressure, psi

ϕ_{800} = porosity under 800 psi net overburden pressure, psi

k_{LNOP} = equivalent liquid permeability under net overburden pressure, psi

k_{L800} = equivalent liquid permeability under 800 psi net overburden pressure, psi

It should be noted that minimum working pressure of the CMS-300 test system is 800 psi. Thus, ϕ_{800} and k_{L800} parameters are set as the initial values of the graphs.

2.1.4. Relative Permeability

The analysis of the production performance is essentially based on the fluid PVT properties and relative permeability data. Relative permeability is a dimensionless measure of at least two phases by modifying Darcy's Equation. The ratio of effective permeability of one phase to absolute permeability of total system is named as relative permeability. Relative permeability is a property of porous medium, so that it can be considered as a function of wettability characteristics of the formation, pore geometry, porosity, permeability, temperature, interfacial tension, saturation history and flow direction and velocity of the reservoir fluids [6, 7, 8].

- $k_{ro} = \frac{k_o}{k}$, relative permeability of oil (2-1/11)

- $k_{rw} = \frac{k_w}{k}$, relative permeability of water (2-1/12)

The wetting phase relative permeability is a function only of its own saturation and is not influenced by the direction of saturation change or the nature of non-wetting phase. In strongly wetted rock, the relative permeability of the wetting phase is often path independent [9, 10].

Relative permeability measurements are generally used to estimate the production that will be obtained by recovery processes, waterflood or gas injection. There are two methods for measuring the relative permeability; "steady state" and "unsteady state" [7]. For the steady state relative permeability measurement methods, certain volumes of two different phases are injected until the pressure drop across the core stabilize and by weighing the core saturations in the core are calculated. The other method, unsteady state method is based on immiscible displacement process and can be made more rapidly than steady state methods. After saturating the core plug samples with one phase, the core is flooded with the other phase at a constant rate or constant pressure.

Core flooding system consists of a constant volume positive displacement pump, two accumulators, one for oil and one for brine, a pressure gauge for the determination of inlet pressure and a triaxial core holder. The schematic diagram is shown in Figure 2.3.

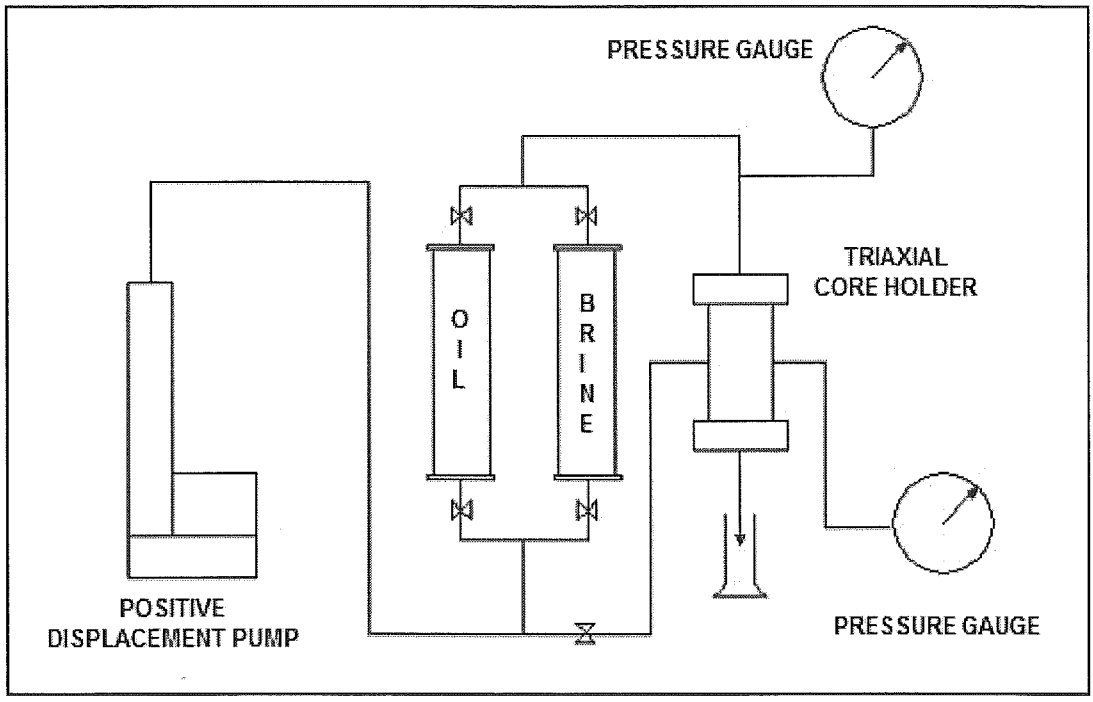

Fig. 2.3. Schematic view of the core flooding system

In order to determine relative permeability data from the unsteady-state experiments, Johnson-Bossler-Naumann method can be used for the calculation of water saturation. Laboratory test results can be normalized by JBN method, base on the moveable hydrocarbon saturation [11].

Firstly, water saturation values can be induced with the help of the following expression;

$$S_w^* = \frac{S_w - S_{wi}}{1 - S_{wi} - S_{or}} \qquad (2\text{-}1/13)$$

Then, relative permeabilities of oil and water phases have to be induced with the following expressions ;

- $$k_{rw}^{*} = \frac{k_{rw}}{k_{rw}@S_{or}} \quad (2\text{-}1/14)$$

- $$k_{ro}^{*} = \frac{k_{ro}}{k_{ro}@S_{wi}} \quad (2\text{-}1/15)$$

After plotting the S_w^* - k_{rw}* and k_{ro}^* graphs, Sw* values against k_{rw}* and k_{ro}* values can be read from the trendline curves. Lastly, porosity and initial water saturation and irreducible oil saturation relations have to be plotted and S_{wi} and S_{or} values against various porosity values have to be read from the bestlines. With the help of these values and the following expressions relative permeability versus porosity models can be plotted.

- $$S_w = (1 - S_{wi} - S_{or})S_w^{*} + S_{wi} \quad (2\text{-}1/16)$$

- $$k_{rw} = k_{rw}^{*}(k_{rw}@S_{or}) \quad (2\text{-}1/17)$$

- $$k_{ro} = k_{ro}^{*}(k_{ro}@S_{wi}) \quad (2\text{-}1/18)$$

2.1.5. Capillary Pressure

In order to evaluate the production potential of an oil field, capillary pressure, relative permeabilty, interfacial tensions and wettability terms of reservoir rock have to be characterized.

Capillary pressure, which is the difference in the pressure across the interface between two immiscible phases, results in a curvature of the interface. "When two immiscible fluids are in contact, a discontinuity in pressure exists between two fluids, which depends on the curvature of the

interface that separate the fluids. This particular difference in pressures is called as the capillary pressure" [12].

The defining equation of capillary pressure in a porous medium is given by the following expression:

$$P_c = P_{non\text{-}wetting\ phase} - P_{wetting\ phase} \qquad (2\text{-}1/19)$$

The Young–Laplace equation states that this pressure difference is proportional to the surface tension, and inversely proportional to the effective radius of the interface [13]. It also depends on the contact angle of the liquid on the surface of the capillary.

$$Pc = \frac{2\sigma(\cos\theta)}{r} \quad , \qquad (2\text{-}1/20)$$

where,

Pc, capillary pressure,

σ, interfacial tension,

θ, contact angle of the liquid

r, effective radius of the interface.

The equation for capillary pressure is only valid under capillary equilibrium, which means that there can not be any flowing phases.

The capillary pressure curve is important for understanding saturation distribution in the reservoir and affects imbibition and multiphase fluid flow through the rock. The capillary pressure that exists within a porous medium is a function of adhesion tension, the average size of the capillaries, saturation distribution of the fluids involved and the saturation history. As the relative saturations of the phases change, the pressure differences across the fluid interfaces also change, resulting in a change in the capillary pressure. Rocks have a distribution of pore throat sizes, so as more pressure is applied to the nonwetting phase, increasingly smaller pore openings are invaded.

The two saturation processes, drainage and imbibition are dependant on the wetting characteristics of fluid phases. Laboratory measurement of capillary pressure is confined to these drainage and imbibiton saturation processes. In drainage, the nonwetting phase displaces the wetting phase and in imbibition is reverse.

Capillary pressure petrophysical reservoir models is used to identify hydraulic units in pressure communication and hydrocarbon / water contacts and highlights rock type differences. In order to prepare the capillary pressure petrophysical model representative capillary pressure measurements on the rock sequence and calculated petrophysical profiles of effective porosity and water saturation have to be known.

Laboratory measurements are aimed to simulate the saturation history of the reservoir. There are three main methods to make capillary pressure measurements; mercury-injection method, centrifuge method and the porous diaphragm.

Mercury Capillary Pressure test system can be used for capillary pressure measurements and bulk volume measurements of core samples. System consists of a mercury pump, visual sample cell and a pressure gauge. A light source is also used in order to observe the mercury level inside the chamber. Volume measuring scales in millimeters with 0.01 vernier. Pump furnished with spare o-ring seals. Maximum working pressure of the system is 1200 psi. Picture of the mercury capillary pressure test system can be seen in Fig.2.4.

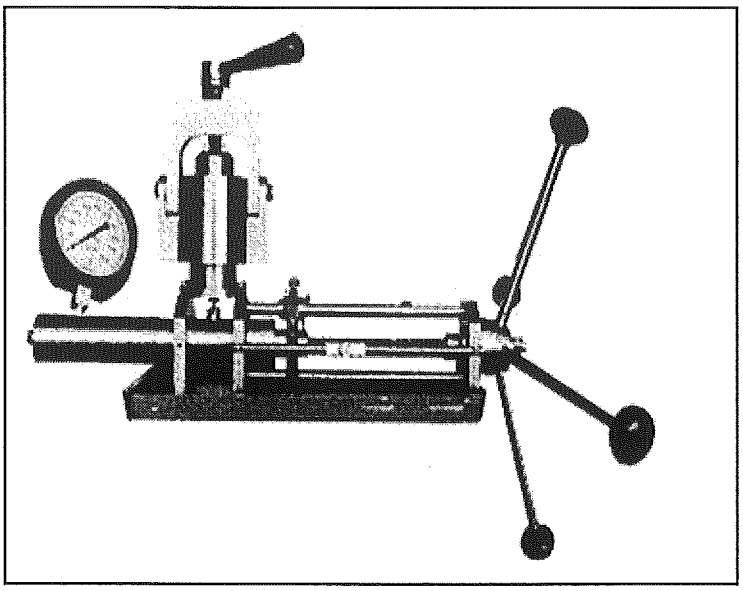

Fig. 2.4. Mercury capillary pressure test system

Mercury is an ideal fluid for capillary pressure measurements, because it is known as a non-wetting phase with all types of gases and liquids. The core plug sample is inserted in the mercury chamber and evacuated. Mercury is introduced into the core at a number of pressure increments and the injected mercury volume is measured. This measured mercury volume represents the non-wetting phase saturation. This procedure is continued until the sample is filled with mercury. This measurement is named as drainage process. Then,

beginning with the last pressure step of the drainage process, pressure is decreased incrementally and the withdrawn mercury volume is measured. This process is named as imbibition process. The disadvantage of mercury-injection method is the difference in wetting properties and the loss of the measured core plug sample [14].

From these capillary pressure measurement data, capillary pressure curves are derived to relate reservoir water saturation to height above the free water level. This laboratory capillary pressure curve for core plug samples of known permeability, porosity or rock type can be used to calculate water saturation versus height for oil-water reservoir conditions. [15]

Mercury injection capillary pressure measurements give air – mercury capillary pressure data. It is important to convert the laboratory data to the field water and oil capillary pressure. Results should represent water oil capillary pressure of a water-wet reservoir rock. In order to make this conversion the following equation is used:

$$P_{C_R} = P_{C_L} \times \frac{(\sigma Cos\,\theta)_R}{(\sigma Cos\,\theta)_L} \qquad (2\text{-}1/21)$$

where,

σ : interfacial tension, dyne/cm

θ : contact angle, degree

R : reservoir conditions

L : laboratory conditions

Washburn (1921) first suggested the use of mercury injection as a laboratory method for determining the pore aperture size distribution in porous rocks [16].

The Washburn equation can be expressed as:

$$P_c = -2\,\gamma\cos\theta/r \qquad (2\text{-}1/22)$$

where,

- P_c = capillary pressure (dynes/cm^2),
- γ = surface tension of Hg (480 dynes/cm),
- θ = contact angle of mercury in air (140°)
- r = radius of pore throat for a cylindrical pore.

In order to calculate the pore throat size, the following expression can be used :

- $$d = C \times \frac{4\sigma Cos\theta}{P_c} \qquad (2\text{-}1/23)$$

where,

d : pore throat diameter, µm

C : unit conversion constant (C = 145x10^{-3})

2.1.5.1. J-Function – Averaging Capillary Preassure Data

As capillary pressure data are obtained on small core samples which represent an extremely small part of the reservoir, it is necessary to combine all the capillary pressure data to classify a particular reservoir. Leverett introduced a dimensionless capillary pressure correlation, J-function, with an

intention to eliminate the effect of rock heterogeneity, such as porosity and permeability variations from the capillary pressure – saturation function. Leverett investigated the effect of fluids interfacial tension and rock properties, porosity and permeability on capillary pressure.

The J-Function correlating term uses the physical properties of the rock and fluid [17]. Modelling of the drainage capillary pressure can be done with the following expressions :

$$- \quad J(S_w) = \frac{P_c}{\sigma Cos\theta}\sqrt{\frac{k}{\phi}} \qquad (2\text{-}1/24)$$

where,

σ = interfacial tension, dyne/cm

θ = contact angle, degree

k = permeability, md

ϕ = porosity, ratio

Since the irreducible water saturations is usually not the same for the different formations, it is normal to expect different J-function curves for those formations. For this reason, using a normalized saturation scale may improve the J-function correlation. The normalized saturation is defined as :

$$- \quad S_w^* = \frac{(S_w - S_{wi})}{(1 - S_{wi})} \qquad (2\text{-}1/25)$$

where,

S_w^* = Induced water saturation

S_w = water saturation

S_{wi} = irreducible water saturation

Using these correlations, all capillary pressure curves will have the same value of $S_w^* = 0$ at irreducible water saturation.

2.2. PVT ANALYSIS

PVT analyses are mainly consist of constant mass expansion, zero-flash (separator) test, viscosity measurement and compositional analysis. These tests are aimed to represent the volumetric changes taking place in the reservoir.

2.2.1. Constant Mass Expansion Test

Constant mass expansion tests are done with a fixed amount of reservoir fluid sample transferred to a PVT cell at various pressure levels and fixed reservoir temperature. Measurements can be done by assuring phase equilibrium of system at every pressure level. Decomposed gas, at pressure levels under bubble point, was preserved within the system and total volumes of oil and gas phases were obtained at equilibrium.

Constant mass expansion test gives information about the saturation pressure at the reservoir temperature and the relative volumes of gas and oil in the reservoir.

The experiment must be started at a pressure higher than the bubble point pressure. Pressure is decreased step by step till the smallest pressure point below bubble point pressure. Volume readings are done against each pressure steps. At each stage of the experiment the relative volume, which is the ratio of the actual volume and the volume at bubble pressure, is recorded.

With the constant mass expansion experiment bubble point pressure, relative volume, density and the isothermal oil compressibility can be calculated.

2.2.2. Zero-Flash Separator Test

Zero-flash separator test is done after constant mass expansion experiment in order to gain an idea about the relative volumes of gas and oil produced from a particular reservoir. At reservoir temperature and a pressure point, a known amount of oil sample is flashed out to standard conditions, atmospheric temperature and pressure. Flashed oil and gas volumes are measured. With the zero-flash separator test gas oil ratio, oil formation volume factor, gas gravity and gas compositions can be found.

2.2.3. Viscosity Test

The aim of the viscosity test is to measure the oil viscosity at reservoir temperature and at decreasing pressure starting from the reservoir pressure. Oil viscosity measurements can be done by using high pressure and high temperature rolling ball viscometer or electromagnetic viscometer. Measurements should be done at reservoir temperature and at various pressure levels starting from a pressure above the reservoir pressure. Below the bubble point pressure the measurements should be done through removing the gas from the system as in the differential liberation test. Gas viscosities at reservoir temperature also can be calculated using standard correlations [18].

2.2.4. Compositional Analysis

The gas chromatograph (GC) is a system comprising two phases: the mobile phase which is a carrier gas, usually helium and the stationary phase that is a microscopic layer of liquid with a high boiling point on an inert solid support inside a column. The column is a glass or metal tubing through which helium gas is allowed to flow. The column is attached to an injection port, and the entire system is heated in an oven. Sample is injected into the column through the injection port. Different chemical constituents of the sample pass at different rates depending on their various chemical and physical properties and their interaction with the specific column filling. To be more precise, the polarity of the compounds and their volatility determines how long they are retained by the column. As each component exit the end of the column a peak is registered on a recorder. Thus, the main function of the stationary phase in the column is to separate different components, causing each one to exit the column at a retention time.

In a GC analysis, a known volume of gas or liquid sample is injected into the inlet of the column, usually using a microsyringe or a gas source. Although the carrier gas sweeps the sample molecules through the column, this motion is inhibited by the adsorption of the sample molecules either onto the column walls or onto packing materials in the column.

The rate at which the molecules progress along the column depends on the strength of adsorption, which in turn depends on the type of molecule and on the stationary phase materials. Since each type of molecule has a different rate of progression, the various components of the sample are separated as they progress along the column and reach the end of the column at different retention times. A detector is used to monitor the outlet stream from the column; thus, the time at which each component reaches the outlet and the amount of that component can be determined. Generally, substances are identified by the order in which they emerge from the column and by the retention time of the sample in the column.

A number of detectors are used in gas chromatography. The most common are the flame ionization detector (FID) and the thermal conductivity detector (TCD). Both are sensitive to a wide range of components, and both work over a wide range of concentrations. While TCDs are essentially universal and can be used to detect any component other than the carrier gas, FIDs are more sensitive to hydrocarbons than TCDs. Both detectors are also quite robust. Since TCD is non-destructive, it can be operated in-series before an FID (destructive), thus providing complementary detection of the same compounds.

The outlet from this process contains a number of light gases including H_2, CO, CO_2 and CH_4, as well as heavier parafinic and olefinic hydrocarbons (C_2-C_{36+}). In a typical experiment, a packed column is used to separate the light gases, which are then detected with a TCD. The hydrocarbons are separated using a capillary column and detected with an FID.

2.2.5. Limited PVT Data Correlations

In situations when the laboratory PVT data is lacking, it becomes necessary to make calculations with the empirically derived correlations [19]. In this section, the usefullness of these correlations is discussed by real PVT test results for the case of lacking PVT data. Equations that are used to estimate oil properties are given in the order of density, gas solubility, bubble point pressure, oil formation volume factor, isothermal compressibility coefficient, viscosity and interfacial tension calculations. Correlations for each property can be seen in Appendix A.

2.2.6. Flow Assurance Potential

The Flow Assurance which is a commonly used term in the oil and gas industry, is used to evaluate the effects of fluid hydrocarbon solids, such as asphaltene, wax and hydrate, scaling, sand and corrosivity. Flow assurannce is vital because of its potential to disrupt production due to fluid hydrocarbon solids deposition in the flow system. The term was firstly used in the early 1990's by Petrobras as "Garantia de Fluxo", meaning "Flow Assurance" in English.

Asphaltenes are responsible for many of the field problems experienced by production companies. It is a component class that may precipitate from petroleum reservoir fluids as a highly viscous and sticky material that cause deposition problems. The deposition of asphaltenes has been observed in producing wells and associated transfer and storage facilities. Some of these depositions occur in the reservoir pore space, pipelines, well chokes, casing perforations, the suction side of the pumps, storage tanks, pipelines, wellbore and well tubing and severely restrict the fluid flow.

The asphaltene precipitation is a complex phenomenon that involves asphaltenes and resins which are aromatic heterocompounds. Resins have a strong tendency to associate with asphaltenes in oil with aliphatic substitutions and they form the most polar fraction of crude oil. Asphaltenes are sensitive to shearing forces and electrostatic interactions [20].

Alongside deposition, there are various other problems, resulting from the asphaltene content in crude oils such as viscosity problems and production rate and flow rate decreases. Generally crude oils with high asphaltene content have high viscosity values. The viscosity of the crude oil depends on asphaltenes molecular weight and its high dispersion throughout the crude mix determine the viscosity of the crude oil.

"In order to determine the effect of asphaltene molecular weight on crude oil viscosity, asphaltene concentration and average chain length of the polysulfide-linked constituents must be known". Determining the asphaltene concentration is easy and can be performed by injecting in large quantities which forces the asphaltenes to precipitate from crude oil samples. But, determining the polysulfide constituents is a difficult task [20].

One of the basic characteristics of any chemical compound is its molecular weight which has a vital effect on the physical properties of the compound as solubility, density, phase behaviour, and intermolecular interaction. Asphaltenes are aromatic organic substances with high molecular weight and they are soluble in aromatic solvents but precipitated by the addition of n-heptane and n-pentane. Further, the molecular weight of asphaltenes varies from 1000 to several hundreds of thousands [21, 19].

Asphaltene solubility is dependent on the composition, pressure and temperature. The heavy and aromatic the crude oil, the higher the asphaltene solubility is. High asphaltene solubility increases the stability of the crude oil and it gets harder to dissolve asphaltenes. If the temperature, pressure or the compositional changes affect the stability of the crude oil, asphaltenes may start to precipitate. When thinking about a live bottom hole oil sample at reservoir pressure and temperature, decreasing the pressure below the upper asphaltene onset pressure will destabilize asphaltenes which cause asphaltene deposition in the wellbore. Moreover, the composition change will damage the asphaltene stability because the paraffin amount within the crude mix directly affects the precipitation of asphaltenes. Aromatics increase the solubility of asphaltenes, whereas paraffins act in the opposite way. This fact makes the potential of the asphaltene precipitation from a low density reservoir oil higher. De Boer and Leeriooyer present a generalized plot to identify crude oils with the potential to cause flow assurance problems by comparing the difference in pressures in the reservoir and at the bubble point with in-situ density of the oil (Fig.2.5). This plot summarizes the facts about potential asphaltene precipitation. [19, 22].

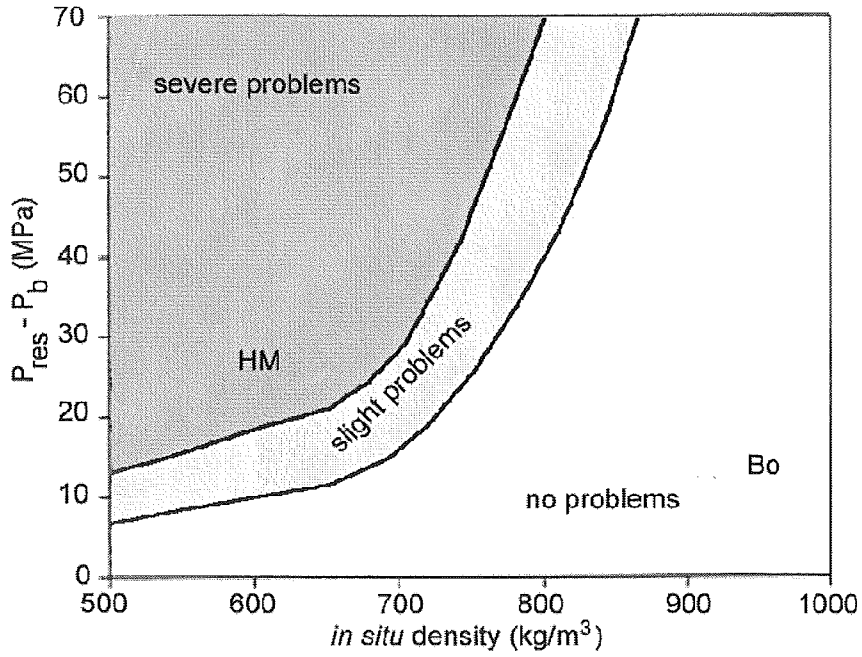

Fig 2.5. De Boer plot

Moreover, Oilphase Schlumberger develops an Asphaltene Stability Index to identify flow assurance problems. According to this approach, if the difference between the density of oil at the initial reservoir pressure and the density at the bubble point pressure is bigger than 0.025 g/cc, system can be thought as unstable. This approach also proves that asphaltene precipitation is more likely to take place from a reservoir fluid of low density. The bigger the gap between initial reservoir oil density and bubble point oil density indicates higher the amount of the light crudes and higher the oil compressibility coefficient.

It is not enough to say there may not be any problem about the asphaltene deposition with De Boer plot and Asphaltene Stability Index. Enhanced oil recovery studies may increase the risk of asphaltene deposition. If any thermal recovery processes or any gas injection processes are applied, it

should be noted that, laboratory tests should be done to specify the Lower and Upper Asphaltene Onset Pressure values.

The pressure at which the last asphaltenes go into solution is called the Lower Asphaltene Onset Pressure whereas, the pressure at which the asphaltene phase will disappear is called the Upper Asphaltene Onset Pressure.

In order to detect these asphaltene onset pressure points, there are six commonly used techniques including gravimetric, acoustic resonance, light-scattering, filtration and high-pressure microscope techniques. The gravimetric method is performed in a conventional PVT cell by reducing the pressure at a constant temperature value, whereas the acoustic resonance technique allows the formation of a new phase to be determined acoustically. Acoustic resonance technique can be performed just for determining the upper asphaltene onset pressure. By the Light-Scattering Technique, the upper asphaltene precipitation onset pressure can be measured with accuracy and power of transmitted light vs. pressure graphs can be drawn. Filtration technique is based on the detection of the increasing pressure drop over the filter which is a result of asphaltene phase precipitation. Finally, with the high pressure microscope the change in size and morphology of asphaltene solids are monitored as a function of temperature, pressure and time. [23]

2.2.7. C_{7+} Characterization

It is essential to make a C_{7+} characterization of hydrocarbon fluid sample, to correlate measured PVT data with equations of state. For pure compounds critical properties that are required to use in equations of state are known. For the petroleum fractions making up heptanes-plus critical properties must be estimated. Correlations of Riazi and Daubert and Edmister can be seen in Appendix B.

2.2.8. Lumping (Pseudoization)

Lumping is the reduction in the number of components used in equations of state calculations. It is important to regroup the original components into a small number without losing the accuracy of the equations of state. Lee et al., Whitson and Behrens and Sandler's proposed methods for lumping can be seen in Appendix C.

2.2.9. Equations of State

An equation of state is based on the well-known equation of state of ideal gas. This equation is modified for real hydrocarbon fluids by relating the pressure, volume and temperature parameters. These parameters are important to determine the phase and the volumetric behaviour of reservoir hydrocarbon fluids.

In compositional simulation studies, it is necessary to perform PVT simulation and compare it with measured laboratory PVT data. The results of this

comparison can be employed as a quality check of the fluid composition. These calculations for oil and gas mixtures are based on van der Waals's cubic equation of state (1873). Furthermore, Redlich and Kwong (1949), Soave (1972), Peng-Robinson (1978) and Peneloux et al. (1982) developed various other cubic equations of state. These equations of state require good C_{7+} characterization and for this case it is neccessary to make some calculations with the dead oil compositional analysis.

For making cubic equation state calculations on a reservoir fluid composition, the critical temperature, the critical pressure and the acentric factor parameters are required for each component within the mixture. When using Peneloux et al.'s equation of state with volume correction, it is required to define a volume shift parameter for each component. C_{7+} characterization comprises representing the heptane plus fraction of hydrocarbons as a convenient number of pseudocomponent and to find the needed equation of state parameters for each of these pseudocomponents. [24]

Correlations for equations of state calculations can be seen in Appendix D.

CHAPTER 3

STATEMENT OF THE PURPOSE

In order to find the storage and flow capacities of reservoir rocks and the production performance both core analysis and PVT analysis subjects have to be studied in detail. Petroleum reservoir rock and fluid properties can be determined with the help of laboratory measurement data. Moreover, there are many studies about the estimations of core and PVT properties in the literature. This study is aimed to be a road map from laboratory measurements to the input data file of reservoir simulation and various approaches are going to be studied.

In petroleum reservoirs, oil, water, and gas may coexist and flow simultaneously. In multiphase reservoirs, the phase saturations add up to one, capillary pressures between phases exist, and phase relative permeability affect flow properties. Although volumetric and viscosity properties of water and gas phases are not different from those in single-phase flow, oil-phase properties are affected by both solution GOR and whether the pressure is below or above the oil bubble-point pressure.

Simulation of multiphase flow involves writing the flow equation for each component in the system and solving all equations for the unknowns in the system. In black-oil simulation, the components are the oil, water and gas and the flow model consists of one equation for each of the three components, the saturation constraint and the oil/water and gas/oil capillary pressures.

The two-phase oil / water, oil / gas and gas / water flow models can be considered as subsets of the black-oil model. In order to solve the model equations, the accumulation terms have to be expanded in a conservative way and expressed in terms of the changes of the primary unknowns over the same time step, the well production rate terms for each phase defined, and the fictitious well rate terms reflecting the boundary conditions need to be defined. In addition, all nonlinear terms have to be linearized.

X-Field, which is chosen for this study, is a carbonate reservoir. Because of lacking of well log data and production data, this study becomes limited. Some approaches like porosity and permeability estimation from well log data or production performance estimation can not be dealt with in this study. However, laboratory measurements can be done on core plug samples. With the help of the laboratory data porosity, permeability, capillary pressure and relative permeability properties are going to be studied. Moreover, averaging and normalizing the reservoir rock properties subjects are going to be discussed.

The analysis of the production performance is essentially based on the fluid PVT properties and relative permeability data. In literature, there are a lot of studies about the PVT data estimation in case of lacking of measurement data. With the help of the previously done PVT laboratory measurements data some of these studies are going to be applied over the X-Field reservoir oil and water properties. After dealing with the correlations with limited PVT data, equations of state are going to be tried to correlate with measured data. In order to make this correlation, C_{7+} properties are going to be estimated. Results of these correlations are going to be discussed in following chapters.

CHAPTER 4

EXPERIMENTAL PROCEDURE

4.1. CORE ANALYSIS

4.1.1. Preparation of core plug samples for test

Core plugs were cleaned from the residues of hydrocarbon, formation water and drilling fluid; firstly by usage of the "soxhlet toluene extraction" device and then via keeping under vacuum and within alcohol. The cleaned core plug samples were made ready for the test upon weight and dimension measurements after drying the samples in a temperature-controlled oven at 70 °C.

4.1.2. Porosity

Porosity values were measured via Helium Porosimeter and Boyle Law and the data obtained from the measurements are utilized in calculating the grain density of the sample.

Two chambers of known volumes were connected. Reference cell is filled with helium at a given pressure and core plug sample is placed in the matrix cup. The helium was expanded into the matrix cup and the equilibrium pressure was recorded to determine the unknown volume of the matrix cup with the core plug. Grain volume of the core plugs were calculated with the help of the Boyle's Law. Moreover, bulk volumes of the core plugs were

determined by measuring its dimensions. Lastly, grain density calculations were also done after weighing the core plug sample.

4.1.3. Permeability

Permeability measurements were done with the help of the air permeameter by transmitting dry air through the sample, placed within Hasler-type core cell, and calculated with Darcy Law. At a constant differential pressure, dry air was injected through the sample until a constant flow rate was attained. The measured air permeability values (k_{air}) were then translated into equivalent liquid permeability value (k_L) through Klinkenberg Correction.

4.1.4. Porosity and Permeability Measurements Under Overburden Pressure

Under overburden pressure, porosity and permeability measurements were done by applying the CMS-300 test system over core plug samples. Minimum working pressure of CMS-300 test system is 800 psi. By regarding the reservoir depth, pressure steps were assigned. Over the core plug samples, located in the system, predetermined net overburden pressures (NOP) were applied and for each of the pressure values, the corresponding porosity and permeability values were determined.

4.1.5. Relative Permeability Tests

Water-oil relative permeability tests were applied over 23 core plug samples according to the "unsteady-state" relative permeability test technique in

laboratory conditions. As test fluid; NaCl solution, bearing 130,000 ppm salinity and laboratory oil with density of 0.85 gr/cm^3 and of viscosity 11.5 cp,at 30 °C was used.

Core plug samples, firstly, were saturated with brine then using the same fluid absolute water permeability values (k_w) were determined. After, samples were reduced to irreducible water saturation through flooding with laboratory oil and the oil permeability values of the samples at irreducible water saturation (k_o @ S_{wi}) was determined. In the next step, flooding with brine at constant flow; the data required for the relative permeability tests were recorded. When the oil outflow from the sample ends, water permeability value at irreducible oil saturation (k_w @ S_{or}) was determined and the test was finalized. The relative permeability calculations were done via JBN method.

4.1.6. Capillary Pressure Tests

The mercury injection capillary pressure apparatus was developed to accelerate the determination of the capillary-pressure/saturation relationship. The core samples were inserted in the mercury chamber and evacuated. Mercury was forced into the core under pressure. The volume of mercury injected at each pressure were read to determine the nonwetting phase saturation. This procedure was continued until the core sample was filled with mercury or the maximum injection pressure of the test system was reached. Besides, capillary pressure imbibition curves were formed from the mercury volume values that outflow from the pores up on decreasing the applied pressure at various levels.

Capillary pressure tests were applied over core plug samples with mercury injection method. Capillary pressure drainage curves were formed via

drawing capillary pressure values against wetting phase saturations that were obtained from calculating the non-wetting phase saturations –namely; mercury that enter into the pores of core plug samples between 3-1215 psia pressure values.

CHAPER 5

EXPERIMENTAL RESULTS AND DISCUSSION

5.1. CORE ANALYSIS

X-Field reservoir rock properties were tried to be found with the help of the laboratory measurements. Laboratory measurement data were evaluated and then, average of porosity, permeability and relative permeability properties were calculated and relative permeability and capillary pressure models of the X-Field were developed. Results of the core analysis can be seen graphically in Figures 5.1 to 5.12. Also calculated and normalized data of reservoir rock properties can be seen in Tables 5.1 to 5.6 and in Appendix E.

5.1.1. Porosity

Porosity measurements were done over 273 core plug samples which were taken from 6 different wells of the X-Field. Results show that, porosity values vary between 0.22 % and 51.23 %. Average of the porosity values is 23.45 %. Also, average grain density value was found as 2.79 g/cc. Summary of the porosity and grain density measurements can be seen on Table 5.1.

In determining the original oil in place in a reservoir with fairly good accuracy, the variation of porosity throughout the reservoir needs to be known. In the X-Field, the porosity distribution can be said as normal distribution. Porosity distribution chart can be seen in Fig. 5.1. Moreover, porosity – permeability cross plot is given in Fig.5.3.

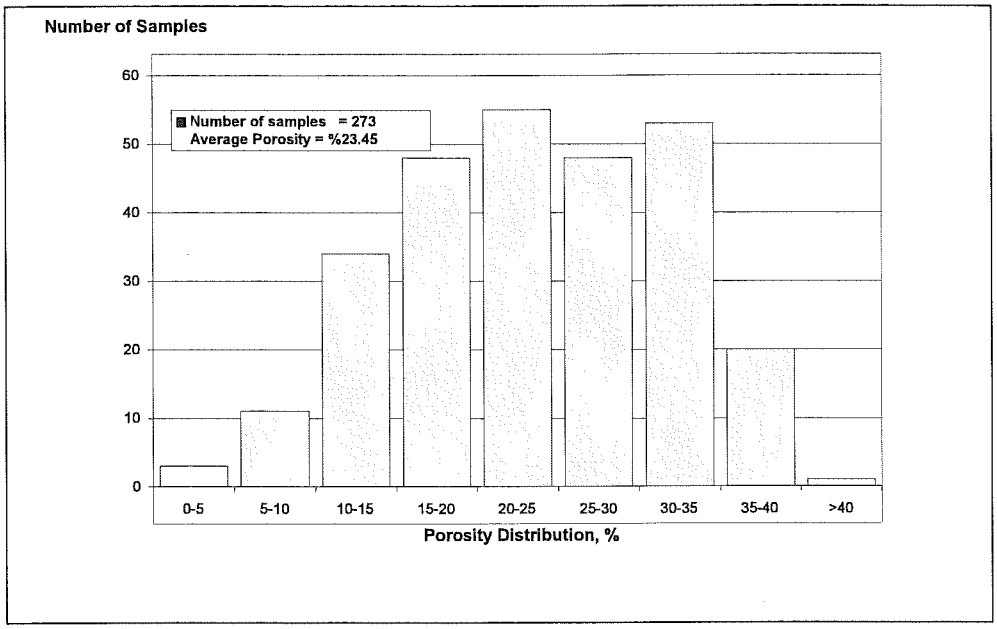

Fig 5.1. X-Field core plug samples porosity distribution histogram.

5.1.2. Permeability

Permeability measurements were done over 273 core plug samples. Permeability values vary between 0.02 md and 58.17 md. Average of the permeability values is 1.69 md. Summary of the permeability measurements can be seen on Table 5.1.

Table 5.1. X-Field core plug samples average porosity and permeability test results

Core	# of samples	Porosity (%)			Permeability (md)			Grain Density (gr/cm^3)		
		Lower Limit	Upper Limit	Average*	Lower Limit	Upper Limit	Average**	Lower Limit	Upper Limit	Average*
X-2	77	6.69	51.23	26.47	0.07	51.77	2.18	2.70	2.88	2.79
X-3	5	15.30	35.16	25.94	0.36	11.02	1.64	2.81	2.96	2.88
X-4	6	18.41	35.02	26.62	0.82	25.74	3.26	2.71	2.98	2.81
X-5	82	0.33	39.20	23.17	0.02	58.17	1.82	2.68	3.18	2.81
X-6	62	0.22	34.70	21.05	0.02	28.56	1.31	2.71	2.89	2.77
X-7	41	5.77	34.56	21.20	0.03	50.32	1.23	2.68	2.88	2.77
Total	*273*	-	-	23.45	-	-	1.69	-	-	2.79

** Aritmethical average.*

*** Geomethrical average.*

Permeability distribution chart can be seen in Fig. 5.2. For the average permeability calculation, geometrical average was preferred. As shown in Fig.5.2 arithmetrical average was calculated as 6.26 md. However, Fig. 5.2 shows that most of the permeability values are below 5 md. Taking arithmetical average for average permeability gives an unexpected value. Permeability distribution chart can be seen as a proof of the validity of geometrical average. This fact is also important to increase the effect of low permeability layers in average permeability.

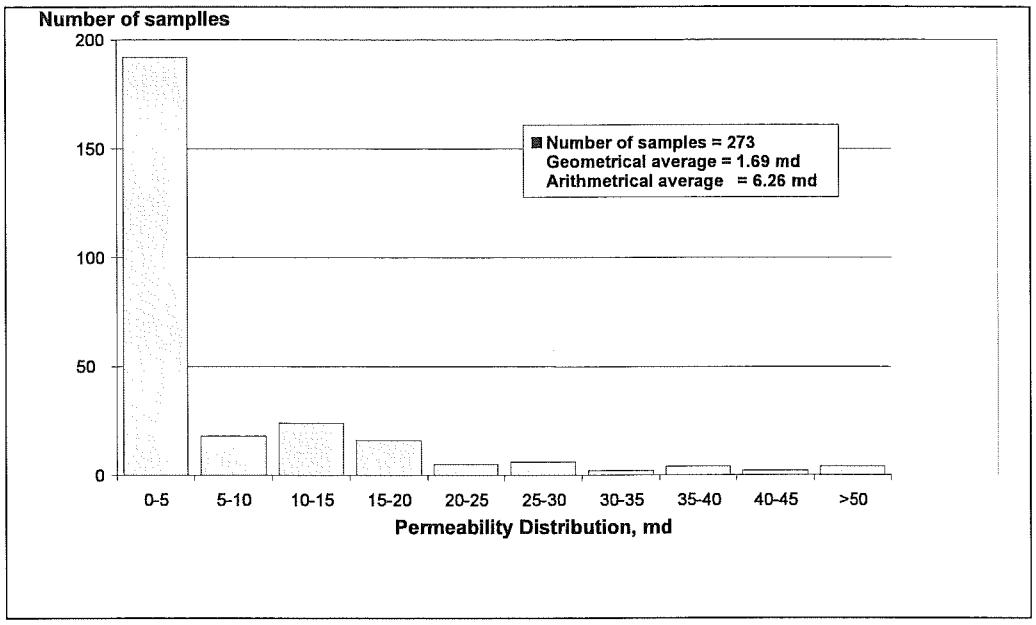

Fig 5.2. X-Field core plug samples permeability distribution histogram.

Reservoir simulation models require permeability values to be defined with a good accuracy in order to predict reservoir performance. Basic models involve plotting of permeabilty versus porosity values as obtained from core analysis on a semilog scale. Porosity – permeability cross plot is shown in Fig.5.3. A logarithmic scale is commonly used for permeability values against porosity, because the permeability variation is more significant than the porosity variation from one point to another in the reservoir. For the X-Field, average permeability value is 1.69 md, whereas the average porosity is 23.45 %. Trendline of the cross-plot shows that at 20 percent of porosity come along nearly 1 md permeability value. This low permeability fact is important for cutoff porosity determination. Moreover, large deviations in values of permeability from the trendline point to significant heterogeneities that exist in the reservoir. For similar porosities, permeability can vary significantly. Besides, it can be said that permeability values increases with increasing porosity as shown in Fig. 5.3. Corresponding to a low permeability value, low porosity cores are not expected to be good conductors of fluids.

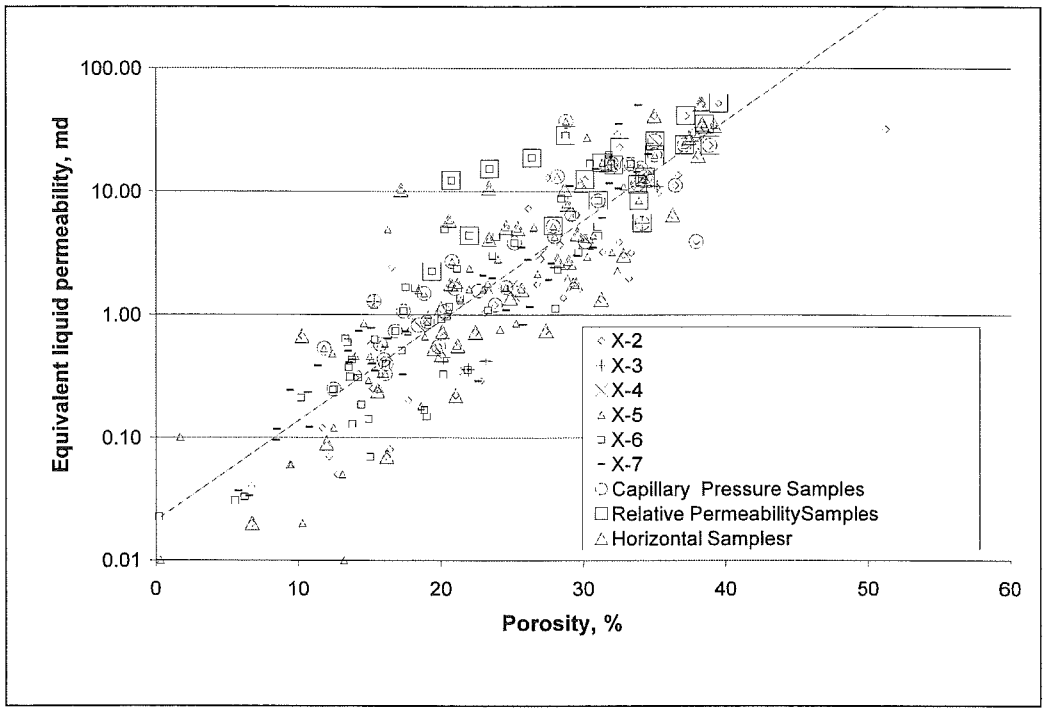

Fig 5.3. X-Field core plug samples porosity-permeability plot.

5.1.3. Porosity and Permeability Measurements Under Netoverburden Pressure

Under overburden pressure, porosity and permeability measurements were done by using the CMS-300 test system over 140 core plug samples. Over the core plug samples, located in the system, respectively 800, 1250, 2000, 3000 and 4000 psi net overburden pressure (NOP) were applied and for each of the pressure values, the corresponding porosity and permeability values were determined.

For the X-Field average depth is known as 1300 m. and the overburden pressure gradient is assumed as 1 psi/ft. With this information pressure steps

for the porosity and permeability measurements under net overburden pressure were choosen as 800, 1250, 2000, 3000 and 4000 psi.

The compressibility of a hydrocarbon-bearing formation under an isothermal condition is a function of change of pore volume with change of pressure. Porosity and permeability changes with increasing pressure can be seen in Fig.5 4. and Fig. 5.5. Results of these measurements can be seen in Table E.2.

Fig. 5.4. shows that, average of nearly 5 % decrease in porosity value can be seen at 4000 psi net overburden pressure. Maximum decline in porosity is more than 20 %.

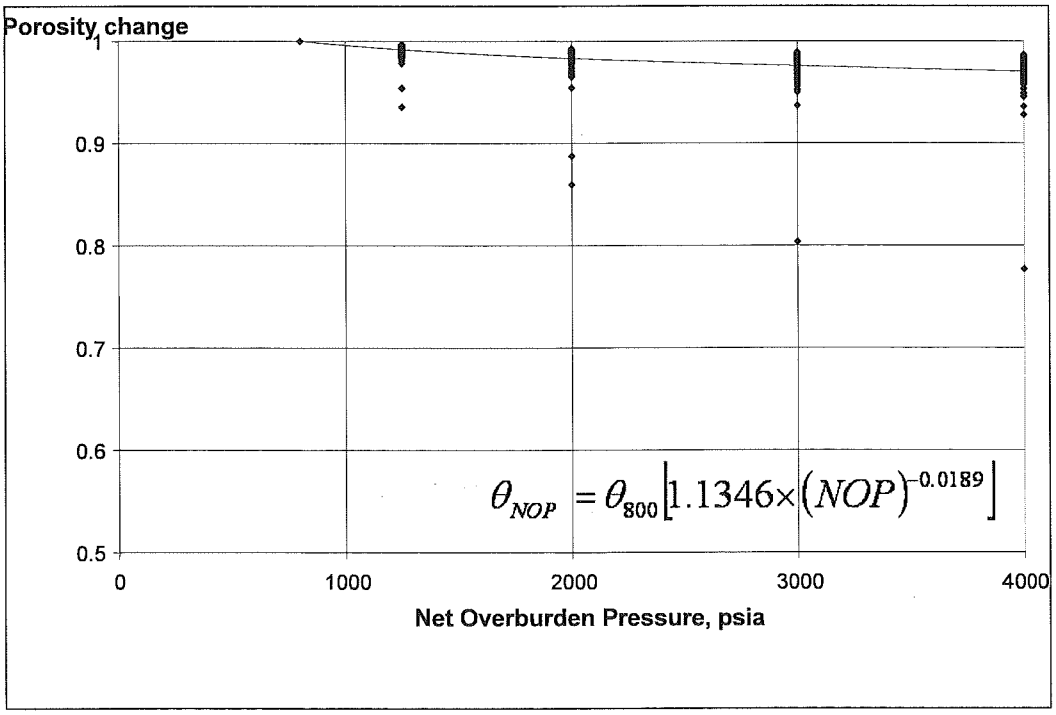

Fig 5.4. X-Field - Porosity change under net overburden pressure

Fig.5.5 is essential to see the importance of the pressure on reservoir rock permeability value. Up to 75 % of porosity decrease is observed in this study. The average permeability decrease is approximately 15 %.

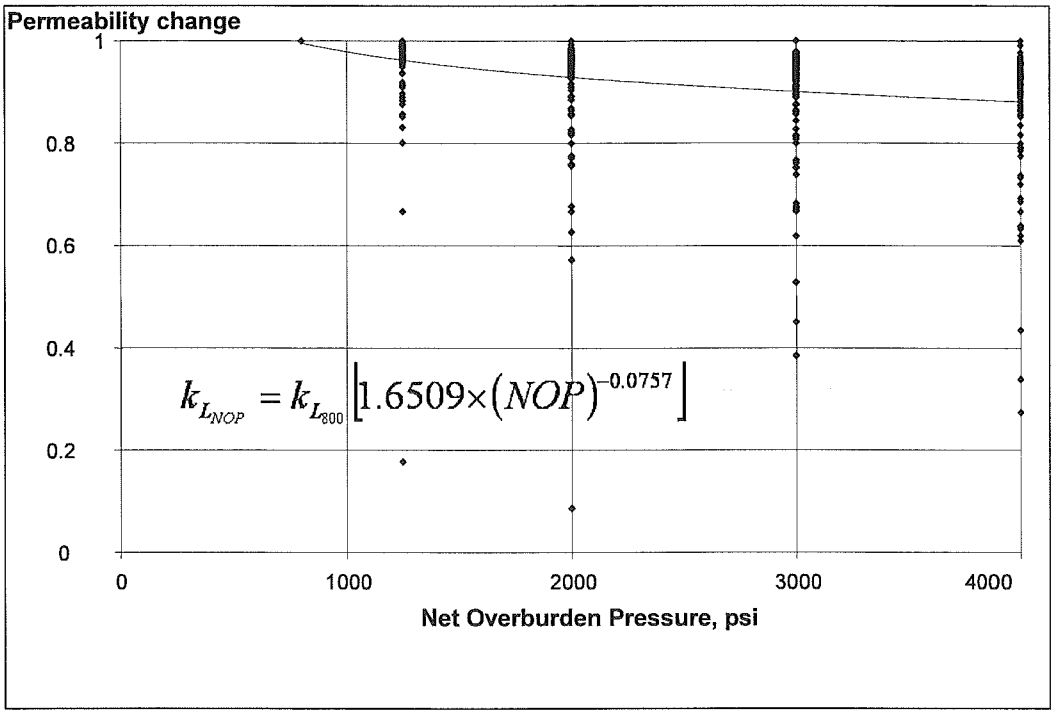

Fig 5.5. X-Field - permeability change under net overburden pressure

The coefficients of the relation between overburden pressure and the porosity and permeability properties found from the slopes of these bestlines can be seen in Table 5.2.

Table 5.2. Coefficients for the equations of the relation between overburden pressure and the porosity and permeability properties

	a	*b*	*C*	*D*
X-Field	1.1346	-0.0189	1.6509	-0.0757

5.1.3. Relative Permeability

Water-oil relative permeability tests are applied over 23 core plug samples according to the "unsteady-state" relative permeability test technique in laboratory conditions. The relative permeability calculations are done via JBN method.

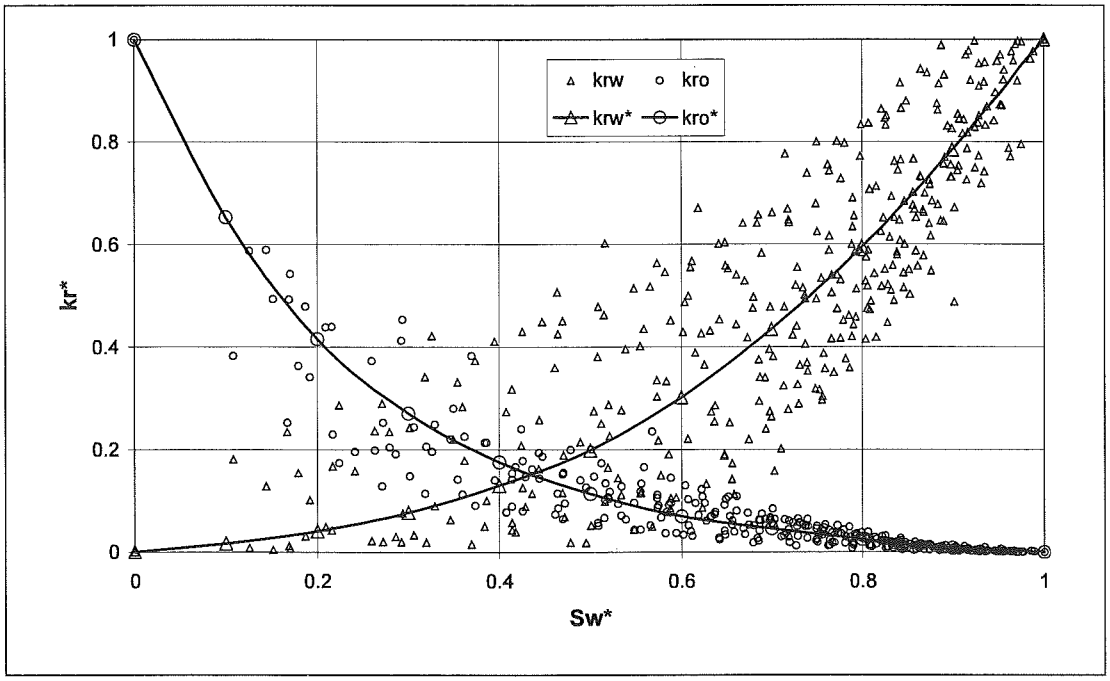

Fig 5.6. X-Field induced relative permeability data

In order to define relative permeability data related to porosity, 15 %, 25 % and 35 % porosity values are determined to use in the calculations. Then, laboratory test results (Table E.3) were tried to be normalized. Induced water saturation values and induced relative permeabilities of oil and water phases S_w^* - k_{rw}^* and k_{ro}^* plots are shown in Fig 5.6. Sw* values against krw* and kro* values which were read from the trendline curves are also shown in Table 5.3.

Table 5.3. S_w^*, k_{rw}^* and k_{ro}^* values read from induced relative permeability graph

S_w^*	k_{rw}^*	k_{ro}^*
0.00	0.00000	1.00000
0.10	0.01700	0.65400
0.20	0.04100	0.41600
0.30	0.07700	0.27100
0.40	0.13000	0.17600
0.50	0.19900	0.11400
0.60	0.30200	0.07000
0.70	0.43500	0.04600
0.80	0.59600	0.02500
0.90	0.78500	0.00800
1.00	1.00000	0.00000

Lastly, porosity and irreducible water saturation and residual oil saturation relations were plotted and S_{wi} and S_{or} values against various porosity values were read from the bestlines.

Similarity of porosity values of the samples used in the relative permeability tests did not allow to determine the relation between porosity and irreducible water saturation. To solve this problem, end-points obtained from both capillary pressure tests and relative permeability tests were used to develop a porosity versus irreducible water saturation plot. (Fig. 5.7). Fig. 5.7. shows that the capillary pressure measurements give end point values in the same manner with relative permeability measurements.

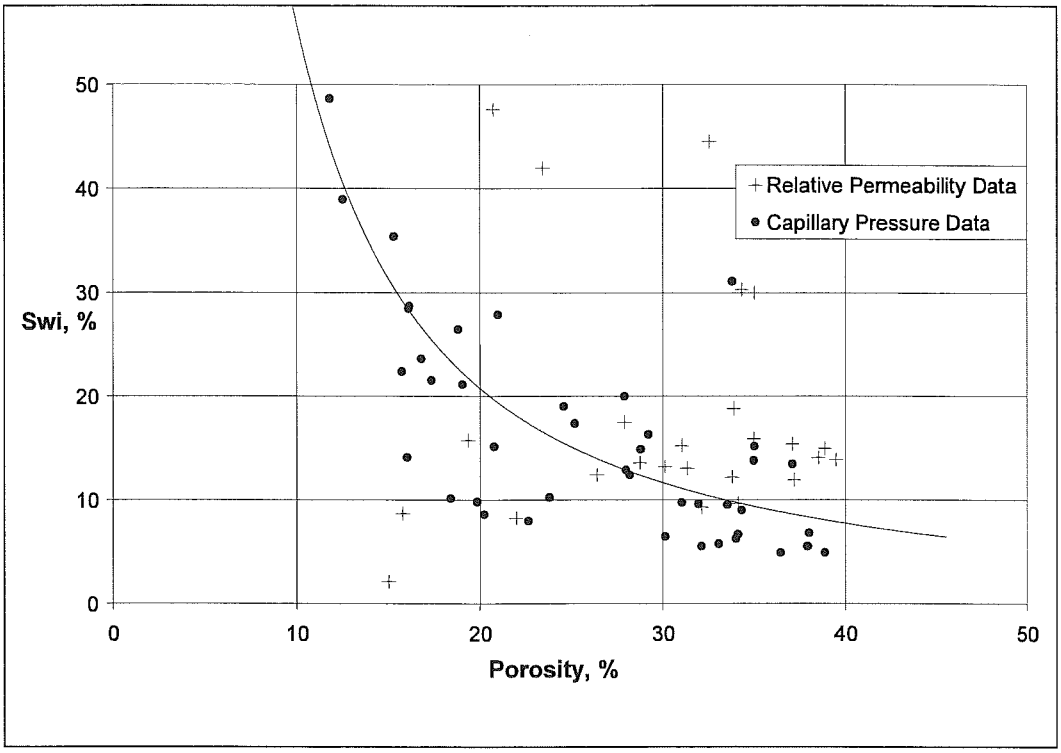

Fig 5.7. X-Field - irreducible water saturation versus porosity

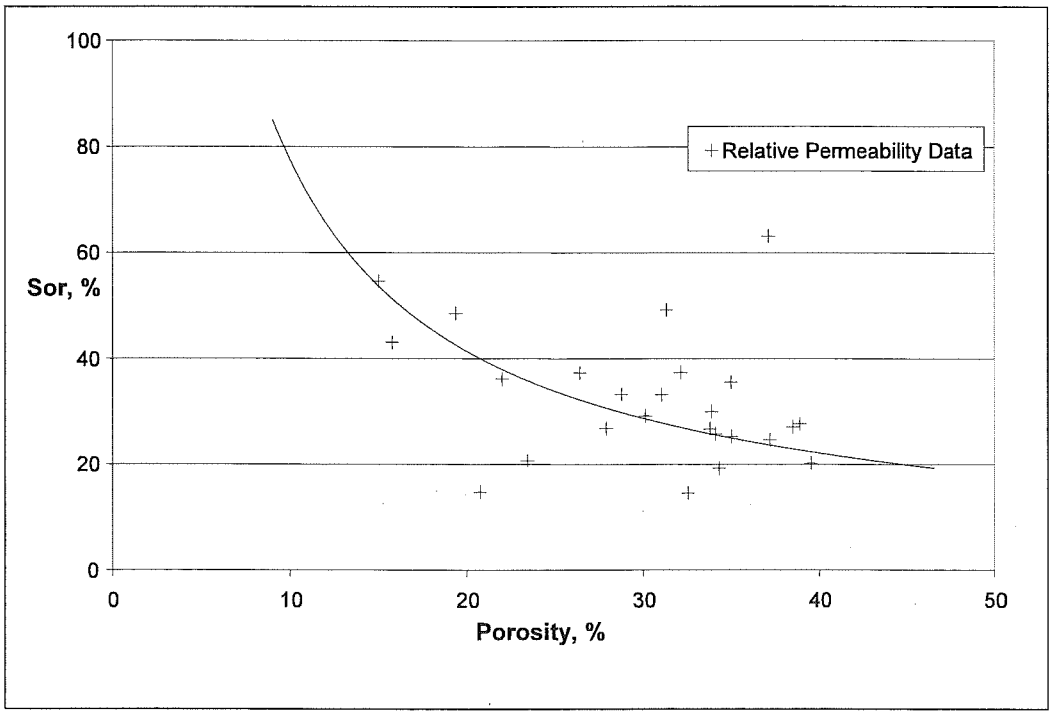

Fig 5.8. X-Field – residual oil saturation versus porosity

With the help of the test data residual oil saturation versus porosity plot was also drawn (Figure 5.8). Finally, after reading residual oil saturation and irreducible water saturation values from these graphs relative permeability models were developed (Table 5.4.) (Figure 5.9).

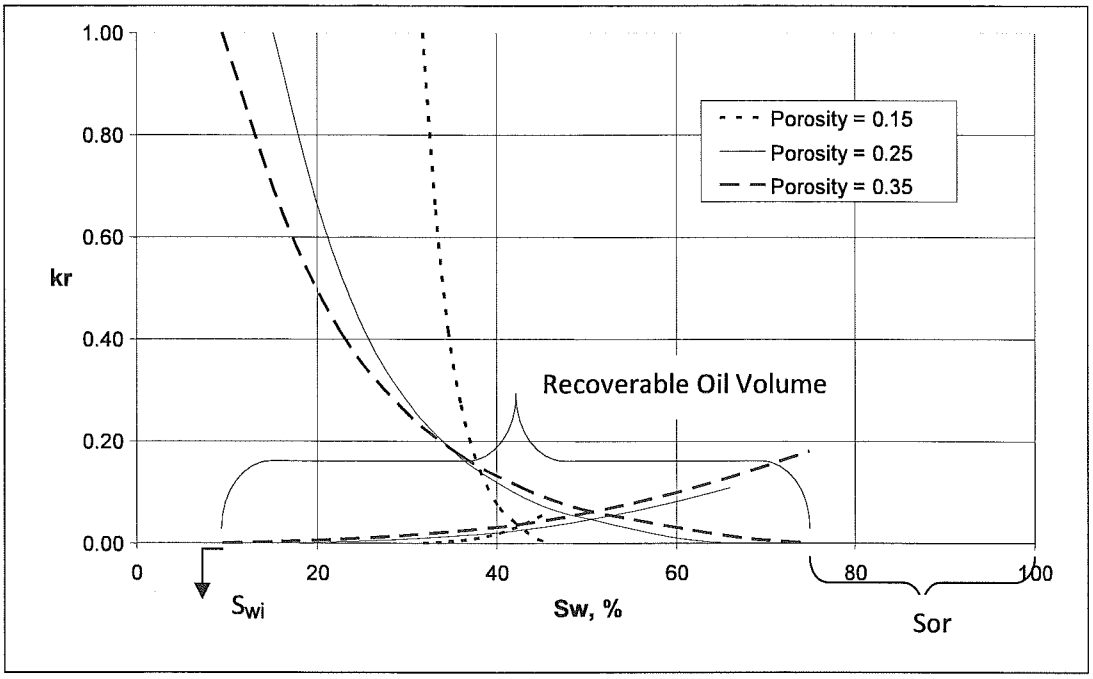

Fig 5.9. X-Field relative permeability models

Table 5.4. X-Field water saturation and relative permeability model data

Porosity = 0.15			Porosity = 0.25			Porosity = 0.35		
S_w (%)	k_{ro}	k_{rw}	S_w (%)	k_{ro}	k_{rw}	S_w (%)	k_{ro}	k_{rw}
31.80	1.00000	0.00000	15.10	1.00000	0.00000	9.50	1.00000	0.00000
33.22	0.65400	0.00107	20.19	0.65400	0.00185	16.04	0.65400	0.00306
34.64	0.41600	0.00258	25.28	0.41600	0.00447	22.58	0.41600	0.00738
36.06	0.27100	0.00485	30.37	0.27100	0.00839	29.12	0.27100	0.01386
37.48	0.17600	0.00819	35.46	0.17600	0.01417	35.66	0.17600	0.02340
38.90	0.11400	0.01254	40.55	0.11400	0.02169	42.20	0.11400	0.03582
40.32	0.07000	0.01903	45.64	0.07000	0.03292	48.74	0.07000	0.05436
41.74	0.04600	0.02741	50.73	0.04600	0.04742	55.28	0.04600	0.07830
43.16	0.02500	0.03755	55.82	0.02500	0.06496	61.82	0.02500	0.10728
44.58	0.00800	0.04946	60.91	0.00800	0.08557	68.36	0.00800	0.14130
46.00	0.00000	0.06300	66.00	0.00000	0.10900	74.90	0.00000	0.18000

Knowledge of relative permeability is crucial in understanding multiphase fluid flow behaviour in a reservoir and for predicting future reservoir performance. The relative permeability characteristics of reservoir fluids usually change from one location to another. Various rock facies in a reservoir may exhibit very different relative permeability trends.

A large amount of relative permeability data is typically incorporated in reservoir models in order to make realistic predictions of recovery. The relative permeability of a fluid phase increases with an increase in the saturation of the phase in porous media. The relationship between two parameters is nonlinear.

Irreducible water saturation is a certain saturation level below which the fluid will not flow through the pores. In Fig. 5.9 irreducible water saturation for 0.35 porosity model is shown as S_{wi}. Moreover S_{or} value for 0.35 porosity is also shown in the figure. The difference between S_{wi} and S_{or} gives the amount of the recoverable oil. To summarize, the bigger the porosity the bigger the difference between irreducible water saturation and residual oil saturation. With the increase in the gap between S_{wi} and S_{or}, the amount of oil can be produced will increase. So, reservoir rock with the 0.35 and 0.25 porosity can be thought as having a good reservoir whereas the reservoir rock with 0.15 porosity have bad quality. This fact is a proof of the importance of the saturation profile while determining the porosity cutoff value.

5.1.4. Capillary Pressure

Capillary Pressure drainage and imbibition tests were done over 42 core plug samples. From the results of these measurements, pore throat size distributions, capillary pressure drainage and imbibition curves were established. Capillary pressure drainage and imbibition data were shown in Table E-4. Results show that, wetting phase saturation data vary between 4.95 % and 48.66 %.

During drainage in a core, the wetting phase fluid is replaced by a flowing wetting phase. In water wet rock, water saturation is reduced as a consequence of the drainage process, while the saturation of the nonwetting phase, oil, is increased.

For the same wetting phase saturation, capillary pressure is observed to be greater during drainage than during imbibition. In other words, a relatively large pressure differential between the nonwetting and wetting fluid phases would be required at a given saturation to drain the wetting phase than to imbibe it.

In order to combine all the capillary data to classify a particular reservoir J-function correlating term was used to plot J-Function versus induced wetting phase saturation graph, which is shown in Fig. 5.10. By the help of the trendline, J function values were read against predetermined induced water saturation values. Data can be seen in Table 5.5.

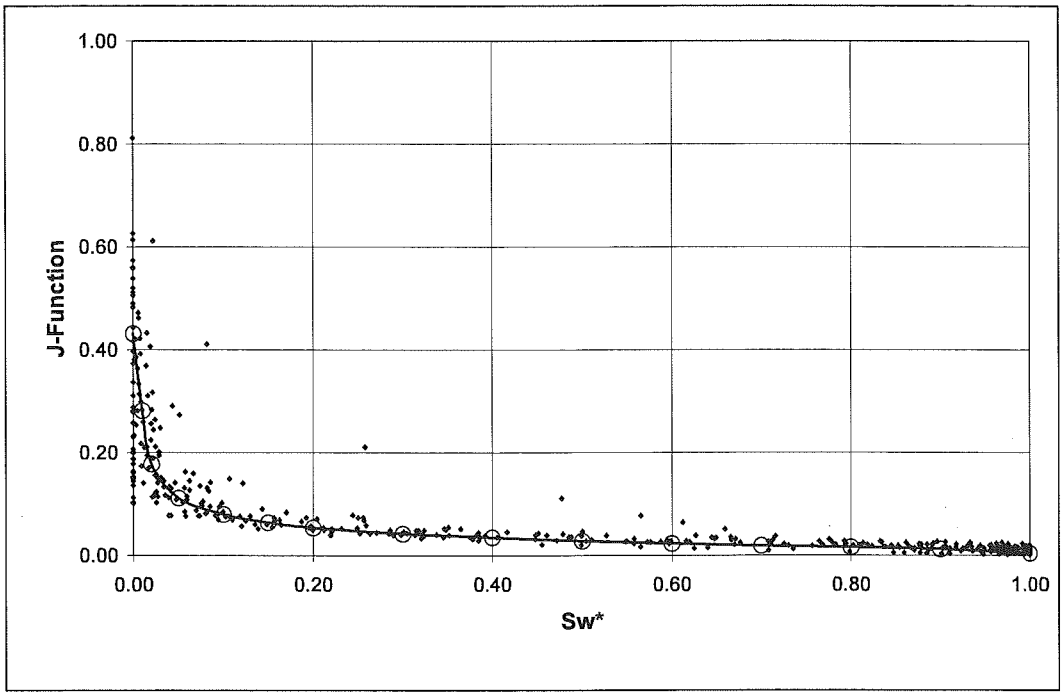

Fig. 5.10. X-Field J-Function vs. induced water saturation graph

Table 5.5. J-S_w* values read from J-Function

J	Sw*
0.4320	0.00
0.2820	0.01
0.1780	0.02
0.1120	0.05
0.0800	0.10
0.0640	0.15
0.0540	0.20
0.0420	0.30
0.0350	0.40
0.0280	0.50
0.0230	0.60
0.0190	0.70
0.0160	0.80
0.0120	0.90
0.0040	1.00

Moreover, threshold pressure versus porosity graph is shown in Fig. 5.11. Threshold pressure is a function of the interfacial tension between the wetting and nonwetting fluid phases and the pore diameter. A certain threshold pressure is required to commence drainage of the oil or water phase. When the rock is either strongly water wet or strongly oil wet, the threshold pressure, also referred to as the displacement pressure, tends to be greater. In contrast, when the core is having intermediate wettability, the threshold pressure is comparatively lower. Small pore diameters in a rock lead to relatively high threshold pressure. As shown in Fig.11, threshold pressure tends to increase with decreasing porosities.

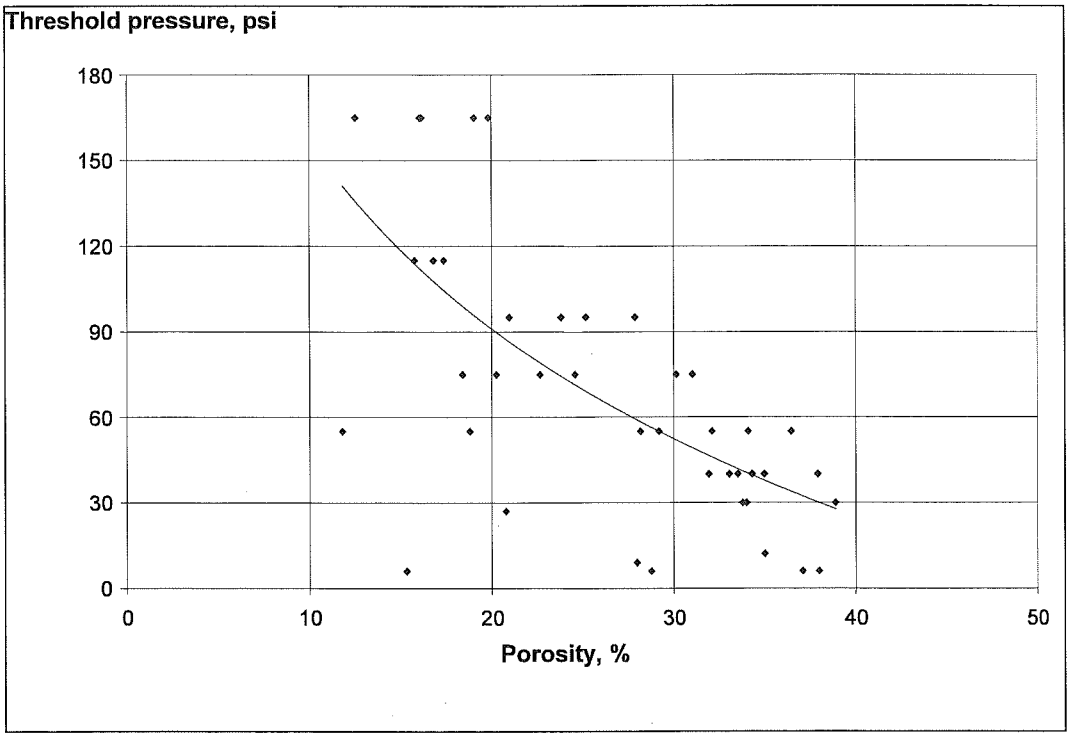

Fig 5.11. X-Field threshold pressure change with porosity

Using the J-Function method, air-mercury capillary pressure models are established for 15 %, 25 % and 35 % porosity values. (Fig. 5.12) (Table 5.6)

Fig. 5.12 can be used to see the reservoir quality at different porosity values. With increasing porosity irreducible water saturation value becomes smaller as expected. This means, with increasing porosity amount of the recoverable oil increase. Capillary pressure curve drawn for 15 % porosity can be regard to have a bad reservoir quality. While determining porosity cutoff value this water saturation versus capillary pressure graph can be present for evidence.

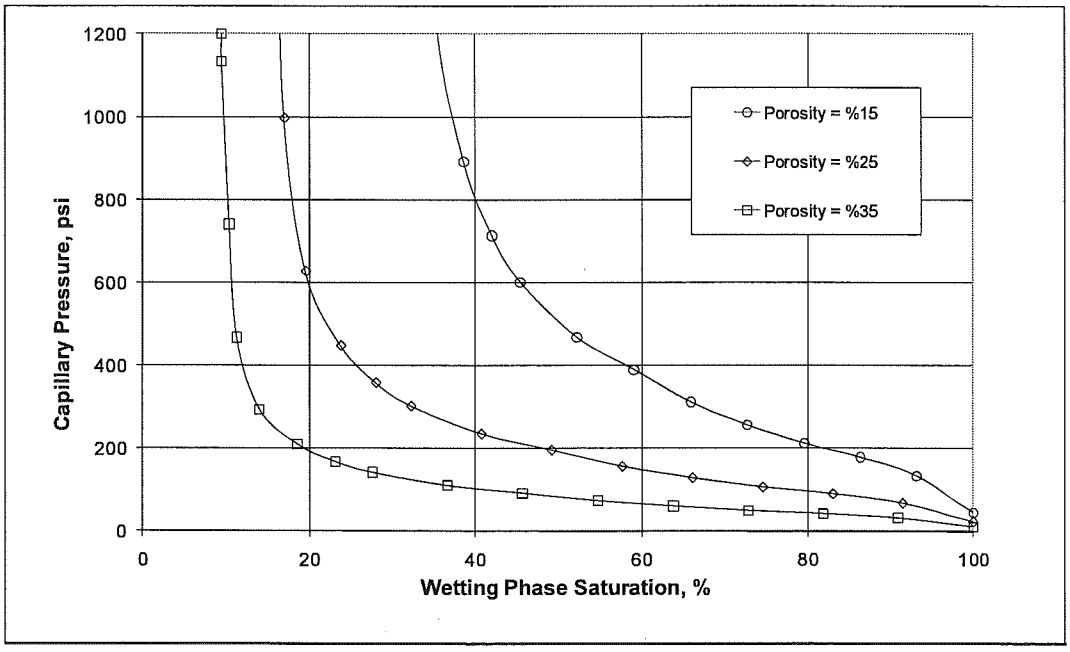

Fig 5.12. X-Field capillary pressure model (drainage) curves

Table 5.6. X-Field data of capillary pressure models

Sw(15%)	Pc(15%)	Sw(25%)	Pc(25%)	Sw(35%)	Pc(35%)
31.80	4814.34	15.30	2418.03	9.50	1200.00
32.48	3142.70	16.15	1578.44	9.50	1133.77
33.16	1983.69	16.99	996.32	10.41	740.10
35.21	1248.16	19.54	626.90	11.31	467.16
38.62	891.54	23.77	447.78	14.03	293.94
42.03	713.24	28.01	358.23	18.55	209.96
45.44	601.79	32.24	302.25	23.08	167.97
52.26	468.06	40.71	235.09	27.60	141.72
59.08	390.05	49.18	195.91	36.65	110.23
65.90	312.04	57.65	156.72	45.70	91.86
72.72	256.32	66.12	128.74	54.75	73.49
79.54	211.74	74.59	106.35	63.80	60.36
86.36	178.31	83.06	89.56	72.85	49.86
93.18	133.73	91.53	67.17	81.90	41.99
100.00	44.58	100.00	22.39	90.95	31.49
				100.00	10.50

5.2. PVT ANALYSIS

Studies about the PVT data estimation in case of lacking of laboratory measurement data are shown in figures and tables. Correlations for density, bubble point pressure, gas solubility, oil formation volume factor, viscosity, compressibility coefficient, reservoir water properties, and flow assurance potential were evaluated and results of the calculations are shown in figures. Then C_{7+} properties are characterized in order to use in equations of state calculations. Finally, equations of state were correlated with real test data.

5.2.1. Constant Mass ExpansionTest

Consant mass expansion test have been done before starting this study. Results show that the bubble point pressure of the X-Field is 105 psi at

reservoir temperature of 125 °F. API gravity was found as 16.5°. Moreover oil density at bubble point pressure was found as 0.9237 g/cc and isothermal oil compressibility at 2000 psi was found as 5.2252×10^{-6} $psig^{-1}$. Relative volume and pressure relation is shown in Table F.1.

5.2.2. Zero-Flash Separator Test

Zero-Flash separator test have been done by flashing the oil sample from reservoir conditions to 70 °F temperature and 13.3 psi atmospheric pressure. Gas oil ratio (R_s) was found as 12.2 scf/STB and oil formation volume factor was found as 1.0351. Relation between the gas / oil ratio and pressure can be seen in Table F.3.

5.2.3. Viscosity Test

Results of the oil viscosity measurement at reservoir temperature can be seen at Table F.2. Oil viscosity at bubble point pressure is 138.0 cp.

5.2.4. Compositional Analysis

Oil and gas samples which were flashed out during the zero-flash separator test were injected to oil and gas GC's. Results of both gas, oil and recombination of these gas and oil compositions are given at Table F.4.

5.2.5. PVT Calculations With Limited PVT Data

5.2.5.1. Density

Oil density at bubble point pressure and at reservoir temperature calculations were done by using Katz's and Standing's methods with the help of the data shown below. Results can be seen in Table 5.7.

- $\rho_{ga} = 0.5401 g/cc$, apparent liquid density
- R_s = 12.2 scf / STB
- γ_g = 0.9865
- γ_o = 0.9561
- API = 16.5°
- T_r = 125 °F
- P_b = 105 psi
- $\Delta\rho_p = 0.050 lb/ft^3$, pressure correction factor, from the "density correction for the compressibility of crude oils" chart.
- $\Delta\rho_T = 1.00 lb/ft^3$, isothermal adjustment factor, from the "density correction for isothermal expansion of crude oils" chart.
- $\rho_{sc} = 0.9537 g/cc$ the liquid density at standard conditions (calculated by Katz' correlation)

Table 5.7. Oil density at reservoir temperature and bubble point pressure

	Katz	*Standing*	*Test Data*
ρ_b *(g/cc)*	0.9384	0.9278	0.9237

5.2.5.2. Gas Solubility

Gas solubility calculations were done by using the Standing's, Vasquez-Begg's, Glaso's and Marhoun's correlations with the help of the following data;

- $x = 0.0925$
- $\gamma_g = 0.9865$
- $T_r = 125$ °F
- API = 16.5°
- $\gamma_{gs} = 0.9235$, gas gravity at the reference separator pressure and temperature, $T_{sep} = 70$°F and $P_{sep} = 13.3$ psi.
- $X = 0.1497$
- $\gamma_o = 0.9561$

Results of the gas solubility correlations can be seen in Table 5.8.

Table 5.8. Results of the gas solubility correlations

	Standing	*Vasquez-Beggs*	*Glaso*	*Marhoun*	*Test Data*
Rs @ Pb (scf/STB)	13.68	11.22	16.26	8.64	12.20

5.2.5.3. Bubble Point Pressure

Bubble point pressure calculations were done by using the Standing's, Lasater's, Vasquez-Begg's, Glaso's, Marhoun's and Al-Shammasi's correlations with the help of the following data;

- R_s = 12.2 scf / STB
- γ_g = 0.9865
- γ_o = 0.9561
- T_{sep} = 70 °F
- P_{sep} = 13.3 psi
- T_r = 125 °F
- API = 16.5°
- $a = -0.0925$ *(Standing's correlation)*
- $\gamma_{gas} = 0.04371$, *(Lasater's correlation)*
- $M_o = 573.96 g/mol$ *(Lasater's correlation)*
- $a = -0.3151$ *(Vasquez-Begg's correlation)*
- $\gamma_{gs} = 0.8739$ *(Vasquez-Begg's correlation)*

- $A = 1.1165$ *(Glaso's correlation)*

Results of the gas solubility correlations can be seen in Table 5.9.

Table 5.9. Results of the bubble point pressure correlations

	Standing	*Lasater*	*Vasquez Beggs*	*Glaso*	*Marhoun*	*Al Shammasi*	*Test Data*
P_b *(psi)*	93.14	93.35	119.26	70.75	134.36	142.35	105

5.2.5.4. Oil Formation Volume Factor

Oil formation volume factor calculations were done by using the Standing's, Vasquez-Beggs's, Glaso's, Marhoun's correlations and material balance equation with the help of the following data;

- API = 16.5°
- R_s = 12.2 scf / STB
- γ_g = 0.9865
- γ_o = 0.9561
- T_r = 125 °F
- $\gamma_{gs} = 0.8739$ *(Vasquez-Beggs correlation)*
- P_{sep} = 13.3 psi *(Vasquez-Beggs correlation)*
- $A = -1.6441$ *(Glaso's correlation)*

- $B_{ob}^{*} = 133.4027$ *(Glaso's correlation)*
- $F = 6.7304$ *(Marhoun's correlation)*

Results of the oil formation volume factor correlations can be seen in Table 5.10.

Table 5.10. Results of the oil formation volume factor correlations

	Standing	*Vasquez - Beggs*	*Glaso*	*Marhoun*	*Material Balance*	*Test Data*
B_o @ P_b	1.0329	1.0268	1.0239	1.0115	1.0023	1.0351

5.2.5.5. Isothermal Compressibility Coefficient

Undersaturated oil compressibility calculations were done by using the Trube's and Standing's correlations with the help of the data shown below. Results of these correlations can be seen in Table 5.11.

- $(\rho_o)_T = 0.7390$
- $(\rho_o)_{60} = 0.7961$
- $(P_b)_{60} = 91.8253$
- $T_{pc} = 1250°R$
- $P_{pc} = 120\,psia$
- P_b = 105 psi

- ρ_{ob} = 0.9310 g/cc

Table 5.11. Results of the isothermal oil compressibility coefficient correlations

	Trube	*Standing*	*Test Data*
Co @ 2000 psi ($psig^{-1}$)	7.5×10^{-6}	1.1127×10^{-5}	5.2252×10^{-6}

5.2.5.6. Crude Oil Viscosity

Dead oil viscosity calculations were done by using the Beal's, Beggs and Robinson's and Glaso's correlations with the help of the data shown below. Results can be seen in Table 5.12.

- API = 16.5°
- Tr = 125 °F
- $A = 8.4110$ *(Beal's correlation)*
- $A = 499.5799$ *(Beggs and Robinson's correlation)*
- $A = -14.8516$ *(Glaso's correlation)*

Table 5.12. Results of the dead oil viscosity correlations

	Beal	*Beggs and Robinson*	*Glaso*	*Test Data*
μ_{od} *(cp)*	130.24	64.96	101.40	184.40

Bubble Point oil viscosity calculations were done by using the Chew-Connaly's, Beggs and Robinson's and Abu-Khamsim and Al-Marhoun's correlations with the help of the data shown below. Results can be seen in Table 5.13.

- $\mu_{od} = 184.40cp$
- R_s = 12.2 scf / STB
- $\rho_{ob} = 0.9237cp$
- $a = -0.0090$ *(Chew-Connaly's correlation)*
- $b = 0.9766$ *(Chew-Connaly's correlation)*
- $c = -0.0011$ *(Chew-Connaly's correlation)*
- $d = -0.0134$ *(Chew-Connaly's correlation)*
- $e = -0.0456$ *(Chew-Connaly's correlation)*
- $a = 0.9424$ *(Beggs and Robinson's correlation)*
- $b = 0.9741$ *(Beggs and Robinson's correlation)*

Table 5.13. Results of the bubble point pressure oil viscosity correlations

	Chew Connaly	*Beggs and Robinson*	*Abu Khamsim Al-Marhoun*	*Test Data*
μ_{ob} *(cp)*	159.83	151.82	178.54	138.00

It should be noted that the gas solubility of X-Field reservoir oil is out of the range of the Chew-Connaly correlation (Rs< 51scf/STB) and Beggs and Robinson correlation.

Undersaturated oil viscosity calculations were done by using the Beal's, Khan's and Vasquez-Beggs's correlations with the help of the data shown below. Results can be seen in Table 5.14 and Fig 5.13.

- $\mu_{ob} = 138.00\, cp$
- P_b = 105 psi

Table 5.14 Results of the undersaturated oil viscosity correlations

	Viscosity, cp			
Pressure (psi)	*Beal*	*Khan*	*Vasquez Beggs*	*Test Data*
3000	324.10	141.89	336.93	207.40
2500	291.96	141.21	280.99	198.40
2000	259.82	140.53	234.57	183.40
1500	227.67	139.86	196.98	172.20
1000	195.53	139.19	167.70	161.90
500	163.39	138.52	146.83	151.60
250	147.32	138.19	140.15	144.00
105	138.00	138.00	138.00	138.00

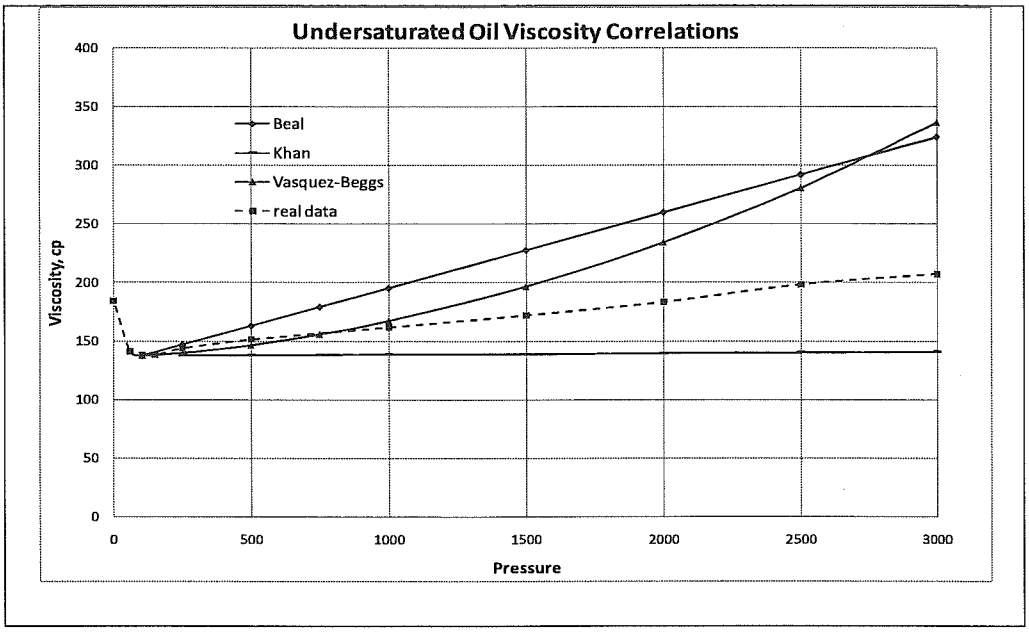

Fig 5.13. Viscosity – Beal, Khan and Vasquez-Beggs correlations and measured data.

5.2.5.7. Interfacial Tension

The modified form of the Katz et al. and Sugden correlation for mixtures gives the interfacial tension as *34.36* dynes/cm with the measured compositional data of both gas and oil phase. Calculation steps of the interfacial tension correlation can be seen in Table 5.15.

Table 5.15. Calculation steps of the interfacial tension correlation.

Comp.	Xi	Yi	Mi	xiMi	yiMi	Pch	Axi	Byi	Pch(Axi-Byi)
C_1	0.00	76.37	16.04	0.00	12.25	106.80	0.00E+00	8.92E-04	-9.53E-02
C_2	0.22	1.82	30.07	0.07	0.55	139.06	1.21E-05	2.12E-05	-1.28E-03
C_3	0.28	0.73	44.10	0.12	0.32	171.32	1.53E-05	8.52E-06	1.17E-03
nC_4	0.57	0.30	58.12	0.33	0.18	203.59	3.12E-05	3.55E-06	5.64E-03
nC_5	1.30	0.17	72.15	0.94	0.12	235.85	7.13E-05	1.93E-06	1.64E-02
C_6	5.77	0.14	84.70	4.89	0.12	264.71	3.16E-04	1.59E-06	8.33E-02
C_{7+}	90.30	0.00	181.39	163.80	0.00	487.10	4.95E-03	0.00E+00	2.41E+00
								Sum Pch(Axi-Byi)	2.42

5.2.5.8. Water Viscosity

Water viscosity at reservoir temperature was calculated with the help of Meehan's and Brill and Beggs's correlations with the help of the following data;

- A = 0.0998
- B = 86.8174
- Y = 130,000 ppm.
- T_{res} = 125 °F

Results can be seen in Table 5.16.

Table 5.16. Results of the water viscosity correlations

	Meehan	*Brill and Beggs*
μ_w @ $T_{res.}(cp)$	0.7944	0.5850

Moreover, water viscosity at reservoir temperature and reservoir pressure was calculated with the help of the McCain et al.'s correlation. Data used in these calculations are listed below;

- A = 109.5684
- B = -1.1182

According the McCain et al.'s correlation water visosity at reservoir temperature and reservoir pressure was calculated as 0.5457 cp.

5.2.5.9. Water Isothermal Compressibility

Water isothermal compressibility at 2000 psi was calculated by Brill and Beggs' correlation.

- $c_w = 2.98 \times 10^{-6}\ psi^{-1}$

where ,

- $C_1 = 3.8566$
- $C_2 = -0.009566$
- $C_3 = 3.7507 \times 10^{-5}$
- $T_{res} = 125\ °F$

5.2.6. Flow Assurance Potential

For the X field both De Boer plot and Asphaltene Stability Index stated that there will be no problem about the asphaltene deposition. However, enhanced oil recovery studies may increase the risk of asphaltene

deposition. If any thermal recovery processes or any gas injection processes are applied, it should be noted that, laboratory tests should be done to specify the Lower and Upper Asphaltene Onset Pressure values.

5.2.7. C_{7+} Characterization

5.2.7.1. Riazi and Daubert

With the help of Riazi and Daubert's correlation T_c, P_c, V_c and T_b parameters of C_{7+} fraction are calculated as;

- T_c = 1335.806 °R,
- P_c = 340.686 psia,
- V_c = 0.0593 ft^3/lb,
- T_b = 966.643 °R.

where,

- γ_{C7+} = 0.9561
- M_{C7+} = 181.39

5.2.7.2. Edmister's Correlation

Edmister correlation for accentric factor estimation gave the following result with the help of the Riazi – Daubert correlation;

- $\omega = 0.5319$

where,

- T_c, Tb, °R

- P_c, psia.

5.2.8. Lumping (Pseudoization)

5.2.8.1. Whitson's Method

By using the Whitson's Method, components can be grouped as

1. Group $C_7 - C_9$
2. Group $C_{10} - C_{13}$
3. Group $C_{14} - C_{17}$
4. Group $C_{18} - C_{25}$
5. Group $C_{25} - C_{30+}$

where,

- $N_g = 5$,
- *Int = integer*
- $M_{C7+} = 181.39$

5.2.8.2. Lee's Mixing Rules

Properties of the groups divided with the help of Whitson's lumping method are shown in the Table 5.17.

Table 5.17. Results of the Whitson's lumping method

		ML	*γ L*	*VL*	*PcL*	*TcL*	*ω L*
Group 1	C_7 - C_9	96.41	0.7506	0.0627	416.11	1038.54	0.3155
Group2	C_{10} - C_{13}	134.82	0.7946	0.0629	325.85	1167.09	0.4207
Group 3	C_{14} - C_{17}	194.01	0.8375	0.0633	252.45	1308.76	0.5567
Group 4	C_{18} - C_{25}	274.21	0.8711	0.0639	201.70	1437.94	0.7132
Group 5	C_{26} - C_{30+}	359.78	0.8976	0.0645	166.61	1553.39	0.8771

5.2.8.3. Behrens and Sandler's Lumping Method

Results of Behrens and Sandler's method are shown in Table 5.18.

Table 5.18. Results of Behrens and Sandler's lumping method

Group	C_n	*Z,*	T_b	*γ*	*M*	T_c	P_c	*Ω*
n_1	9.79	0.62	782	0.7791	131	1119	358	0.3772
n_2	22.58	0.25	1158	0.8789	307	1472	190	0.7575

The integration roots are found from "Behrens and Sandler Roots and Weights for Two-Point Integration" chart.

- r_1 = 0.39024
- r_2 = 1.90420
- ω_1 = 0.71364
- ω_2 = 0.28636

5.2.9. Equations of State

Equation of state calculations were done over the reservoir fluid composition by using the PVT-Sim software and results of the bubble point pressure, relative volume and viscosity estimations were compared with the measued PVT data.

Initially, results of the Riazi and Daubert's correlation for the characterization of the C_{7+} compounds were given as an input for the PVT-Sim software. Moreover, Behrens and Sandler's and Lee's lumping methods were tested with the measured data. Finally, reservoir fluid composition up to C_{36+} compound was directly used in equation of state calculations.

Soave - Redlich – Kwong and Peng – Robinson equations of state calculations were applied over both expressions. Moreover, in order to see its effect, Peneloux correction factor was also used in the calculations.

Main difference of these calculations is the critical properties of the C_{7+} components. Different methods to make the PVT data assumptions close to measured PVT data, were tried to find better results.

5.2.9.1. Equations of State calculations for Riazi and Daubert's correlation

For making cubic equation state calculations on the reservoir fluid composition, the critical temperature, the critical pressure and the acentric factor parameters of C_{7+} component were calculated with the help of Riazi

and Daubert's and Edmister's correlations. C_{7+} characterization comprises representing the heptane plus fraction of hydrocarbons as a convenient number of pseudocomponent and to find the needed equation of state parameters for each of these pseudocomponents.

Soave – Redlich – Kwong equation of state gave an estimation of 193.21 psi for the bubble point pressure whereas Peng - Robinson equation of state gave 180.59 psi. Knowing that the measured bubble point pressure is 105 psi, results can not be seen as satisfied.

On the other hand, relative volume estimations are very close to the measured PVT data for the pressure values above the bubble point pressure. Results can be seen on Table F.5 and Fig 5.14.

Lastly, viscosity results of the equations of state calculations are shown in Table F.6 and Fig 5.15. It should also be noted that Peneloux et al.'s equation of state with volume correction did not change the results of calculations a lot.

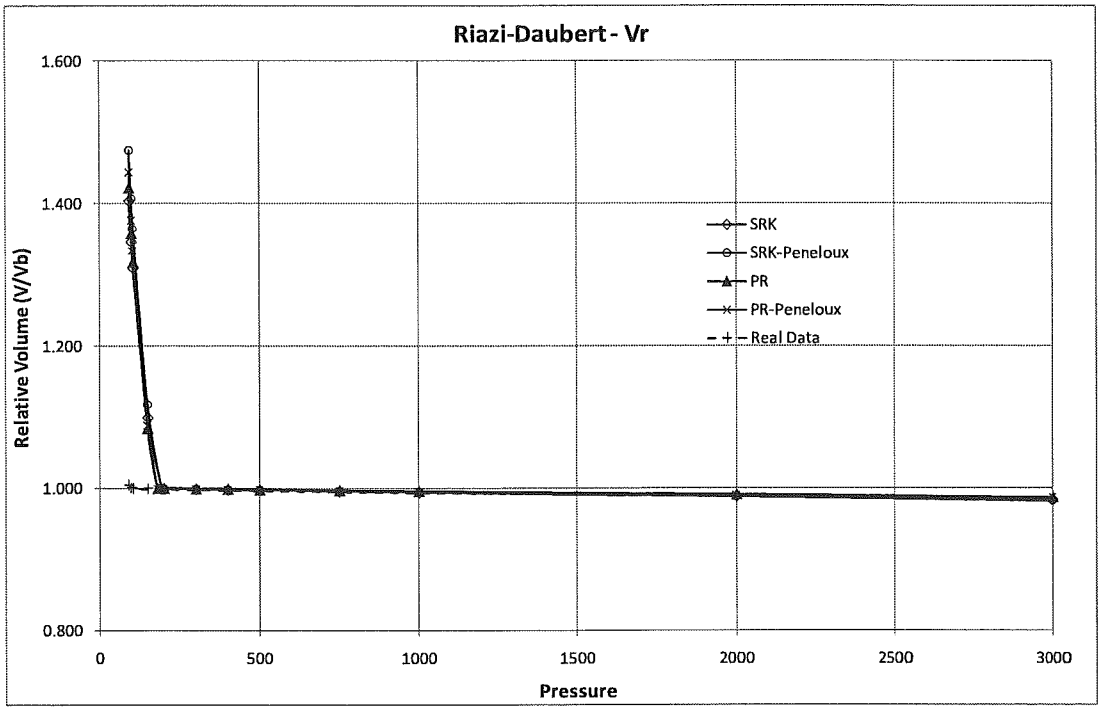

Fig 5.14. Relative volume vs. pressure – EOS results for Riazi and Daubert's correlation.

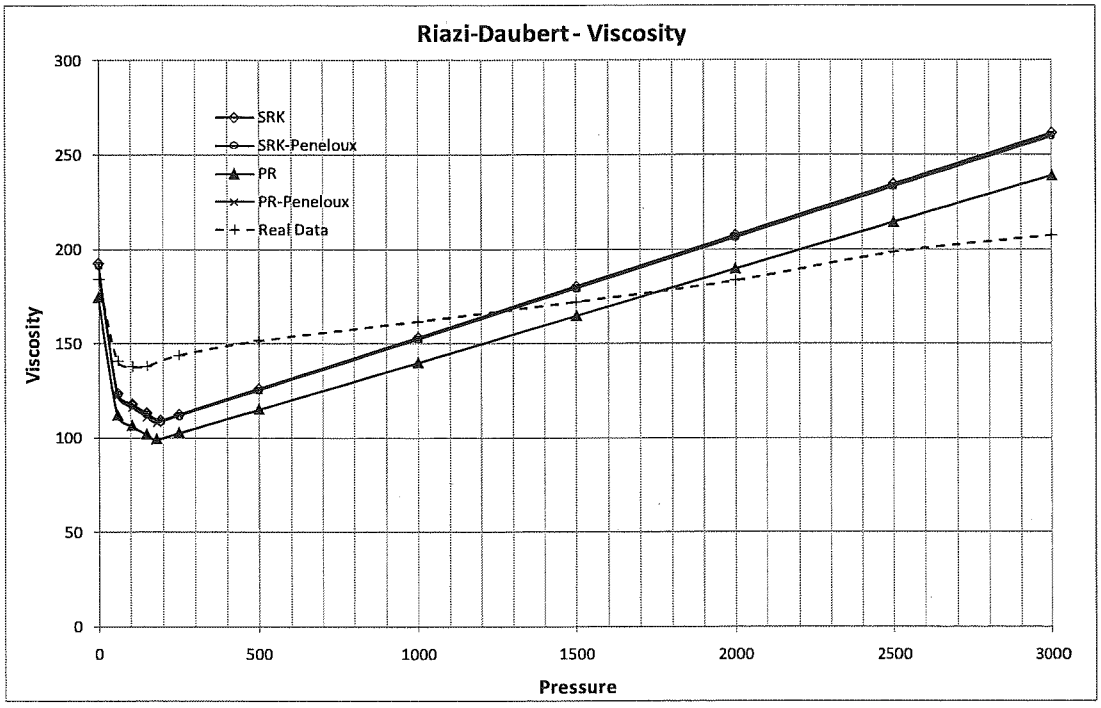

Fig 5.15. Viscosity vs. pressure – EOS results for Riazi and Daubert's correlation.

5.2.9.2. Equations of State calculations for Behrens and Sandler correlation

In order to increase the efficiency of equations of state calculations number of the components of the reservoir fluid composition was tried to be minimized by lumping methods.

In order to replace C_7 to C_{36} compounds of the reservoir fluid composition, two pseudo components, found with the help of the Behrens and Sandler's lumping method, were used. Critical properties which were shown in the previous chapter were used in the equations of state calculations.

Soave – Redlich – Kwong equation of state gave an estimation of 130.26 psi for the bubble point pressure whereas Peng - Robinson equation of state gave 126.63 psi. The measured bubble point pressure is 105 psi.

On the other hand, relative volume estimations are very close to the measured PVT data for the pressure values above the bubble point pressure. Results can be seen on Table F.7 and Fig 5.16.

Lastly, viscosity results of the equations of state calculations are shown in Table F.8 and Fig 5.17. It should also be noted that Peneloux et al.'s equation of state with volume correction did not change the results of calculations a lot.

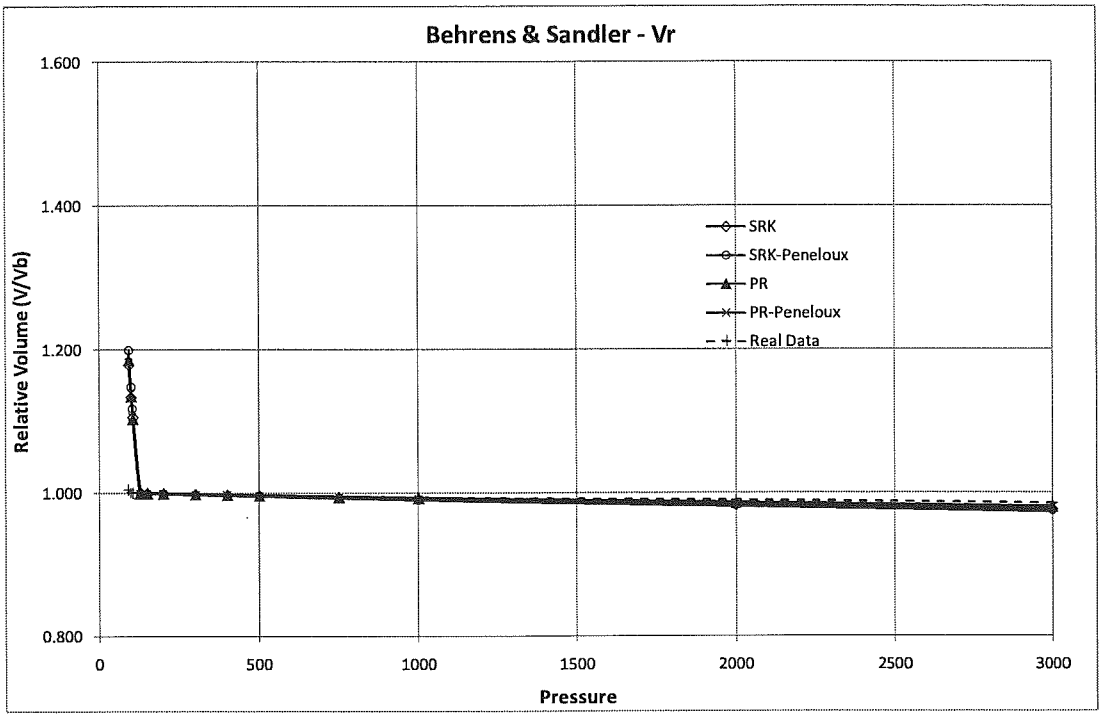

Fig 5.16. Relative volume vs. pressure – EOS results for Behrens and Sandler's correlation.

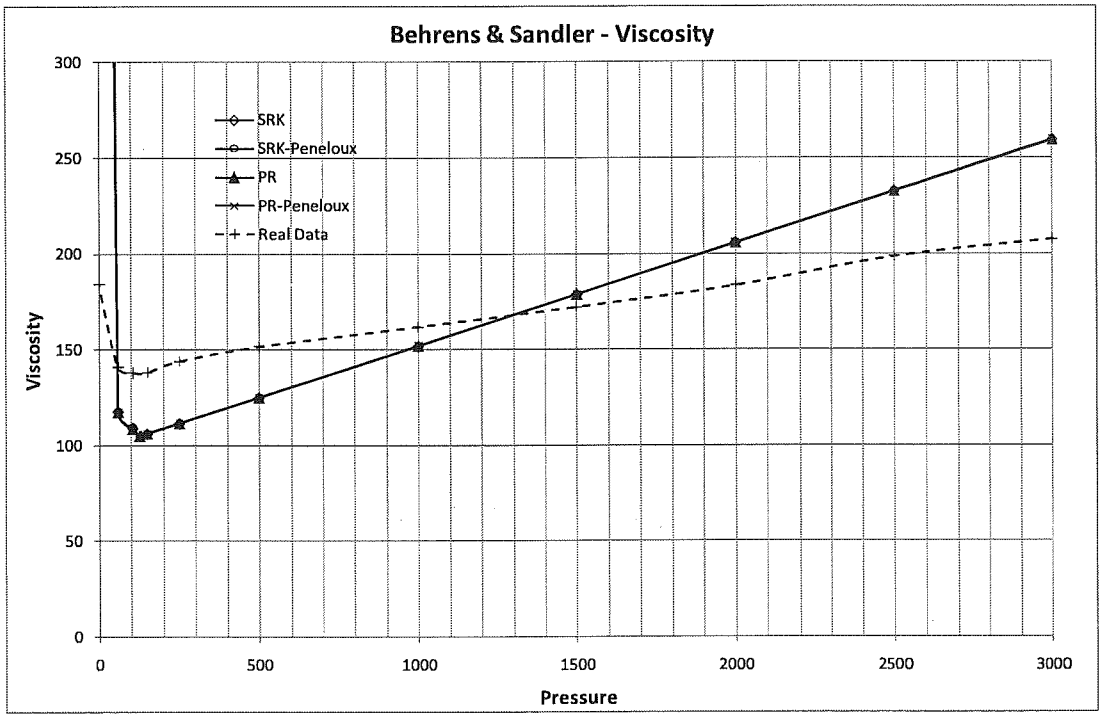

Fig 5.17. Viscosity vs. pressure – EOS results for Behrens and Sandler's correlation.

5.2.9.3. Equations of State calculations for Lee's lumping method

Critical properties of five pseudo components which had already been found with the help of the Whitson and Lee's lumping method, were used in the equations of state calculations.

Soave – Redlich – Kwong equation of state gave an estimation of 130.69 psi for the bubble point pressure whereas Peng - Robinson equation of state gave 126.92 psi.

Relative volume estimations are again very close to the measured PVT data for the pressure values above the bubble point pressure. Results can be seen on Table B.9 and Fig 5.18.

Viscosity results of the equations of state calculations are shown in Table F.10 and Fig 5.19. It should also be noted that Peneloux et al.'s equation of state with volume correction did not change the results of calculations a lot.

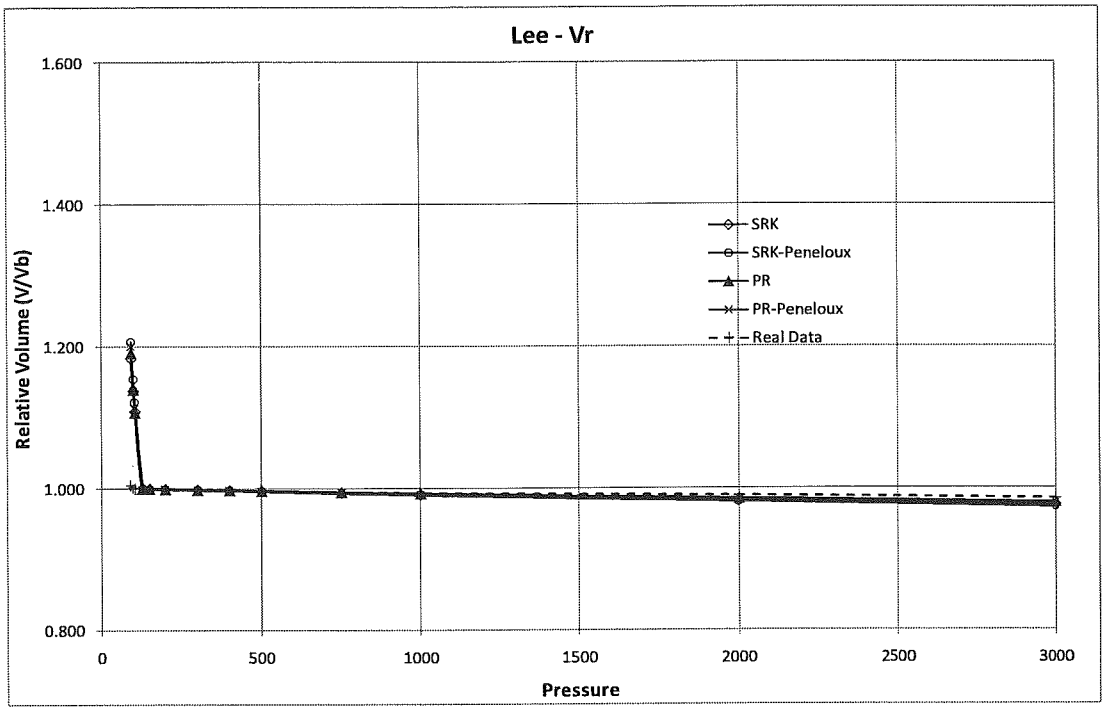

Fig 5.18. Relative volume vs. pressure – EOS results for Lee's lumping method.

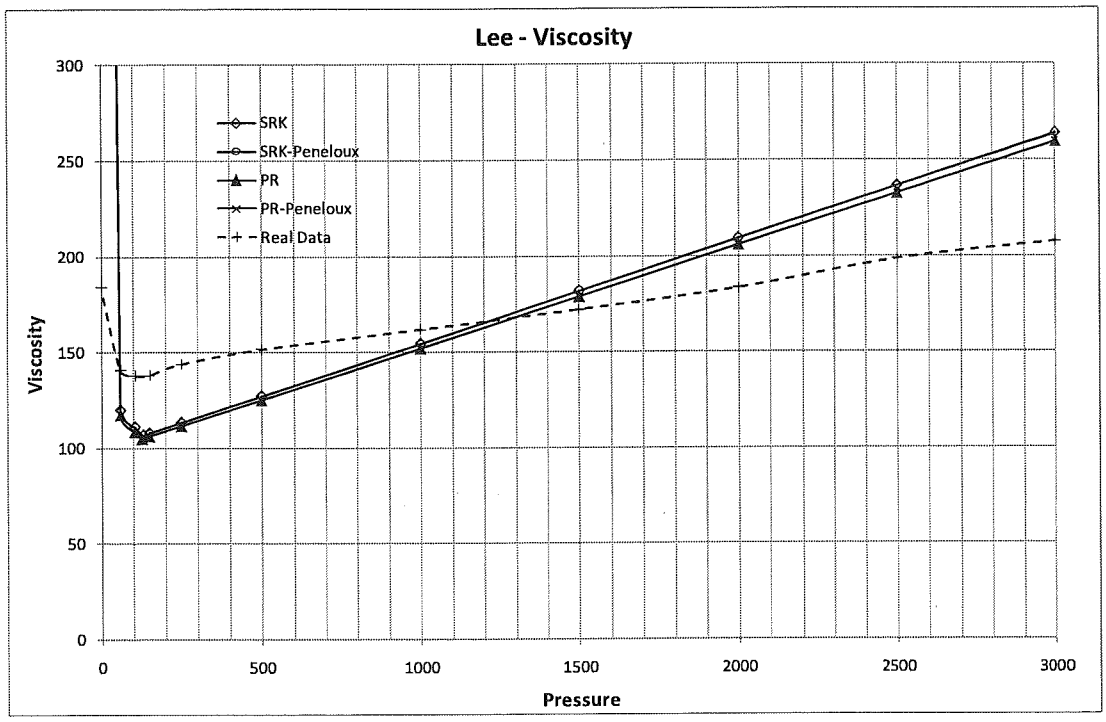

Fig 5.19. Viscosity vs. pressure – EOS results for Lee's lumping method.

5.2.9.4. Equations of State calculations with the original composition of the oil sample

Soave – Redlich – Kwong equation of state gave an estimation of 155.06 psi for the bubble point pressure whereas Peng - Robinson equation of state gave 152.16 psi.

Relative volume estimations can be seen on Table F.11 and Fig. 5.20. Results are again close to the measured PVT data for the pressure values above the bubble point pressure. Viscosity results of the equations of state calculations are shown in Table B.12 and Fig 5.21.

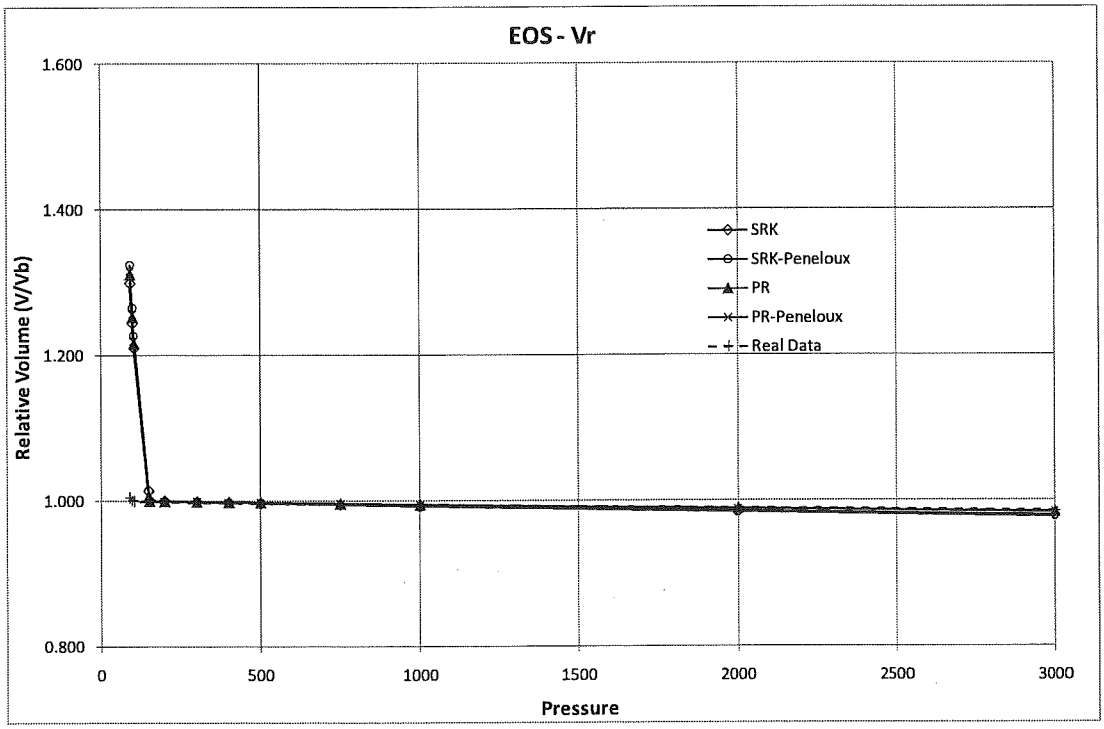

Fig 5.20. Relative volume vs. pressure – EOS results for reservoir fluid composition.

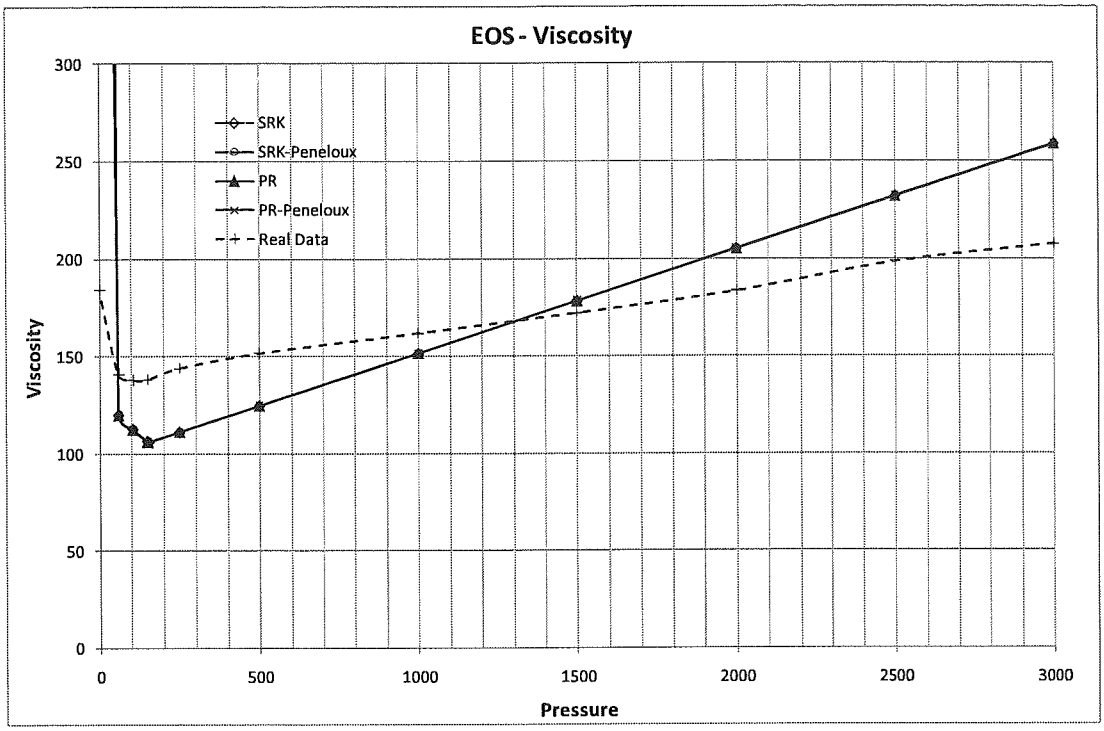

Fig 5.21. Viscosity vs. pressure – EOS results for reservoir fluid composition.

CHAPTER 6

CONCLUSIONS

An integrated reservoir management study should be based on reservoir simulation studies which require representative input data for reservoir rock and fluid properties in order to find the storage and flow capacities of reservoir rocks and the production performance. To identify petroleum reservoir rock and fluid properties, laboratory measurement data can well be employed in core analysis and PVT analysis.

In this regard, the main objective of this study was to elaborate a road map from laboratory measurements to the input data file of reservoir simulation by using the reservoir rock and fluid properties of a selected oil field of Turkey (the X-Field). To be more concrete, via using various approaches to make a probabilistic approach for the estimation of unknown parameters, raw data of reservoir rock and fluid properties of the X-Field will be interpreted and prepared in a way that they will be used as input data of a simulator.

To mention the findings of this study; firstly it should be mentioned that the X-Field, chosen for this study, is a carbonate reservoir. Laboratory measurement data were evaluated and then, permeability and relative permeability estimations were studied. Average of porosity, permeability and relative permeability properties were calculated and relative permeability and capillary pressure models of the X-Field were developed. Results of Core Analysis were illustrated graphically in Chapter 5.

Average of the porosity values was found as 23.45 % wheras the average of the permeability values is 1.69 md. Also, average grain density value was found as 2.79 g/cc. In order to determine the variation of porosity throughout the reservoir, porosity distribution chart was established. In the X-Field, the porosity distribution can be said as normal distribution. Moreover, porosity – permeability cross plot on a semilog scale was drawn. Trendline of the cross-plot shows that at 20 percent of porosity come along nearly 1 md permeability value. Then, average of nearly 5 % decrease in porosity value was observed in porosity and permeability measurements under overburden pressure measurements, whereas the average permeability decrease is approximately 15 %. After, relative permeability models were developed for 0.15, 0.25 and 0.35 porosity reservoir rocks. These models show that the 0.15 porosity reservoir rock have a bad reservoir quality. Finally, capillary pressure drainage and imbibition measurements were done and utilising the J-Function method, air-mercury capillary pressure models were established for 15 %, 25 % and 35 % porosity values. Same as the relative permeability results, capillary pressure curve drawn for 15% porosity can be regarded to have a bad reservoir quality. While determining porosity cutoff value, these relative permeability and capillary pressure models should be taken into consideration.

Studies about the PVT data estimation in case of lacking of laboratory measurement data were denoted in figures and tables. Correlations for density, bubble point pressure, gas solubility, oil formation volume factor, viscosity, compressibility coefficient, reservoir water properties, and flow assurance potential were evaluated and results of the calculations were shown in figures. Then C_{7+} properties were characterized in order to use in equations of state calculations. Finally, equations of state were correlated with real test data. It was noted that heavy oil properties estimations are not easy to make. This fact makes the limited PVT data calculations, C_{7+}

characterization correlations, lumping methods and compositional equations of state calculations difficult.

Correlations to use in the lack of laboratory data, C_{7+} characterization and equations of state calculations were introduced in the PVT analysis section. A number of correlations were tested to use in the lack of reservoir oil and water properties and equations of state were applied with the oil and gas compositional analysis. Results of the density at bubble point pressure and oil formation volume factor correlations are very close to the measured data. Standing's correlation for the density at bubble point pressure estimation and both Standing's and Vasquez-Beggs' correlations for oil formation volume factor gives less than 1% of error. Vasquez-Beggs correlations for gas solubility and bubble point pressure data give better results. Trube's correlation gives relatively good result for isothermal oil compressibility coefficient, whereas Beal's method gives better for the dead oil viscosity.

Results of the C_{7+} characterization and equations of state calculations are shown in Chapter 5. Equations of state calculations were applied over compositions of the original oil, calculated from C_{7+} characterization methods and lumping methods. Relative volume and viscosity estimations were done with the help of equations of state. Results of the relative volume calculations for each composition are close to the measured PVT data. Viscosity results, on the other hand, are good in undersaturated oil viscosity calculations. However, the only satisfactory result for the dead oil viscosity was calculated with the composition obtained from Riazi and Daubert's C_{7+} characterization method.

REFERENCES

1. Oilfield Review, http://www.slb.com/media/services/resources/oilfieldreview/ors00/sum00/p30_41.pdf, last visited on November 2009.

2. Danesh, A.," PVT and Phase Behaviour of Petroleum Reservoir Fluids," Elsevier Science B. V., Amsterdam, The Netherlands, 1998, 301-326

3. Dandekar, A. Y.,"Petroleum Reservoir Rock and Fluid Properties," CRC Press, Taylor & Francis Group, Boca Raton, FL, 2006, 13-26.

4. Monicard, R. P.,"Properties of Reservoir Rocks: Core Analysis." Institut Francais du Petrole Publications, Editions Technip, Paris, 1980, 43-47.

5. Klinkenberg, L. J.:"The Permeability of Porous Media to Liquids and Gases", Drilling and Production Practices, American Petroleum Institute, 1941.

6. Anderson, W. G.: "Wettability Literature Survey-Part 5: The Effects of Wettability on Relative Permeability", SPE 16323, J. Pet. Tech. (November 1987), 1453-1468.

7. Honarpour, M. M., Koederitz, L. F., and Harvey, A. H.,"Relative Permeability of Petroleum Reservoirs," CRC Press, INC., Boca Raton, FL, 1986, 15-41.

8. Crotti, M. A., Inlab S. A.,Rosbaco J. A.: "The Influence of Flow Direction and Heterogeneties. Dependence of End Point Saturations on Displacement Mechanisms." SPE/DOE 11th Symposium on Improved Oil Recovery, Tulsa OK, 19 -22 April 1998, pp. 39-45.

9. Karabakal, U.: "Determination of Wettability and Its Effect on Waterflood Performance In Limestone Medium", Unpublished Master Thesis, METU, May, 2000.

10. Chang, Y. C., Mohanty, K. K., Huang, D. D., Honarpour, M. M.: "The impact of Wettability and Core-Scale Heterogeneities on Relative Permeability", Journal of Petroleum Science and Engineering 18, 1997, 1-19.

11. Johnson, E. F., Bossler, D. P. and Naumann, V. O.:"Calculation of Relative Permeability from Displacement Experiment", J.Pet. Tech (Jan.1959), 61-63, Trans.AIME(1959), Vol.216.

12. Dandekar, A. Y.,"Petroleum Reservoir Rock and Fluid Properties," CRC Press, Taylor & Francis Group, Boca Raton, FL, 2006, 185-217.

13. Schramm, L. L.;"Emulsions, Foams, and Suspensions – Fundamentals and Applications," Wiley-VCH Verlag GmbH & Co. KgaA, Weinheim, 2005, 53-76

14. Bradley, H. B., et al.,"Petroleum Engineering Handbook," SPE, 3rd printing, Richardson, TX., USA, 1-29,1992.

15. LeRoy, L. W., LeRoy, D. O.;" Subsurface Geology," Core Laboratories Inc., 1977.

16. Washburn, E. W.,"Note on a Method of Determining the Distribution of Pore Sizes in a Porous Material," Proceedings of the National Academy of Science, v. 7, p. 115-116, 1921.

17. Leverett, M. C.;"Capillary Behaviour in Porous Solids", Trans.AIME, Vol.142, 151-169, 1941.

18. Carr, N. L., Kobayashi, R., and Burrows, D. B., 1954. Viscosity of Hydrocarbon Gases under Pressure. Trans. AIME, 201: 264-272.

19. Ahmed, T.;"Equations of State and PVT Analysis – Applications for Improved Reservoir Modeling" Gulf Publishing Company, Houston, TX, 2007,181-321.

20. Becker, J. R.,"Crude Oil, Waxes, Emulsions and Asphaltenes." Tulsa: Penn Well Publishing Company, 1997.

21. Mullins, O. C., et al.,"Asphaltenes, Heavy oils and Petroleomics." Springer Street, New York: Springer Science+Busines Media, LLC, 2007.

22. De Boer, R., Leeriooyer, K., Eigner, M., and van Bergen, A.: "Screening of Crude Oils for Asphaltene Precipitation: Theory, Practice, and the Selection of Inhibitors," SPE, Feb, 1995.

23. Çalışgan, H., Susuz, O.: "Laboratory Study of Asphaltene Deposition by Solid Detection System", presented in 17th International Petroleum and Natural Gas Congress and Exhibition of Turkey, Ankara, May 13-15, 2009.

24. Pedersen, K. S., Christensen, P. L.,"Phase Behaviour of Petroleum Reservoir Fluids" CRC Press, Taylor & Francis Group, Boca Raton, FL, 2007, 185-217, 13-281.

25. Katz, D., et al.,"Drilling and Production Practice", American Petroleum Institute, Dallas, 1942.

26. Standing, M. B.,"Volumetric and Phase Behaviour of Oil Field Hydrocarbon Systems," Society of Petroleum Engineers, 9th ed.,Dallas, 1981.

27. Standing, M. B.,"A Pressure-Volume-Temperature Correlation for Mixtures of California Oils and Gases." Drilling and Production Practice, API, 275-287, 1947.

28. Vasquez, M., and Beggs, H. D.," Correlations for Fluid Physical Property Prediction." Journal of Petroleum Technology, 968-970, June, 1980.

29. Glaso, O.,"Generalized Pressure-Volume-Temperature Correlations", Journal of Petroleum Technology, 785-795, May 1980.

30. Marhoun, M. A.,"PVT Correlation for Middle East Crude Oils." Journal of Petroleum Technology 650-665, May 1988.

31. Lasater, J. A.,"Bubble-Point Pressure Correlation." Transactions of the AIME 213, 379-381, 1958.

32. Cragoe, C.,"Thermodynamic Properties of Petroleum Products." Washington DC: U.S. Department of Commerce, 1997, p.97.

33. Al Shammasi, A.,"Bubble-Point Pressure and Formation Volume Factor Correlations."SPE Paper 53185, Presented at the SPE Middle East Conference, Bahrain, February 20-23, 1999.

34. Trube, A. S.,"Compressibility of Undersaturated Hydrocarbon Reservoir Fluids."Transactions of the AIME 210, 341-344, 1957.

35. Standing, M. B.,"Petroleum Engineering Data Book." Trondheim: Norwegian Institute of Technology, 1974.

36. Beal, C.,"The Viscosity of Air, Water, Natural Gas, Crude Oils and Its Associated Gases at Oil Field Temperatures and Pressures." Transactions of AIME 165, 94-112, 1946.

37. Beggs, H. D., and Robinson, J. R.,"Estimating the Viscosity of Crude Oil Systems." Journal of Petroleum Technology, 1140-1141, September 1975.

38. Chew, J., Connally,Jr., C. A.,"A Viscosity Correlation for Gas-Saturated Crude Oils."Transactions of the AIME 216, 23-25, 1959.

39. Abu-Khamsin, A., and Al-Marhoun, M.,"Development of a New Correlation for Bubble-Point Viscosity." Arabian Journal of Science and Engineering 16, no.2A, 99, April 1991.

40. Khan, S., et al.,"Handbook of Natural Gas Engineering." New York: McGraw-Hill, 1959.

41. Weinaug, C., and Katz, D. L.,"Surface Tension of Methane-Propane Mixtures." Industrial Engineering and Chemistry 25, 35-43, 1943.

42. Sugden, S.,"The Variation of Surface Tension. VI. The Variation of Surface Tension with Temperature and Some Related Functions." Journal of Chemistry Society 125, 32-39, 1924.

43. Meehan, D. N.,"A Correlation for Water Compressibility." Petroleum Engineer, 125-126, November 1980.

44. Brill, J., and Beggs, D.,"A Study of Two-Phase Flow in Inclined Pipes." Journal of Petroleum Technology, May 1973.

45. McCain, W., et al.,"The Coefficient of Isothermal Compressibility of Black Oils at Pressures below Bubble Point." SPE Formation Evaluation, September 1988.

46. McCain, W.,"The Properties of Petroleum Fluids."Tulsa: Penn Well Publishing Company, 1991.

47. Riazi, M. R. and Daubert, T. E.,"Characterization Parameters for Petroleum Fractions", Ind. Eng. Chem. Res., 1987, Vol.26, No.24, pp. 755-759.

48. Edmister, W. C.,"Applied Hydrocarbon Thermodynamic, Part 4: Compressibility Factor and Equations of State", Petroleum Refiner, April 1958, Vol.37, pp. 173-179.

49. Whitson, C.,"Characterizing Hydrocarbon-Plus Fractions." Society of Petroleum Engineers Journal, 685-696, Dec.1984.

50. Lee, S., et al., "Experimental and Theoretical Studies on the Fluid Properties Required for Simulation of Thermal Processes," SPE Paper 8393 presented at the SPE 54th Annual Technical Conference, Las Vegas, NV, Sep. 23–26, 1979.

51. Behrens, R., and Sandler, S., "The Use of Semi-Continuous Description to Model the C_{7+} Fraction in Equation of State Calculation," SPE/DOE Paper 14925 presented at the 5th Annual Symposium on EOR, Tulsa, OK, April 20–23, 1986.

52. Van der Waals, J. D., "On the Continuity of the Liquid and Gaseous State." Ph.D. dissertation, Sigth-off, Leiden, 1873.

53. Redlich, O., and Kwong, J. N. S., "On the Thermodynamics of Solutions. An Equation of State. Fugacities of Gaseous Solutions." Chemical Reviews.44, 233-247, 1949.

54. Soave, G.,"Equilibrium Constants from a Modified Redlich-Kwong Equation of State," Chemical Engineering and Science 27, 1197-1203, 1972.

55. Peng, D., and Robinson, D. B.,"A New Two-Constant Equation of State." Industrial Engineering and Chemistry Fundamentals 15, 59-64, 1976.

56. Peng, D., and Robinson, D. B.,"The Characterization of the Heptanes and Heavier Fractions for the GPA Peng-Robinson Programs, GPA Research Report, RR-28, 1978.

APPENDICES

APPENDIX A

PVT CALCULATIONS WITH LIMITED PVT DATA

A.1. Density Correlations

Both Katz and Standing proposed correlations with the help of gas gravity, oil gravity, and gas solubility parameters for density determination of hydrocarbon liquid mixtures at reservoir pressure and temparature.

1) Katz's Method [25]

The liquid density at standard conditions;

- $$\rho_{sc} = \frac{350.376\gamma_o + \left(\frac{R_s\gamma_g}{13.1}\right)}{5.615 + \left(\frac{R_s\gamma_g}{13.1\rho_{ga}}\right)} \qquad \text{(A/1)}$$

where,

apparent liquid density is;

- $$\rho_{ga} = (38.52)10^{-0.00326API} + [94.75 - 33.93\log(API)]\log(\gamma_g) \qquad \text{(A/2)}$$

Pressure correction factor can be found from the "density correction for the compressibility of crude oils" chart and from the "density correction for isothermal expansion of crude oils" chart isothermal adjustment factor can also be found. Then, the oil density at reservoir

temperature and bubble point pressure can be calculated with the following expression.

- $$\rho_o = \rho_{sc} + \Delta\rho_p - \Delta\rho_T \qquad \text{(A/3)}$$

2) Standing's Method [26]

The oil density at a specified pressure and temperature can be calculated as;

- $$\rho_o = \frac{62.4\gamma_o + 0.0136 R_s \gamma_g}{0.972 + 0.000147\left[R_s\left(\frac{\gamma_g}{\gamma_o}\right)^{0.5} + 1.25(T-460)\right]^{1.175}} \qquad \text{(A/4)}$$

A.2. Gas Solubility

To use in the absence of measured gas solubility parameter, five emprical correlations were tested, Standing's, Vasquez-Beggs's, Glaso's and Marhoun's correlations.

1) Standing's Correlation [27]

Gas solubility can be calculated as;

- $$R_s = \gamma_g\left[\left(\frac{p}{18.2} + 1.4\right)10^x\right]^{1.2048}, \qquad \text{(A/5)}$$

where,

- $x = 0.0125API - 0.00091(T - 460)$ (A/6)

2) Vasquez-Begg's Correlation [28]

- $R_s = C_1 \gamma_{gs} p^{C_2} \exp\left[C_3\left(\frac{API}{T}\right)\right]$, (A/7)

where,

Table A.1. Coefficients of Vasquez-Beggs' Correlation for Gas Solubility

Coefficients	API ≤ 30	API > 30
C1	0.362	0.0178
C2	1.0937	1.187
C3	25.7240	23.931

and gas gravity at the reference separator pressure is,

- $\gamma_{gs} = \gamma_g\left[1 + 5.912(10^{-5})(API)(T_{sep} - 460)\log\left(\frac{P_{sep}}{114.7}\right)\right]$ (A/8)

3) Glaso's Correlation [29]

- $R_s = \gamma_g\left\{\left[\frac{API^{0.989}}{(T-460)^{0.172}}\right](A)\right\}^{1.2255}$ (A/9)

where,

- $A = 10^{X}$, (A/10)

and,

- $X = 2.8869 - \left[14.1811 - 3.3093\log(p)^{0.5}\right]$ (A/11)

4) Marhoun's Correlation [30]

- $R_s = \left[a\gamma_g^b \gamma_o^c T^d p\right]^e$ (A/12)

where a-e coefficients are,

$a = 185.843208$
$b = 1.877840$
$c = -3.1437$
$d = -1.32657$
$e = 1.39844$

A.3. Bubble-Point Pressure

1) Standing's Correlation [26, 27]

- $P_b = 18.2\left[\left(\frac{R_s}{\gamma_g}\right)^{0.83}(10)^a - 1.4\right]$ (A/13)

where,

- $a = 0.00091(T - 460) - 0.0125(API)$, (A/14)

2) Lasater's Correlation [31]

- $$P_b = \left(\frac{T}{\gamma_g}\right)A \qquad \text{(A/15)}$$

where,

- $$A = 0.83918\left[10^{1.17664\gamma_{gas}}\right]\gamma_{gas}^{0.57146}, \gamma_{gas} \le 0.6, \qquad \text{(A/16)}$$

- $$A = 0.83918\left[10^{1.08000\lambda_{gas}}\right]\gamma_{gas}^{0.31109}, \gamma_{gas} > 0.6 \qquad \text{(A/17)}$$

and,

- $$\gamma_{gas} = \frac{M_o R_s}{M_o R_s + 133000\gamma_o}, \qquad \text{(A/18)}$$

Mo value can be calculated from the following expression of Cragoe [32] ;

- $$M_o = \frac{6084}{API - 5.9} \qquad \text{(A/19)}$$

3) Vasquez-Beggs's Correlation [28]

- $$P_b = \left[\left(C_1 \frac{R_s}{\gamma_{gs}}\right)(10)^a\right]^{C_2}, \qquad \text{(A/20)}$$

where,

- $$a = C_3\left(\frac{API}{T}\right) \qquad \text{(A/21)}$$

and,

- $$\gamma_{gs} = \gamma_g \left[1 + 5.912(10^{-5})(API)(T_{sep} - 460)\log\left(\frac{p_{sep}}{114.7}\right)\right], \qquad \text{(A/22)}$$

and,

Table A.2. Coefficients of Vasquez-Beggs' Correlation for Bubble Point Pressure

Coefficients	API ≤ 30	API > 30
C1	27.624	56.18
C2	10.914328	0.84246
C3	-11.172	-10.393

4) Glaso's Correlation [29]

- $$\log(p_b) = 1.7669 + 1.7447\log(A) - 0.30218[\log(A)]^2 \qquad \text{(A/23)}$$

where,

- $$A = \left(\frac{R_s}{\gamma_g}\right)^{0.816} \frac{(T - 460)^{0.172}}{(API)^{0.989}} \qquad \text{(A/24)}$$

5) Marhoun's Correlation [30]

- $$P_b = aR_s^{\,b}\gamma_g^{\,c}\gamma_o^{\,d}T^{\,e}, \qquad \text{(A/25)}$$

where,

$a = 5.38088 \times 10^{-3}$

$b = 0.715082$

- $c = -1.87784$

$d = 3.1437$

$e = 1.32657$

6) Al-Shammasi's Correlation [33]

- $$P_b = \gamma_o^{5.527215} e^{-1.841408[\gamma_o \gamma_g]} \left[R_s T \gamma_g\right]^{0.783716} \quad \text{(A/26)}$$

A.4. Oil Formation Volume Factor

1) Standing' Correlation [26, 27]

- $$B_o = 0.9759 + 0.00120\left[R_s\left(\frac{\gamma_g}{\gamma_o}\right)^{0.5} + 1.25(T - 460)\right]^{1.2} \quad \text{(A/27)}$$

2) Vasquez and Beggs's Correlation [28]

- $$B_o = 1.0 + C_1 R_s + (T - 520)\left(\frac{API}{\gamma_{gs}}\right)\left[C_2 + C_3 R_s\right], \quad \text{(A/28)}$$

where,

- $$\gamma_{gs} = \gamma_g\left[1 + 5.912(10^{-5})(API)(T - 460)\log\left(\frac{p_{sep}}{114.7}\right)\right], \quad \text{(A/29)}$$

Table A.3. Coefficients of Vasquez-Beggs' Correlation for Oil Formation Volume Factor

Coefficients	API ≤ 30	API > 30
C1	4.677×10^{-4}	4.677×10^{-4}
C2	1.751×10^{-5}	1.100×10^{-5}
C3	-1.811×10^{-8}	1.337×10^{-9}

3) Glaso's Correlation [29]

- $B_o = 1.0 + 10^A$, (A/30)

where,

- $A = -6.58511 + 2.91329 \log B_{ob}^* - 0.27683 \left(\log B_{ob}^*\right)^2$, (A/31)

and,

- $B_{ob}^* = R_s \left(\frac{\gamma_g}{\gamma_o}\right)^{0.526} + 0.968(T - 460)$ (A/32)

4) Marhoun's Correlation [30]

- $B_o = 0.497069 + 0.000862963T + 0.00182594F + 0.00000318099F^2$ (A/33)

where,

- $F = R_s^a \gamma_g^b \gamma_o^c$, (A/34)

$a = 0.742390,$

- $b = 0.323294,$

$c = -1.202040.$

5) Material Balance Equation

- $$B_o = \frac{62.4\gamma_o + 0.0136 R_s \gamma_g}{\rho_o} \quad \text{(A/35)}$$

A.5. Isothermal Compressibility Coefficient

1) Trube' Correlation for Undersaturated Oil Compressibility [34]

- $$c_o = \frac{c_r}{P_{pc}} \quad \text{(A/36)}$$

where,

- $$(\rho_o)_T = \frac{dp/dh}{0.433} \quad \text{(A/37)}$$

- $$(\rho_o)_{60} = (\rho_o)_T + 0.00046(T - 520) \quad \text{(A/38)}$$

- $$(P_b)_{60} = \frac{1.134 P_b}{10^{0.00091(T-460)}} \quad \text{(A/39)}$$

Pseudo-reduced compressibility and pseudo-critical temperature and pressure values can be estimated with the help of Trube's pseudo-reduced compressibility of undersaturated oil, Trube's pseudo-critical temperature correlation, Trube's pseudo-critical properties correlation graphs [34].

2) Vasquez-Begg's Correlation for Undersaturated Oil Compressibility [28]

- $$c_o = \frac{-1433 + 5R_{sb} + 17.2(T - 460) - 1180\gamma_{gs} + 12.61API}{10^5 p} \quad \text{(A/40)}$$

3) Standing's Correlation for Undersaturated Oil Compressibility [35]

- $$c_o = 10^{-6} \exp\left[\frac{\rho_{ob} + 0.004347(P - P_b) - 79.1}{0.0007141(P - P_b) - 12.938}\right] \quad \text{(A/41)}$$

A.6. Crude Oil Viscosity

1) Beal's Correlation [36]

Dead oil viscosity can be calculated as;

- $$\mu_{od} = 0.32 + \frac{18(10^7)}{API^{4.53}}\left(\frac{360}{T - 260}\right)^A, \quad \text{(A/42)}$$

where,

- $A = 10^{0.42+\left(\frac{8.33}{API}\right)}$ (A/43)

2) Beggs and Robinson's Correlation [37]

Beggs and Robinson suggest the following expression for dead oil viscosity calculations;

- $\mu_{od} = 10^{A(T-460)^{-1.163}} - 1.0,$ (A/44)

where,

- $A = 10^{3.0324-0.02023API}$ (A/45)

3) Glaso's Correlation [29]

Glaso's expression for dead oil viscosity;

- $\mu_{od} = \left[3.141\left(10^{10}\right)\right](T-460)^{-3.444}\left[\log(API)\right]^{A},$ (A/46)

where,

- $A = 10.313\left[\log(T-460)\right] - 36.447$ (A/47)

Glaso's expression can be used within the range of 50 – 300 °F for the temperature and 20-48° for the API gravity.

4) Chew-Connaly Correlation for Bubble Point Oil Viscosity [38]

Standing expressed the Chew-Connaly's graphical correlation in a mathematical form:

- $\mu_{ob} = (10)^{a}(\mu_{od})^{b}$ (A/48)

where,

- $a = R_s\left[2.2(10^{-7})R_s - 7.4(10)^{-4}\right]$ (A/49)
- $b = 0.68(10)^{c} + 0.25(10)^{d} + 0.062(10)^{e}$ (A/50)
- $c = -0.0000862R_s$ (A/51)
- $d = -0.0011R_s$ (A/52)
- $e = -0.00374R_s$ (A/53)

It should be noted that Chew-Connaly used experimental properties of oil samples with the gas solubility of the reservoir oil between 51 – 3,544 scf/STB, the temperature of 72 – 292 °F, pressure between 132 – 5,645 psia and the dead oil viscosity in the range of 0.377 – 50 cp, to develop their correlation.

5) Beggs-Robinson Correlation for Bubble Point Oil Viscosity [37]

- $\mu_{ob} = a(\mu_{od})^{b}$, (A/54)

where,

- $a = 10.715(R_s + 100)^{-0.515}$ (A/55)
- $b = 5.44(R_s + 150)^{-0.338}$ (A/56)

Experimental results to develop Beggs and Robinson's equation are in the following ranges;

- Pressure : 131 – 5,265 psia
- Temperature : 70 – 295 °F
- Gas Solubility : 20 – 2.070 scf/STB
- API Gravity : 16 – 58 °

6) Abu Khamsim and Al-Marhoun for Bubble Point Oil Viscosity [39]

- $\ln(\mu_{ob}) = 8.484462\rho_{ob}^4 - 2.652294$ (A/57)

7) Beal's Correlation for Undersaturated Oil Viscosity [36]

- $\mu_o = \mu_{ob} + 0.001(P - P_b)\left[0.024\mu_{ob}^{1.6} + 0.038\mu_{ob}^{0.56}\right]$ (A/58)

8) Khan's Correlation for Undersaturated Oil Viscosity [40]

- $\mu_o = \mu_{ob} \exp\left[9.6(10^{-6})(P - P_b)\right]$ (A/59)

9) Vasquez-Begg's Correlation for Undersaturated Oil Viscosity [28]

Vasquez-Beggs used a total of 3,593 data points in order to develop the following expression;

- $$\mu_o = \mu_{ob}\left(\frac{P}{P_b}\right)^m, \qquad \text{(A/60)}$$

where,

- $$m = 2.6P^{1.187}10^A \qquad \text{(A/61)}$$
- $$A = -3.9\left(10^{-5}\right)P - 5 \qquad \text{(A/62)}$$

Data used to develop Vasquez-Beggs' equation are in the following ranges;

- Pressure : 141 – 9,151 psia
- Viscosity : 0.117 – 148 cp
- Gas solubility : 9.3 – 2.199 scf/STB
- API gravity : 15.3 – 59.5 °
- Gas gravity : 0.511 – 1.351

A.7. Interfacial Tension

The modified form of the Katz et al. and Sugden correlation for mixtures by introducing compositions of two phases into equation is; [41], [42]

- $$\sigma^{1/4} = \sum_{i=1}^{n}\left[(P_{ch})_i(Ax_i - By_i)\right] \qquad \text{(A/63)}$$

where,

- $A = \frac{\rho_o}{62.4 M_o}$ (A/64)

- $B = \frac{\rho_g}{62.4 M_g}$ (A/65)

- $(P_{ch})_i = 69.9 + 2.3 M_i$ (A/66)

A.8. Water Viscosity

Water viscosity calculations were made by using Meehan's (1980), Brill and Beggs (1973) and McCain et al.'s water viscosity correlations.

(1) Meehan's correlation [43]

brine viscosity at any pressure and temperature

- $\mu_w = \mu_{wD} (1 + 3.5 \times 10^{-2} p^2 (T-40))$, (A/67)

brine viscosity at 14.7 psi and reservoir temperature

- $\mu_{wD} = A + B / T$, (A/68)

where,

- $A = 4.518 \times 10^{-2} + 9.313 \times 10^{-7} Y - 3.93 \times 10^{-12} Y^2$ (A/69)

- $B = 70.634 + 9.576 \times 10^{-10} Y^2$ (A/70)

- Y is the water salinity, ppm.

(2) Brill and Beggs equation [44]

- $\mu_w = \exp (1.003 - 1.479 \times 10^{-2} T + 1.982 \times 10^{-5} T^2)$ (A/71)

(3) McCain et al. [45]

brine viscosity at any pressure and temperature

- $\mu_w = \mu_{w1} (0.9994 + 0.0000450295\ p + 3.1062 \times 10^{-9}\ p^2)$ (A/72)

brine viscosity at 14.7 psi and reservoir temperature

- $\mu_{w1} = AT^B$ (A/73)

where,

- $A = 109.574 - 0.0840564\ \omega_s + 0.313314(\omega_s)^2 + 0.00872213\ (\omega_s)^3$ (A/74)

- $B = -1.12166 + 0.0263951\ \omega_s - 0.000679461\ (\omega_s)^2 - 0.0000547119\ (\omega_s)^3 + 1.55586 \times 10^{-6}\ (\omega_s)^4$ (A/75)

- ω_s, water salinity, percent by weight, solids.

A.9. Water Isothermal Compressibility

Brill and Beggs (1978) and McCain (1991) proposed the following equations for estimating water isothermal compressibility

(1) Brill and Beggs [44]

- $c_w = (C_1 + C_2T + C_3T^2) \times 10^{-6}$ (A/76)

where

- $C_1 = 3.8546 - 0.000134p$ (A/77)
- $C_2 = -0.01052 + 4.77 \times 10^{-7}p$ (A/78)
- $C_3 = 3.9267 \times 10^{-5} - 8.8 \times 10^{-10}p$ (A/79)

(2) McCain (1991) [46]

McCain suggested the following equation,

- $$c_w = \frac{1}{7.033P + 541.55C_{sw} - 537.0T + 403300},$$ (A/80)

where,

- C_{sw}, the salinity of the water.

APPENDIX B

CORRELATIONS FOR THE C_{7+} CHARACTERIZATION

B.1. Riazi and Daubert

Riazi and Daubert developed the following equation for predicting the physical properties of pure compounds and undefined hydrocarbon mixtures. [47]

- $$\theta = a(M)^b \gamma^c EXP\left[d(M) + e\gamma + f(M)\gamma\right] \qquad \text{(B/1)}$$

where,

- Θ, any physical property
- M, molecular weight
- γ, specific gravity
- a-f, constants, can be seen in Table B.1

Table B.1. Constants for Riazi – Daubert's correlation

Θ	a	B	c	d	e	F
Tc, °R	544.4	0.2998	1.0555	-1.3478×10^{-4}	-0.61641	0.0
Pc, psia	4.5203×10^{4}	-0.8063	1.6015	-1.8078×10^{-3}	-0.3084	0.0
Vc, ft^3/lb	1.206×10^{-2}	0.20378	-1.3036	-2.657×10^{-3}	0.5287	2.6012×10^{-3}
Tb, °R	6.77857	0.401673	-1.58262	3.77409×10^{-3}	2.984036	-4.25288×10^{-3}

B.2. Edmister's Correlation

Edmister proposed a correlation for accentric factor estimation. [48]

- $$\omega = \frac{3[\log(P_c/14.7)]}{7[(T_c/T_b - 1)]} - 1, \qquad \text{(B/2)}$$

where,

- Tc, Tb,°R
- Pc, psia.

APPENDIX C

LUMPING METHODS

C.1. Whitson's Method [49]

- $$M_I = M_{C_{7+}}\left(\frac{M_{N+}}{M_{C_7}}\right)^{\frac{I}{N_g}}, \qquad \text{(C/1)}$$

where,

- $$N_g = Int\left[1+3.3\log(N-n)\right], \qquad \text{(C/2)}$$
- Int = integer

C.2. Lee's Mixing Rules

In order to determine the lumped fraction properties Lee et al. propose the following equations [50].

- $$z_i^* = \frac{z_i}{\sum_{i=L}^{L} z_i},$$ Normalized mole fraction of a component. (C/3)
- $$M_L = \sum_{i=L}^{L} z_i^* M_i,$$ Pseudo-molecular weight. (C/4)

- $\gamma_L = \dfrac{M_L}{\sum_{i=L}^{L}\left[\dfrac{z_i^* M_i}{\gamma_i}\right]}$, Pseudo-density. (C/5)

- $V_{cL} = \sum_{i=L}^{L}\left[\dfrac{z_i^* M_i V_{ci}}{M_L}\right]$, Pseudo-critical volume. (C/6)

- $P_{cL} = \sum_{i=L}^{L}\left[z_i^* P_{ci}\right]$, Pseudo-critical pressure. (C/7)

- $T_{cL} = \sum_{i=L}^{L}\left[z_i^* T_{ci}\right]$, Pseudo-critical temperature. (C/8)

- $\omega_L = \sum_{i=L}^{L}\left[z_i^* \omega_i\right]$, Pseudo-accentric factor. (C/9)

C.3. Behrens and Sandler's Lumping Method

Behrens and Sandler [51] propose the following equations ;

- $\bar{c}_n = \dfrac{M_{C_{+7}} + 4}{14}$, (C/10)

- $\dfrac{1}{\alpha} - \bar{c}_n + A - \dfrac{[A-B]e^{-B\alpha}}{e^{-A\alpha} - e^{-B\alpha}} = 0$, (C/11)

- $c = (B-A)\alpha$, (C/12)

- $n_1 = \dfrac{r_1}{\alpha} + A$, (C/13)

- $n_2 = \frac{r_2}{\alpha} + A$, (C/14)

- $z_1 = \omega_1 z_{+7}$, (C/15)

- $z_2 = \omega_2 z_{+7}$, (C/16)

APPENDIX D

EQUATIONS OF STATE

D.1. Van der Waals' Equation of State

The difference between the expression developed by Van der Waals (1873) and the ideal gas equation of state is the 'a' and 'b' parameters [52]. The aim of using these parameters is to modify the ideal gas equation of state to eliminate two assumptions. The first assumption is "*the volume of the gas molecules is insignificant compared to both the volume of the container and distance between the molecules*". The second assumption is *"there are no attractive or repulsive forces between the molecules or the walls of the container"*. Van der Waals developed the following expression with a and b parameters, where a is the attraction parameter and b is the repulsion parameter:

$$P = \frac{RT}{V-b} - \frac{a}{V^2}, \qquad \text{(D/1)}$$

$$a = \frac{27R^2T_c^2}{64P_c}, \qquad \text{(D/2)}$$

$$b = \frac{RT_c}{8P_c}, \qquad \text{(D/3)}$$

The modified cubic equation of state of Van der Waals is ;

$$V^3 - \left(b + \frac{RT}{P}\right)V^2 + \left(\frac{a}{P}\right)V - \left(\frac{ab}{P}\right) = 0 \qquad \text{(D/4)}$$

D.2. Redlich – Kwong's Equation of State

This equation of state can be seen as a modified Van der Waals' equation of state. It is considered as the first modern equation of state [53].

$$P = \frac{RT}{V-b} - \frac{a}{V(V+b)\sqrt{T}}, \qquad \text{(D/5)}$$

In order to improve the vapor pressure predictions, the attractive term gained more temperature dependence.

$$a = \frac{0.42747 R^2 T_c^{2.5}}{P_c}, \qquad \text{(D/6)}$$

$$b = \frac{0.08664 R T_c}{P_c}, \qquad \text{(D/7)}$$

Replacing molar volume with ZRT / P, the following equation is obtained;

$$Z^3 - Z^2 + (A - B - B^2)Z - AB = 0, \qquad \text{(D/8)}$$

where,

$$A = \frac{aP}{R^2 T^{2.5}}, \qquad \text{(D/9)}$$

$$B = \frac{bP}{RT}. \qquad \text{(D/10)}$$

D.3. Soave – Redlich – Kwong's Equation of State

With a more general temperature-dependent term, Soave (1972) improved the accuracy of vapour pressures of pure components [54]. This term is denoted as α(T).

- $P = \frac{RT}{V-b} - \frac{a\alpha(T)}{V(V+b)}$, (D/11)
- $\alpha(T) = \left(1 + m\left(1 - \sqrt{T_r}\right)\right)^2$, (D/12)
- $m = 0.480 + 1.574\omega - 0.176\omega^2$ (D/13)
- $a = \frac{0.42747 R^2 T_c^2}{P_c}$, (D/14)
- $b = \frac{0.08664 RT_c}{P_c}$, (D/15)

where,

- ω : acentric factor
- T_r : reduced temperature (T/T_c)

By replacing molar volume with ZRT/P, the Soave-Redlich-Kwong equation of state becomes as the following expression;

- $Z^3 - Z^2 + \left(A - B - B^2\right)Z - AB = 0$, (D/16)

where,

- $A = \frac{(a\alpha(T))P}{R^2T^2}$, (D/17)

- $$B = \frac{bP}{RT} \qquad \text{(D/18)}$$

D.4. Peng – Robinson's Equation of State

In order to predict the density, and other fluid properties of hydrocarbons, Peng and Robinson (1976a) developed a new equation.

- $$P = \frac{RT}{V-b} - \frac{a\alpha}{(V+b)^2 - cb^2} \qquad \text{(D/19)}$$

Then by giving an optimized value for c parameter the equation is modified to the commonly known Peng-Robinson Equation of State [55].

- $$P = \frac{RT}{V-b} - \frac{a\alpha}{V(V+b)-b(V-b)} \qquad \text{(D/20)}$$
- $$\alpha = \left(1 + m\left(1 - \sqrt{T_r}\right)\right)^2 \qquad \text{(D/21)}$$
- $$m = 0.3796 + 1.54226\omega - 0.2699\omega^2 \qquad \text{(D/22)}$$
- $$a = \frac{0.457247 R^2 T_c^2}{P_c} \qquad \text{(D/23)}$$
- $$b = \frac{0.07780 RT_c}{P_c} \qquad \text{(D/24)}$$

For heavy components, ω > 0.49, 'm' parameter can be calculated as ; [56]

- $$m = 0.379642 + 1.48503\omega - 0.1644\omega^2 + 0.016667\omega^3 \qquad \text{(D/25)}$$

By replacing the molar volume with ZRT/P, the Peng-Robinson equation of state becomes as the following expression;

$$- \quad Z^3 - (B-1)Z^2 + (A - 3B^2 - 2B)Z - (AB - B^2 - B^3) = 0 \quad , \qquad \text{(D/26)}$$

where,

$$- \quad A = \frac{(a\alpha(T))_m P}{R^2 T^2} \quad , \qquad \text{(D/27)}$$

$$- \quad B = \frac{b_m P}{RT} \qquad \text{(D/28)}$$

APPENDIX E

PETROPHYSICAL PROPERTIES

Table E.1. X-Field core plug samples average core analysis results

	# of samples	Porosity (%)			Permeability (md)			Grain Density (g/cc)		
		Min.	Max.	Average*	Min.	Max.	Average**	Min.	Max.	Average*
X-2	77	6.69	51.23	26.47	0.07	51.77	2.18	2.70	2.88	2.79
X-3	5	15.30	35.16	25.94	0.36	11.02	1.64	2.81	2.96	2.88
X-4	6	18.41	35.02	26.62	0.82	25.74	3.26	2.71	2.98	2.81
X-5	82	0.33	39.20	23.17	0.02	58.17	1.82	2.68	3.18	2.81
X-6	62	0.22	34.70	21.05	0.02	28.56	1.31	2.71	2.89	2.77
X-7	41	5.77	34.56	21.20	0.03	50.32	1.23	2.68	2.88	2.77
Total	*273*	-	-	23.45	-	-	1.69	-	-	2.79

** Arithmetical average.*

*** Geomethrical average.*

Table E.2. X-Field porosity and permeability change under overburden pressure

	Sample	NOP, psi	ø, %	k_L, md	k_{air}, md	$\frac{k_L}{k_{L@800psi}}$	$\frac{\phi}{\phi_{@800psi}}$
X-5	96	800	2.40	0.13	0.13	1.00	1.00
		1250	2.29	0.02	0.05	0.18	0.95
		2000	2.13	0.01	0.03	0.09	0.89
		3000	-	< 0.01	-	-	-
		4000	-	< 0.01	-	-	-
X-5	97	800	13.07	0.54	0.74	1.00	1.00
		1250	12.96	0.54	0.73	0.99	0.99
		2000	12.81	0.52	0.71	0.97	0.98
		3000	12.68	0.51	0.69	0.95	0.97
		4000	12.58	0.50	0.68	0.93	0.96
X-5	98	800	22.36	1.42	2.03	1.00	1.00
		1250	22.27	1.41	2.01	0.99	1.00
		2000	22.15	1.39	1.98	0.98	0.99
		3000	22.05	1.37	1.95	0.96	0.99
		4000	21.97	1.36	1.94	0.95	0.98
X-5	99	800	29.25	2.01	3.06	1.00	1.00
		1250	28.87	1.93	2.95	0.96	0.99
		2000	28.33	1.86	2.86	0.93	0.97
		3000	27.79	1.88	2.80	0.94	0.95
		4000	27.37	1.83	2.73	0.91	0.94
X-5	100	800	30.41	2.93	4.28	1.00	1.00
		1250	30.22	2.89	4.24	0.99	0.99
		2000	29.98	2.85	4.18	0.97	0.99
		3000	29.79	2.81	4.11	0.96	0.98
		4000	29.67	2.77	4.07	0.95	0.98
X-5	101	800	24.32	0.76	1.17	1.00	1.00
		1250	24.17	0.71	1.11	0.94	0.99
		2000	23.98	0.66	1.04	0.87	0.99
		3000	23.82	0.62	0.98	0.82	0.98
		4000	23.70	0.60	0.95	0.79	0.97
X-5	102	800	16.78	0.29	0.48	1.00	1.00
		1250	16.70	0.28	0.48	0.99	1.00
		2000	16.59	0.28	0.47	0.97	0.99
		3000	16.50	0.27	0.46	0.94	0.98
		4000	16.43	0.26	0.45	0.92	0.98
X-5	103	800	19.73	1.17	1.77	1.00	1.00
		1250	19.57	1.07	1.66	0.91	0.94
		2000	19.39	0.97	1.52	0.83	0.86
		3000	19.22	0.90	1.42	0.77	0.80
		4000	19.10	0.86	1.38	0.74	0.78
X-5	104	800	32.54	15.87	19.91	1.00	1.00
		1250	32.36	15.71	19.72	0.99	0.99
		2000	32.14	15.50	19.46	0.98	0.99
		3000	31.94	15.28	19.19	0.96	0.98
		4000	31.80	15.11	18.99	0.95	0.98

Table E.2. (Cont.)

	Sample	NOP, psi	ø, %	k_L, md	k_{air}, md	$\frac{k_L}{k_{L@800psi}}$	$\frac{\phi}{\phi_{@800psi}}$
X-5	105	800	9.73	0.05	0.11	1.00	1.00
		1250	9.61	0.05	0.10	0.91	0.99
		2000	9.47	0.04	0.09	0.82	0.97
		3000	9.37	0.04	0.09	0.75	0.96
		4000	9.32	0.04	0.08	0.72	0.96
X-5	106	800	15.36	0.72	1.06	1.00	1.00
		1250	15.22	0.66	0.98	0.92	0.99
		2000	15.05	0.59	0.89	0.82	0.98
		3000	14.91	0.53	0.80	0.74	0.97
		4000	14.82	0.49	0.75	0.69	0.96
X-5	107	800	12.92	0.04	0.09	1.00	1.00
		1250	12.79	0.04	0.09	0.88	0.99
		2000	12.65	0.03	0.08	0.76	0.98
		3000	12.54	0.03	0.07	0.68	0.97
		4000	12.48	0.03	0.07	0.64	0.97
X-5	108	800	23.06	1.63	2.33	1.00	1.00
		1250	22.82	1.46	2.12	0.90	0.99
		2000	22.54	1.26	1.86	0.78	0.98
		3000	22.33	1.10	1.63	0.67	0.97
		4000	22.20	0.99	1.49	0.61	0.96
X-5	109	800	16.06	4.92	6.53	1.00	1.00
		1250	15.91	4.09	5.02	0.83	0.99
		2000	15.72	3.08	3.71	0.63	0.98
		3000	15.55	2.21	2.70	0.45	0.97
		4000	15.43	1.67	2.09	0.34	0.96
X-5	110	800	18.22	1.54	2.03	1.00	1.00
		1250	18.09	1.49	1.97	0.97	0.99
		2000	17.93	1.43	1.88	0.93	0.98
		3000	17.79	1.37	1.81	0.89	0.98
		4000	17.69	1.34	1.76	0.87	0.97
X-5	111	800	23.17	1.77	2.55	1.00	1.00
		1250	22.99	1.74	2.51	0.98	0.99
		2000	22.77	1.71	2.46	0.97	0.98
		3000	22.59	1.67	2.42	0.95	0.97
		4000	22.46	1.65	2.39	0.93	0.97
X-5	112	800	15.78	0.40	0.69	1.00	1.00
		1250	15.66	0.39	0.68	0.98	0.99
		2000	15.52	0.37	0.65	0.94	0.98
		3000	15.39	0.54	0.76	1.38	0.98
		4000	15.31	0.53	0.75	1.35	0.97
X-5	113	800	35.70	14.48	18.89	1.00	1.00
		1250	35.49	14.32	18.72	0.99	0.99
		2000	35.24	14.12	18.45	0.97	0.99
		3000	35.01	13.91	18.19	0.96	0.98
		4000	34.85	13.76	18.02	0.95	0.98

Table. E.2. (Cont.)

	Sample	NOP, psi	ø, %	k_L, md	k_{air}, md	$\frac{k_L}{k_{L@800psi}}$	$\frac{\phi}{\phi_{@800psi}}$
X-5	114	800	23.35	0.61	1.02	1.00	1.00
		1250	23.24	0.60	1.01	0.99	1.00
		2000	23.10	0.60	1.00	0.97	0.99
		3000	22.98	0.59	0.99	0.96	0.98
		4000	22.90	0.58	0.98	0.95	0.98
X-5	115	800	30.75	4.26	5.94	1.00	1.00
		1250	30.58	4.20	5.86	0.99	0.99
		2000	30.37	4.12	5.76	0.97	0.99
		3000	30.19	4.04	5.65	0.95	0.98
		4000	30.06	3.97	5.56	0.93	0.98
X-5	116	800	16.85	0.48	0.80	1.00	1.00
		1250	16.72	0.47	0.78	0.97	0.99
		2000	16.57	0.45	0.76	0.94	0.98
		3000	16.44	0.44	0.74	0.91	0.98
		4000	16.35	0.43	0.72	0.90	0.97
X-5	117	800	14.91	0.28	0.50	1.00	1.00
		1250	14.82	0.27	0.49	0.96	0.99
		2000	14.70	0.28	0.47	0.99	0.99
		3000	14.60	0.27	0.47	0.98	0.98
		4000	14.53	0.27	0.46	0.98	0.97
X-5	118	800	31.41	4.21	6.13	1.00	1.00
		1250	31.25	4.17	6.07	0.99	0.99
		2000	31.06	4.12	5.99	0.98	0.99
		3000	30.90	4.05	5.91	0.96	0.98
		4000	30.79	4.00	5.84	0.95	0.98
X-5	119	800	23.27	2.07	2.98	1.00	1.00
		1250	23.07	1.94	2.80	0.94	0.99
		2000	22.83	1.79	2.61	0.86	0.98
		3000	22.60	1.67	2.47	0.81	0.97
		4000	22.44	1.60	2.38	0.78	0.96
X-5	120	800	24.78	2.73	4.07	1.00	1.00
		1250	24.57	2.72	4.01	1.00	0.99
		2000	24.34	2.66	3.92	0.98	0.98
		3000	24.14	2.59	3.82	0.95	0.97
		4000	24.02	2.54	3.75	0.93	0.97
X-5	121	800	19.00	0.99	1.47	1.00	1.00
		1250	18.88	0.98	1.46	0.99	0.99
		2000	18.74	0.96	1.44	0.98	0.99
		3000	18.61	0.95	1.42	0.96	0.98
		4000	18.52	0.94	1.40	0.95	0.97
X-5	122	800	15.67	0.24	0.42	1.00	1.00
		1250	15.52	0.23	0.41	0.98	0.99
		2000	15.33	0.23	0.40	0.96	0.98
		3000	15.15	0.22	0.38	0.93	0.97
		4000	15.03	0.21	0.38	0.90	0.96

Table E.2. (Cont.)

	Sample	NOP, psi	ø, %	k_L, md	k_{air}, md	$\frac{k_L}{k_{L@800psi}}$	$\frac{\phi}{\phi_{@800psi}}$
X-5	123	800	27.25	5.12	7.07	1.00	1.00
		1250	27.12	5.06	6.99	0.99	1.00
		2000	26.96	4.98	6.88	0.97	0.99
		3000	26.83	4.89	6.78	0.96	0.98
		4000	26.74	4.83	6.70	0.94	0.98
X-5	124	800	33.36	10.73	14.13	1.00	1.00
		1250	33.23	10.62	13.99	0.99	1.00
		2000	33.08	10.48	13.82	0.98	0.99
		3000	32.94	10.34	13.65	0.96	0.99
		4000	32.85	10.25	13.53	0.96	0.98
X-5	125	800	30.98	27.77	33.10	1.00	1.00
		1250	30.88	27.55	32.85	0.99	1.00
		2000	30.75	27.26	32.52	0.98	0.99
		3000	30.64	26.96	32.18	0.97	0.99
		4000	30.56	26.74	31.93	0.96	0.99
X-5	126	800	18.20	0.17	0.27	1.00	1.00
		1250	17.86	0.15	0.24	0.88	0.98
		2000	17.59	0.13	0.22	0.86	0.97
		3000	17.62	0.11	0.20	0.75	0.97
		4000	17.49	0.10	0.18	0.69	0.96
X-5	127	800	38.80	28.96	35.40	1.00	1.00
		1250	38.55	28.29	34.58	0.98	0.99
		2000	38.26	27.39	33.49	0.95	0.99
		3000	37.99	26.47	32.37	0.91	0.98
		4000	37.81	25.79	31.58	0.89	0.97
X-5	128	800	15.90	1.22	1.77	1.00	1.00
		1250	15.80	1.21	1.75	0.99	0.99
		2000	15.68	1.19	1.73	0.98	0.99
		3000	15.57	1.18	1.71	0.97	0.98
		4000	15.49	1.16	1.69	0.96	0.97
X-5	129	800	31.84	17.31	21.67	1.00	1.00
		1250	31.69	17.08	21.39	0.99	1.00
		2000	31.50	16.77	21.02	0.97	0.99
		3000	31.34	16.49	20.68	0.95	0.98
		4000	31.24	16.29	20.44	0.94	0.98
X-5	131	800	16.80	10.24	11.65	1.00	1.00
		1250	16.66	10.12	11.51	0.99	0.99
		2000	16.50	9.94	11.30	0.97	0.98
		3000	16.35	9.75	11.09	0.95	0.97
		4000	16.25	9.61	10.92	0.94	0.97
X-5	132	800	26.94	2.13	2.98	1.00	1.00
		1250	26.81	2.12	2.98	0.99	1.00
		2000	26.65	2.07	2.92	0.97	0.99
		3000	26.51	2.05	2.88	0.96	0.98
		4000	26.42	2.01	2.84	0.95	0.98

Table. E.2. (Cont.)

	Sample	NOP, psi	ø, %	k_L, md	k_{air}, md	$\frac{k_L}{k_{L@800psi}}$	$\frac{\phi}{\phi_{@800psi}}$
X-5	133	800	10.16	0.02	0.06	1.00	1.00
		1250	10.07	0.02	0.05	0.97	0.99
		2000	9.97	0.02	0.05	0.94	0.98
		3000	9.89	0.02	0.05	0.91	0.97
		4000	9.85	0.02	0.05	0.90	0.97
X-5	134	800	13.09	0.01	0.02	1.00	1.00
		1250	12.88	0.01	0.02	1.09	0.98
		2000	12.64	0.01	0.02	1.03	0.97
		3000	12.47	0.01	0.02	0.98	0.95
		4000	12.38	0.01	0.01	0.88	0.95
X-5	135	800	20.99	1.62	2.25	1.00	1.00
		1250	20.90	1.61	2.23	0.99	1.00
		2000	20.79	1.59	2.21	0.98	0.99
		3000	20.68	1.57	2.18	0.97	0.99
		4000	20.60	1.56	2.16	0.96	0.98
X-5	136	800	9.51	0.06	0.10	1.00	1.00
		1250	9.40	0.05	0.10	0.97	0.99
		2000	9.26	0.05	0.09	0.94	0.97
		3000	9.17	0.05	0.09	0.93	0.96
		4000	9.12	0.05	0.09	0.95	0.96
X-5	137	800	27.88	5.17	7.02	1.00	1.00
		1250	27.79	5.13	6.98	0.99	1.00
		2000	27.67	5.08	6.92	0.98	0.99
		3000	27.56	5.03	6.85	0.97	0.99
		4000	27.48	4.99	6.80	0.97	0.99
X-5	138	800	22.01	1.59	2.38	1.00	1.00
		1250	21.86	1.56	2.34	0.98	0.99
		2000	21.67	1.52	2.29	0.96	0.98
		3000	21.51	1.49	2.23	0.93	0.98
		4000	21.41	1.46	2.20	0.92	0.97
X-5	139	800	21.04	1.69	2.48	1.00	1.00
		1250	20.87	1.62	2.39	0.96	0.99
		2000	20.66	1.53	2.28	0.90	0.98
		3000	20.48	1.46	2.18	0.86	0.97
		4000	20.35	1.41	2.12	0.84	0.97
X-5	140	800	20.61	2.65	3.65	1.00	1.00
		1250	20.46	2.55	3.52	0.96	0.99
		2000	20.29	2.43	3.37	0.92	0.98
		3000	20.12	2.33	3.23	0.88	0.98
		4000	20.01	2.26	3.15	0.85	0.97
X-5	141	800	20.44	1.79	2.60	1.00	1.00
		1250	20.27	1.73	2.53	0.97	0.99
		2000	20.07	1.66	2.43	0.93	0.98
		3000	19.88	1.60	2.34	0.89	0.97
		4000	19.74	1.56	2.28	0.87	0.97

Table E.2. (Cont.)

	Sample	NOP, psi	ø, %	k_L, md	k_{air}, md	$\frac{k_L}{k_{L@800psi}}$	$\frac{\phi}{\phi_{@800psi}}$
X-5	142	800	34.88	19.53	24.32	1.00	1.00
		1250	34.73	19.35	24.09	0.99	1.00
		2000	34.55	19.09	23.78	0.98	0.99
		3000	34.37	18.81	23.46	0.96	0.99
		4000	34.24	18.59	23.18	0.95	0.98
X-5	143	800	15.13	0.42	0.64	1.00	1.00
		1250	15.01	0.41	0.63	0.98	0.99
		2000	14.86	0.40	0.61	0.94	0.98
		3000	14.74	0.43	0.60	1.02	0.97
		4000	14.66	0.42	0.59	0.99	0.97
X-5	144	800	12.39	0.49	0.66	1.00	1.00
		1250	12.22	0.47	0.65	0.97	0.99
		2000	12.02	0.46	0.63	0.94	0.97
		3000	11.86	0.44	0.61	0.91	0.96
		4000	11.75	0.44	0.60	0.89	0.95
X-5	145	800	32.12	17.51	21.88	1.00	1.00
		1250	31.99	17.34	21.69	0.99	1.00
		2000	31.84	17.11	21.43	0.98	0.99
		3000	31.71	16.88	21.16	0.96	0.99
		4000	31.62	16.70	20.94	0.95	0.98
X-5	146	800	25.28	0.84	1.36	1.00	1.00
		1250	25.12	0.82	1.33	0.97	0.99
		2000	24.91	0.79	1.29	0.94	0.99
		3000	24.74	0.76	1.25	0.90	0.98
		4000	24.62	0.74	1.22	0.88	0.97
X-5	147	800	27.99	4.06	5.38	1.00	1.00
		1250	27.80	3.61	4.89	0.89	0.99
		2000	27.57	3.13	4.35	0.77	0.98
		3000	27.36	2.77	3.92	0.68	0.98
		4000	27.21	2.57	3.69	0.63	0.97
X-5	148	800	29.27	4.45	6.20	1.00	1.00
		1250	28.91	4.23	5.89	0.95	0.99
		2000	28.49	3.97	5.55	0.89	0.97
		3000	28.14	3.76	5.28	0.84	0.96
		4000	27.92	3.64	5.12	0.82	0.95
X-5	149	800	25.24	1.59	2.33	1.00	1.00
		1250	24.99	1.56	2.29	0.98	0.99
		2000	24.68	1.52	2.24	0.96	0.98
		3000	24.39	1.49	2.19	0.93	0.97
		4000	24.20	1.46	2.15	0.92	0.96
X-5	150	800	28.04	12.98	16.18	1.00	1.00
		1250	27.88	12.83	15.99	0.99	0.99
		2000	27.69	12.62	15.74	0.97	0.99
		3000	27.52	12.41	15.49	0.96	0.98
		4000	27.41	12.26	15.32	0.94	0.98

Table E.2. (Cont.)

	Sample	NOP, psi	ø, %	k_L, md	k_{air}, md	$\frac{k_L}{k_{L@800psi}}$	$\frac{\phi}{\phi_{@800psi}}$
X-5	151	800	23.11	4.01	5.49	1.00	1.00
		1250	22.96	3.96	5.42	0.99	0.99
		2000	22.79	3.89	5.33	0.97	0.99
		3000	22.63	3.82	5.23	0.95	0.98
		4000	22.52	3.77	5.16	0.94	0.97
X-5	152	800	20.54	5.77	7.22	1.00	1.00
		1250	20.41	5.53	6.96	0.96	0.99
		2000	20.26	5.24	6.60	0.91	0.99
		3000	20.12	4.99	6.30	0.86	0.98
		4000	20.02	4.82	6.09	0.84	0.97
X-5	153	800	29.37	1.72	2.65	1.00	1.00
		1250	29.18	1.71	2.63	0.99	0.99
		2000	28.93	1.69	2.60	0.98	0.99
		3000	28.70	1.67	2.57	0.97	0.98
		4000	28.54	1.65	2.55	0.96	0.97
X-5	154	800	32.40	2.23	3.44	1.00	1.00
		1250	32.23	2.22	3.41	0.99	0.99
		2000	32.01	2.19	3.37	0.98	0.99
		3000	31.80	2.16	3.33	0.97	0.98
		4000	31.65	2.14	3.30	0.96	0.98
X-5	155	800	31.90	3.18	4.61	1.00	1.00
		1250	31.74	3.15	4.57	0.99	0.99
		2000	31.56	3.10	4.51	0.98	0.99
		3000	31.39	3.06	4.44	0.96	0.98
		4000	31.27	3.02	4.40	0.95	0.98
X-5	156	800	33.88	8.40	11.00	1.00	1.00
		1250	33.71	8.31	10.91	0.99	0.99
		2000	33.52	8.17	10.74	0.97	0.99
		3000	33.35	8.01	10.54	0.95	0.98
		4000	33.24	7.87	10.38	0.94	0.98
X-5	157	800	24.47	1.65	2.57	1.00	1.00
		1250	24.27	1.62	2.53	0.98	0.99
		2000	24.03	1.57	2.47	0.95	0.98
		3000	23.83	1.53	2.41	0.93	0.97
		4000	23.70	1.51	2.37	0.91	0.97
X-5	158	800	23.57	1.55	2.35	1.00	1.00
		1250	23.36	1.52	2.31	0.98	0.99
		2000	23.11	1.49	2.27	0.96	0.98
		3000	22.88	1.46	2.22	0.94	0.97
		4000	22.73	1.44	2.19	0.93	0.96
X-5	159	800	28.74	6.14	8.08	1.00	1.00
		1250	28.57	6.02	7.95	0.98	0.99
		2000	28.36	5.85	7.74	0.95	0.99
		3000	28.16	5.66	7.51	0.92	0.98
		4000	28.02	5.50	7.32	0.90	0.97

Table E.2. (Cont.)

	Sample	NOP, psi	ø, %	k_L, md	k_{air}, md	$\frac{k_L}{k_{L@800psi}}$	$\frac{\phi}{\phi_{@800psi}}$
X-5	160	800	29.05	2.54	3.30	1.00	1.00
		1250	28.90	2.46	3.20	0.97	0.99
		2000	28.71	2.37	3.10	0.93	0.99
		3000	28.54	2.30	3.02	0.91	0.98
		4000	28.43	2.27	2.94	0.89	0.98
X-5	161	800	37.10	23.74	27.75	1.00	1.00
		1250	36.88	23.39	27.35	0.99	0.99
		2000	36.57	22.86	26.76	0.96	0.99
		3000	36.26	22.26	26.09	0.94	0.98
		4000	36.01	21.75	25.54	0.92	0.97
X-5	162	800	37.84	50.36	57.75	1.00	1.00
		1250	37.67	49.69	56.97	0.99	1.00
		2000	37.46	48.68	55.88	0.97	0.99
		3000	37.26	47.52	54.60	0.94	0.98
		4000	37.11	46.54	53.53	0.92	0.98
X-5	163	800	37.20	27.06	31.60	1.00	1.00
		1250	37.00	26.71	31.22	0.99	0.99
		2000	36.73	26.19	30.63	0.97	0.99
		3000	36.45	25.58	29.95	0.95	0.98
		4000	36.23	25.07	29.39	0.93	0.97
X-5	164	800	17.80	0.72	1.13	1.00	1.00
		1250	17.68	0.71	1.12	0.99	0.99
		2000	17.54	0.70	1.10	0.97	0.99
		3000	17.41	0.69	1.09	0.96	0.98
		4000	17.32	0.68	1.07	0.95	0.97
X-5	165	800	16.12	0.32	0.56	1.00	1.00
		1250	16.02	0.32	0.56	0.99	0.99
		2000	15.89	0.31	0.55	0.97	0.99
		3000	15.78	0.31	0.54	0.95	0.98
		4000	15.71	0.30	0.53	0.94	0.97
X-5	166	800	23.22	10.54	14.76	1.00	1.00
		1250	23.04	10.28	14.36	0.98	0.99
		2000	22.84	9.89	13.88	0.94	0.98
		3000	22.68	9.46	13.33	0.90	0.98
		4000	22.60	9.10	12.86	0.86	0.97
X-5	167	800	28.73	36.89	50.39	1.00	1.00
		1250	28.49	36.13	49.54	0.98	0.99
		2000	28.22	35.10	48.20	0.95	0.98
		3000	27.99	34.04	46.75	0.92	0.97
		4000	27.85	33.24	45.48	0.90	0.97
X-5	168	800	28.14	2.74	4.07	1.00	1.00
		1250	28.00	2.67	4.03	0.98	1.00
		2000	27.83	2.60	3.92	0.95	0.99
		3000	27.69	2.55	3.86	0.93	0.98
		4000	27.60	2.52	3.82	0.92	0.98

Table E.2. (Cont.)

	Sample	NOP, psi	ø, %	k_L, md	k_{air}, md	$\frac{k_L}{k_{L@800psi}}$	$\frac{\phi}{\phi_{@800psi}}$
X-5	169	800	21.15	0.56	0.90	1.00	1.00
		1250	21.06	0.55	0.90	0.98	1.00
		2000	20.94	0.54	0.87	0.96	0.99
		3000	20.85	0.53	0.87	0.95	0.99
		4000	20.79	0.52	0.85	0.94	0.98
X-5	170	800	13.96	0.46	0.60	1.00	1.00
		1250	13.89	0.45	0.59	0.98	0.99
		2000	13.81	0.43	0.57	0.95	0.99
		3000	13.73	0.28	0.47	0.62	0.98
		4000	13.69	0.29	0.46	0.64	0.98
X-5	171	800	12.39	0.12	0.17	1.00	1.00
		1250	12.19	0.10	0.15	0.85	0.98
		2000	11.96	0.08	0.12	0.68	0.97
		3000	11.80	0.06	0.10	0.53	0.95
		4000	11.71	0.05	0.08	0.43	0.95
X-5	172	800	12.46	0.08	0.13	1.00	1.00
		1250	12.19	0.07	0.11	0.80	0.98
		2000	11.89	0.05	0.08	0.57	0.95
		3000	11.67	0.03	0.06	0.38	0.94
		4000	11.56	0.02	0.04	0.27	0.93
X-5	173	800	38.62	34.82	41.22	1.00	1.00
		1250	38.36	34.26	40.54	0.98	0.99
		2000	38.05	33.46	39.61	0.96	0.99
		3000	37.76	32.58	38.60	0.94	0.98
		4000	37.55	31.87	37.77	0.92	0.97
X-5	174	800	39.45	33.55	40.06	1.00	1.00
		1250	39.19	32.60	38.98	0.97	0.99
		2000	38.87	31.25	37.43	0.93	0.99
		3000	38.57	29.83	35.77	0.89	0.98
		4000	38.35	28.72	34.59	0.86	0.97
X-5	175	800	24.53	5.07	6.40	1.00	1.00
		1250	24.43	5.02	6.34	0.99	1.00
		2000	24.31	4.96	6.26	0.98	0.99
		3000	24.21	4.90	6.18	0.97	0.99
		4000	24.14	4.85	6.12	0.96	0.98
X-5	176	800	25.58	5.01	6.67	1.00	1.00
		1250	25.42	4.95	6.59	0.99	0.99
		2000	25.23	4.87	6.49	0.97	0.99
		3000	25.06	4.79	6.39	0.96	0.98
		4000	24.95	4.73	6.32	0.95	0.98
X-5	177	800	27.67	8.11	10.84	1.00	1.00
		1250	27.56	8.05	10.77	0.99	1.00
		2000	27.42	7.95	10.64	0.98	0.99
		3000	27.29	7.86	10.52	0.97	0.99
		4000	27.19	7.78	10.43	0.96	0.98

Table E.2. (Cont.)

	Sample	NOP, psi	ø, %	k_L, md	k_{air}, Md	$\frac{k_L}{k_{L@800psi}}$	$\frac{\phi}{\phi_{@800psi}}$
X-6	42	800	21.41	0.28	0.46	1.00	1.00
		1250	21.25	0.27	0.44	0.96	0.99
		2000	21.05	0.25	0.42	0.89	0.98
		3000	20.86	0.24	0.40	0.86	0.97
		4000	20.72	0.24	0.39	0.86	0.97
X-6	43	800	21.35	0.26	0.47	1.00	1.00
		1250	21.21	0.26	0.46	1.00	0.99
		2000	21.05	0.26	0.45	1.00	0.99
		3000	20.92	0.26	0.44	1.00	0.98
		4000	20.83	0.26	0.42	1.00	0.98
X-6	44	800	14.68	0.07	0.13	1.00	1.00
		1250	14.47	0.06	0.12	0.86	0.99
		2000	14.25	0.06	0.12	0.86	0.97
		3000	14.08	0.06	0.11	0.86	0.96
		4000	13.99	0.06	0.11	0.86	0.95
X-6	45	800	24.83	3.08	4.01	1.00	1.00
		1250	24.66	3.05	3.96	0.99	0.99
		2000	24.46	3.00	3.90	0.97	0.99
		3000	24.27	2.95	3.83	0.96	0.98
		4000	24.13	2.91	3.78	0.94	0.97
X-6	46	800	19.90	0.08	0.18	1.00	1.00
		1250	19.73	0.08	0.18	1.00	0.99
		2000	19.52	0.08	0.17	1.00	0.98
		3000	19.35	0.08	0.17	1.00	0.97
		4000	19.24	0.08	0.16	1.00	0.97
X-6	49	800	15.77	0.08	0.17	1.00	1.00
		1250	15.53	0.08	0.16	1.00	0.98
		2000	15.27	0.08	0.15	1.00	0.97
		3000	15.07	0.07	0.14	0.88	0.96
		4000	14.97	0.07	0.14	0.88	0.95
X-6	50	800	29.15	1.16	1.74	1.00	1.00
		1250	28.99	1.15	1.72	0.99	0.99
		2000	28.78	1.13	1.69	0.97	0.99
		3000	28.59	1.11	1.66	0.96	0.98
		4000	28.45	1.09	1.64	0.94	0.98
X-6	51	800	8.34	0.01	0.02	1.00	1.00
		1250	-	< 0.01	-	-	-
		2000	-	< 0.01	-	-	-
		3000	-	< 0.01	-	-	-
		4000	-	< 0.01	-	-	-
X-6	53	800	19.00	0.09	0.21	1.00	1.00
		1250	18.91	0.09	0.19	1.00	1.00
		2000	18.81	0.09	0.18	1.00	0.99
		3000	18.74	0.08	0.18	0.89	0.99
		4000	18.70	0.08	0.18	0.89	0.98

Table E.2. (Cont.)

	Sample	NOP, psi	ø, %	k_L, md	k_{air}, Md	$\frac{k_L}{k_{L@800psi}}$	$\frac{\phi}{\phi_{@800psi}}$
X-6	54	800	22.82	0.29	0.48	1.00	1.00
		1250	22.70	0.28	0.47	0.97	0.99
		2000	22.54	0.28	0.47	0.97	0.99
		3000	22.41	0.28	0.46	0.97	0.98
		4000	22.32	0.27	0.45	0.93	0.98
X-6	55	800	32.45	4.69	6.62	1.00	1.00
		1250	32.27	4.63	6.54	0.99	0.99
		2000	32.06	4.54	6.43	0.97	0.99
		3000	31.88	4.46	6.31	0.95	0.98
		4000	31.75	4.40	6.24	0.94	0.98
X-6	56	800	32.13	3.26	4.62	1.00	1.00
		1250	31.96	3.24	4.58	0.99	0.99
		2000	31.75	3.20	4.53	0.98	0.99
		3000	31.56	3.16	4.47	0.97	0.98
		4000	31.44	3.12	4.43	0.96	0.98
X-6	57	800	15.06	0.25	0.42	1.00	1.00
		1250	14.94	0.25	0.41	1.00	0.99
		2000	14.80	0.24	0.40	0.96	0.98
		3000	14.67	0.24	0.39	0.96	0.97
		4000	14.58	0.23	0.38	0.92	0.97
X-6	58	800	26.79	3.70	5.04	1.00	1.00
		1250	26.66	3.68	5.01	0.99	1.00
		2000	26.50	3.65	4.98	0.99	0.99
		3000	26.37	3.62	4.93	0.98	0.98
		4000	26.30	3.59	4.89	0.97	0.98
X-6	59	800	29.29	1.95	2.82	1.00	1.00
		1250	29.11	1.92	2.78	0.98	0.99
		2000	28.90	1.88	2.73	0.96	0.99
		3000	28.73	1.84	2.68	0.94	0.98
		4000	28.62	1.82	2.65	0.93	0.98
X-6	60	800	17.42	0.43	0.63	1.00	1.00
		1250	17.28	0.42	0.62	0.98	0.99
		2000	17.11	0.42	0.61	0.98	0.98
		3000	16.96	0.41	0.60	0.95	0.97
		4000	16.86	0.41	0.59	0.95	0.97
X-6	61	800	14.73	0.48	0.75	1.00	1.00
		1250	14.59	0.45	0.71	0.94	0.99
		2000	14.43	0.41	0.66	0.85	0.98
		3000	14.29	0.39	0.63	0.81	0.97
		4000	14.20	0.38	0.61	0.79	0.96
X-6	62	800	30.94	27.55	32.60	1.00	1.00
		1250	30.74	27.29	32.34	0.99	0.99
		2000	30.50	26.93	31.94	0.98	0.99
		3000	30.29	26.56	31.53	0.96	0.98
		4000	30.15	26.28	31.22	0.95	0.97

Table E.2. (Cont.)

	Sample	NOP, psi	ø, %	k_L, md	k_{air}, md	$\frac{k_L}{k_{L@800psi}}$	$\frac{\phi}{\phi_{@800psi}}$
X-6	63	800	29.89	8.78	11.35	1.00	1.00
		1250	29.69	8.67	11.21	0.99	0.99
		2000	29.44	8.53	11.04	0.97	0.98
		3000	29.23	8.39	10.87	0.96	0.98
		4000	29.08	8.30	10.74	0.95	0.97
X-6	64	800	30.47	6.02	8.14	1.00	1.00
		1250	30.32	5.91	8.00	0.98	1.00
		2000	30.14	5.78	7.84	0.96	0.99
		3000	29.98	5.67	7.69	0.94	0.98
		4000	29.87	5.60	7.61	0.93	0.98
X-6	65	800	33.14	14.86	18.61	1.00	1.00
		1250	32.95	14.71	18.43	0.99	0.99
		2000	32.73	14.51	18.19	0.98	0.99
		3000	32.52	14.29	17.94	0.96	0.98
		4000	32.38	14.13	17.74	0.95	0.98
X-6	66	800	13.75	0.25	0.38	1.00	1.00
		1250	13.67	0.24	0.37	0.96	0.99
		2000	13.56	0.24	0.37	0.96	0.99
		3000	13.46	0.23	0.35	0.92	0.98
		4000	13.38	0.23	0.35	0.92	0.97
X-6	67	800	14.42	0.69	0.92	1.00	1.00
		1250	14.35	0.68	0.91	0.99	1.00
		2000	14.26	0.67	0.90	0.97	0.99
		3000	14.19	0.66	0.89	0.96	0.98
		4000	14.14	0.65	0.88	0.94	0.98
X-6	68	800	18.84	1.61	2.21	1.00	1.00
		1250	18.75	1.60	2.19	0.99	1.00
		2000	18.64	1.58	2.17	0.98	0.99
		3000	18.55	1.56	2.14	0.97	0.98
		4000	18.48	1.55	2.12	0.96	0.98
X-6	69	800	16.10	0.05	0.12	1.00	1.00
		1250	15.90	0.05	0.11	1.00	0.99
		2000	15.67	0.04	0.11	0.80	0.97
		3000	15.50	0.04	0.10	0.80	0.96
		4000	15.41	0.04	0.09	0.80	0.96
X-6	70	800	32.09	4.20	6.02	1.00	1.00
		1250	31.91	4.16	5.77	0.99	0.99
		2000	31.69	4.09	5.67	0.97	0.99
		3000	31.51	4.00	5.55	0.95	0.98
		4000	31.40	3.94	5.47	0.94	0.98
X-6	71	800	24.55	1.09	1.66	1.00	1.00
		1250	24.41	1.08	1.64	0.99	0.99
		2000	24.24	1.07	1.62	0.98	0.99
		3000	24.09	1.05	1.59	0.96	0.98
		4000	24.00	1.04	1.57	0.95	0.98

Table E.2. (Cont.)

	Sample	NOP, psi	ø, %	k_L, md	k_{air}, md	$\frac{k_L}{k_{L@800psi}}$	$\frac{\phi}{\phi_{@800psi}}$
X-6	72	800	32.40	8.21	10.90	1.00	1.00
		1250	32.23	8.12	10.78	0.99	0.99
		2000	32.03	7.99	10.62	0.97	0.99
		3000	31.84	7.85	10.46	0.96	0.98
		4000	31.70	7.75	10.33	0.94	0.98
X-6	73	800	14.96	0.68	0.83	1.00	1.00
		1250	14.87	0.68	0.81	1.00	0.99
		2000	14.76	0.66	0.80	0.97	0.99
		3000	14.67	0.65	0.78	0.96	0.98
		4000	14.61	0.64	0.77	0.94	0.98
X-6	74	800	25.85	1.63	2.38	1.00	1.00
		1250	25.68	1.62	2.36	0.99	0.99
		2000	25.48	1.60	2.33	0.98	0.99
		3000	25.31	1.57	2.30	0.96	0.98
		4000	25.20	1.56	2.27	0.96	0.97
X-6	75	800	21.73	9.23	10.85	1.00	1.00
		1250	21.52	8.16	9.66	0.88	0.99
		2000	21.26	7.01	8.34	0.76	0.98
		3000	21.05	6.17	7.38	0.67	0.97
		4000	20.92	5.72	6.87	0.62	0.96
X-6	76	800	11.77	0.15	0.26	1.00	1.00
		1250	11.64	0.15	0.26	1.00	0.99
		2000	11.49	0.15	0.25	1.00	0.98
		3000	11.37	0.15	0.25	1.00	0.97
		4000	11.29	0.14	0.24	0.93	0.96
X-6	77	800	31.15	2.70	3.92	1.00	1.00
		1250	30.95	2.66	3.86	0.99	0.99
		2000	30.70	2.61	3.80	0.97	0.99
		3000	30.49	2.57	3.74	0.95	0.98
		4000	30.35	2.54	3.70	0.94	0.97
X-6	78	800	16.60	0.03	0.05	1.00	1.00
		1250	16.33	0.02	0.06	0.67	0.98
		2000	16.02	0.02	0.05	0.67	0.97
		3000	15.80	0.02	0.04	0.67	0.95
		4000	15.69	0.02	0.04	0.67	0.95
X-6	79	800	18.68	0.87	1.35	1.00	1.00
		1250	18.57	0.83	1.29	0.95	0.99
		2000	18.43	0.77	1.20	0.89	0.99
		3000	18.31	0.72	1.13	0.83	0.98
		4000	18.21	0.69	1.09	0.79	0.97
X-6	80	800	21.23	0.88	1.41	1.00	1.00
		1250	21.08	0.86	1.38	0.98	0.99
		2000	20.90	0.84	1.35	0.95	0.98
		3000	20.74	0.82	1.32	0.93	0.98
		4000	20.62	0.81	1.29	0.92	0.97

Table E.2. (Cont.)

	Sample	NOP, psi	ø, %	k_L, md	k_{air}, md	$\frac{k_L}{k_{L@800psi}}$	$\frac{\phi}{\phi_{@800psi}}$
X-6	81	800	18.30	0.46	0.78	1.00	1.00
		1250	18.18	0.45	0.77	0.98	0.99
		2000	18.03	0.44	0.75	0.96	0.99
		3000	17.89	0.43	0.73	0.93	0.98
		4000	17.81	0.42	0.72	0.91	0.97
X-6	82	800	21.96	0.91	1.37	1.00	1.00
		1250	21.73	0.90	1.36	0.99	0.99
		2000	21.47	0.88	1.34	0.97	0.98
		3000	21.28	0.87	1.31	0.96	0.97
		4000	21.18	0.85	1.29	0.93	0.96
X-6	83	800	23.12	1.84	2.71	1.00	1.00
		1250	22.91	1.68	2.55	0.91	0.99
		2000	22.67	1.51	2.35	0.82	0.98
		3000	22.46	1.40	2.20	0.76	0.97
		4000	22.33	1.35	2.13	0.73	0.97
X-6	84	800	21.66	1.13	1.74	1.00	1.00
		1250	21.49	1.11	1.72	0.98	0.99
		2000	21.29	1.09	1.69	0.96	0.98
		3000	21.13	1.07	1.65	0.95	0.98
		4000	21.02	1.05	1.63	0.93	0.97
X-6	85	800	35.21	12.07	15.02	1.00	1.00
		1250	34.97	11.82	14.71	0.98	0.99
		2000	34.68	11.43	14.28	0.95	0.98
		3000	34.42	11.01	13.80	0.91	0.98
		4000	34.22	10.65	13.33	0.88	0.97
X-6	86	800	16.16	0.21	0.39	1.00	1.00
		1250	16.00	0.21	0.38	1.00	0.99
		2000	15.81	0.21	0.37	1.00	0.98
		3000	15.63	0.20	0.37	0.95	0.97
		4000	15.51	0.20	0.36	0.95	0.96
X-6	87	800	20.12	0.79	1.25	1.00	1.00
		1250	20.00	0.78	1.23	0.99	0.99
		2000	19.85	0.76	1.20	0.96	0.99
		3000	19.71	0.74	1.17	0.94	0.98
		4000	19.60	0.73	1.16	0.92	0.97
X-6	88	800	24.66	15.30	19.32	1.00	1.00
		1250	24.50	15.06	19.01	0.98	0.99
		2000	24.32	14.73	18.60	0.96	0.99
		3000	24.18	14.40	18.20	0.94	0.98
		4000	24.09	14.16	17.83	0.93	0.98
X-6	89	800	22.18	2.45	3.25	1.00	1.00
		1250	22.08	2.43	3.21	0.99	1.00
		2000	21.96	2.39	3.17	0.98	0.99
		3000	21.85	2.35	3.12	0.96	0.99
		4000	21.78	2.32	3.08	0.95	0.98

Table E.2. (Cont.)

	Sample	NOP, psi	ø, %	k_L, md	k_{air}, md	$\frac{k_L}{k_{L@800psi}}$	$\frac{\phi}{\phi_{@800psi}}$
X-6	90	800	32.58	16.85	20.98	1.00	1.00
		1250	32.46	16.67	20.78	0.99	1.00
		2000	32.31	16.44	20.50	0.98	0.99
		3000	32.18	16.21	20.24	0.96	0.99
		4000	32.09	16.04	20.03	0.95	0.98
X-6	91	800	13.55	0.20	0.33	1.00	1.00
		1250	13.46	0.20	0.33	1.00	0.99
		2000	13.35	0.19	0.32	0.95	0.99
		3000	13.25	0.19	0.31	0.95	0.98
		4000	13.18	0.18	0.30	0.90	0.97
X-6	92	800	35.61	22.84	28.25	1.00	1.00
		1250	35.44	22.58	27.96	0.99	1.00
		2000	35.22	22.22	27.54	0.97	0.99
		3000	35.03	21.84	27.08	0.96	0.98
		4000	34.90	21.54	26.73	0.94	0.98
X-6	93	800	22.63	1.51	2.05	1.00	1.00
		1250	22.51	1.48	2.01	0.98	0.99
		2000	22.34	1.44	1.96	0.95	0.99
		3000	22.19	1.40	1.91	0.93	0.98
		4000	22.08	1.38	1.88	0.91	0.98
X-6	94	800	32.62	20.12	24.35	1.00	1.00
		1250	32.45	19.86	24.06	0.99	0.99
		2000	32.25	19.51	23.64	0.97	0.99
		3000	32.07	19.15	23.23	0.95	0.98
		4000	31.95	18.89	22.94	0.94	0.98
X-6	95	800	16.43	0.54	0.85	1.00	1.00
		1250	16.35	0.53	0.83	0.98	1.00
		2000	16.24	0.51	0.81	0.94	0.99
		3000	16.14	0.50	0.79	0.93	0.98
		4000	16.06	0.49	0.77	0.91	0.98
X-6	96	800	18.53	0.68	1.06	1.00	1.00
		1250	18.40	0.68	1.05	1.00	0.99
		2000	18.24	0.67	1.03	0.99	0.98
		3000	18.08	0.66	1.02	0.97	0.98
		4000	17.98	0.65	1.00	0.96	0.97
X-6	97	800	32.26	16.32	20.15	1.00	1.00
		1250	32.06	16.15	19.96	0.99	0.99
		2000	31.82	15.92	19.69	0.98	0.99
		3000	31.60	15.69	19.42	0.96	0.98
		4000	31.45	15.51	19.21	0.95	0.97
X-6	98	800	33.62	16.20	20.27	1.00	1.00
		1250	33.46	16.00	20.04	0.99	1.00
		2000	33.25	15.72	19.70	0.97	0.99
		3000	33.06	15.42	19.35	0.95	0.98
		4000	32.92	15.20	19.09	0.94	0.98

Table E.3. X-Field water-oil relative permeability data

Sample 2184				Sample 193				Sample 2201			
X-2				X-2				X-2			
Sw %	*krw*	*kro*	*krw/kro*	*Sw %*	*krw*	*kro*	*krw/kro*	*Sw %*	*krw*	*kro*	*krw/kro*
44.5129	0.0000	1.0000	0.0000	11.9601	0.0000	1.0000	0.0000	13.2075	0.0000	1.0000	0.0000
58.8163	0.0538	0.2808	0.1917	47.2315	0.0391	0.1341	0.2916	30.1258	0.0270	0.4540	0.0595
62.8237	0.1101	0.1869	0.5888	50.4983	0.0748	0.1032	0.7244	42.7044	0.0892	0.1739	0.5129
65.6597	0.1476	0.1346	1.0965	53.4330	0.0856	0.0697	1.2274	47.1069	0.1607	0.1452	1.1066
68.0025	0.1382	0.0872	1.5849	55.9247	0.1152	0.0646	1.7824	50.7547	0.1969	0.1082	1.8197
69.8520	0.1644	0.0726	2.2646	57.8627	0.1434	0.0576	2.4889	53.5849	0.2355	0.0849	2.7733
71.8866	0.1573	0.0464	3.3884	59.5238	0.1672	0.0510	3.2810	55.7862	0.2629	0.0644	4.0832
73.7978	0.1903	0.0369	5.1523	61.1849	0.1798	0.0367	4.8978	57.6730	0.2849	0.0523	5.4450
75.2158	0.1960	0.0258	7.6033	62.7353	0.1975	0.0264	7.4817	59.2453	0.2963	0.0380	7.7983
76.4488	0.1953	0.0179	10.9396	64.0089	0.2118	0.0207	10.2329	60.5031	0.3073	0.0307	10.0000
77.5586	0.2049	0.0132	15.4882	65.0055	0.2207	0.0164	13.4586	61.7610	0.3253	0.0228	14.2561
78.3600	0.2085	0.0103	20.1837	65.7254	0.2317	0.0141	16.4816	63.0189	0.3349	0.0164	20.4174
79.2848	0.2155	0.0080	26.9153	66.8328	0.2478	0.0111	22.2331	64.4025	0.3514	0.0119	29.5121
81.0111	0.2280	0.0046	50.0035	68.7708	0.2812	0.0077	36.3078	66.1006	0.3476	0.0065	53.4564
82.8607	0.2340	0.0015	152.4053	70.9856	0.3075	0.0032	96.8278	67.9874	0.3607	0.0027	133.9677
84.2170	0.2427	0.0005	497.7371	72.6467	0.3181	0.0015	206.0630	69.5597	0.3621	0.0007	532.1083
85.4501	0.2449	0.0000	-	75.4153	0.3381	0.0000	-	70.8176	0.3554	0.0000	-

Table E.3. (Cont.)

Sample 2225				Sample 2235				Sample 2239			
X-2				X-2				X-2			
Sw %	*krw*	*kro*	*krw/kro*	*Sw %*	*krw*	*kro*	*krw/kro*	*Sw %*	*krw*	*kro*	*krw/kro*
13.8655	0.0000	1.0000	0.0000	9.3369	0.0000	1.0000	0.0000	14.9578	0.0000	1.0000	0.0000
38.2353	0.0048	0.3834	0.0125	20.8390	0.0129	0.4400	0.0293	25.6936	0.0087	0.4795	0.0182
46.9013	0.0164	0.2008	0.0817	28.6198	0.0542	0.2259	0.2399	39.5657	0.0250	0.1472	0.1698
52.6786	0.0330	0.0959	0.3443	33.0176	0.0781	0.1444	0.5408	51.5078	0.0716	0.0738	0.9705
57.1429	0.0447	0.0537	0.8318	37.0771	0.0871	0.1039	0.8375	55.0060	0.1113	0.0617	1.8030
60.0315	0.0831	0.0562	1.4791	40.4601	0.1010	0.0784	1.2882	57.1170	0.1451	0.0540	2.6853
62.6576	0.1110	0.0507	2.1878	43.0311	0.1308	0.0690	1.8967	58.8058	0.1657	0.0426	3.8905
65.0210	0.1310	0.0369	3.5481	45.6022	0.1506	0.0520	2.8973	60.3739	0.1845	0.0348	5.2966
67.0168	0.1494	0.0285	5.2481	48.1732	0.1682	0.0314	5.3580	61.7612	0.2007	0.0255	7.8705
68.7500	0.1605	0.0202	7.9433	50.0677	0.1867	0.0232	8.0353	62.9674	0.2146	0.0197	10.9144
70.0630	0.1732	0.0154	11.2202	51.4208	0.1921	0.0180	10.6660	64.1737	0.2157	0.0131	16.5196
71.1134	0.1816	0.0129	14.1254	52.4357	0.2141	0.0153	14.0281	65.6815	0.2461	0.0097	25.4097
72.4265	0.2031	0.0093	21.8776	54.1272	0.2257	0.0102	22.2331	67.4910	0.2728	0.0054	50.5825
74.2647	0.2282	0.0057	39.8107	56.4953	0.2610	0.0051	50.8159	69.3004	0.2843	0.0023	121.6186
76.2605	0.2643	0.0027	97.7237	58.3897	0.2788	0.0023	122.4616	70.8082	0.2804	0.0008	369.8282
77.9937	0.2888	0.0009	331.1311	59.9459	0.2899	0.0012	243.7811	72.3764	0.2812	0.0000	-
79.8319	0.3139	0.0000	-	62.6522	0.3026	0.0000	-				

Table E.3. (Cont.)

Sample 2241				Sample 4				Sample 9			
X-2				X-3				X-4			
Sw %	*krw*	*kro*	*krw/kro*	*Sw %*	*krw*	*kro*	*krw/kro*	*Sw %*	*krw*	*kro*	*krw/kro*
30.3030	0.0000	1.0000	0.0000	9.6774	0.0000	1.0000	0.0000	29.9544	0.0000	1.0000	0.0000
40.8586	0.0210	0.4389	0.0479	55.6129	0.0445	0.0303	1.4702	38.5535	0.0316	0.3419	0.0925
46.9192	0.0387	0.2496	0.1549	58.0645	0.0703	0.0229	3.0690	42.4829	0.0727	0.2048	0.3548
51.7172	0.0895	0.2408	0.3715	59.3548	0.0772	0.0189	4.0832	45.8428	0.1029	0.1423	0.7228
55.7576	0.1179	0.1478	0.7980	60.6452	0.0927	0.0163	5.7016	48.5194	0.0986	0.0897	1.0990
58.5354	0.1870	0.1663	1.1246	61.9355	0.1041	0.0128	8.1283	50.7973	0.1319	0.0861	1.5311
60.8081	0.2096	0.1304	1.6069	63.2258	0.1150	0.0099	11.5878	53.0752	0.1434	0.0672	2.1330
63.0808	0.2400	0.1033	2.3227	64.3871	0.1201	0.0071	17.0216	55.3531	0.1606	0.0527	3.0479
65.1010	0.2505	0.0746	3.3574	65.2258	0.1294	0.0059	21.9786	57.3462	0.1722	0.0413	4.1687
66.6162	0.2782	0.0609	4.5709	66.1935	0.1412	0.0047	30.1301	59.0547	0.1871	0.0340	5.4954
68.1313	0.2920	0.0459	6.3680	67.8065	0.1611	0.0032	50.2343	60.6492	0.1989	0.0269	7.3961
69.4949	0.3130	0.0357	8.7700	69.7419	0.1843	0.0016	112.4605	62.2437	0.1992	0.0191	10.4232
70.6061	0.3315	0.0286	11.5878	71.3548	0.1918	0.0008	237.6840	64.2369	0.2304	0.0139	16.6341
72.0202	0.3579	0.0221	16.2181	74.3226	0.2201	0.0000	-	66.9704	0.2623	0.0085	30.7610
74.3434	0.4015	0.0149	26.8534					69.7039	0.2831	0.0033	85.1138
77.0202	0.4282	0.0049	87.4984					71.6970	0.2953	0.0015	197.2423
79.0404	0.4193	0.0016	267.9168					74.8292	0.3097	0.0000	-
80.8081	0.4293	0.0000	-								

Table E.3. (Cont.)

Sample 11				Sample 129				Sample 137			
X-4				X-5				X-5			
Sw %	*krw*	*kro*	*krw/kro*	*Sw %*	*krw*	*kro*	*krw/kro*	*Sw %*	*krw*	*kro*	*krw/kro*
12.2183	0.0000	1.0000	0.0000	17.4935	0.0000	1.0000	0.0000	15.8933	0.0000	1.0000	0.0000
41.0439	0.0189	0.0955	0.1978	49.1384	0.0090	0.2356	0.0380	30.1044	0.0062	0.4130	0.0150
44.8399	0.0306	0.0718	0.4266	52.2193	0.0157	0.1084	0.1445	36.1949	0.0127	0.1668	0.0759
48.5172	0.0291	0.0375	0.7762	54.1775	0.0205	0.0399	0.5129	42.8654	0.0367	0.1187	0.3090
51.7794	0.0521	0.0415	1.2560	56.1358	0.0437	0.0525	0.8318	47.7958	0.0549	0.0616	0.8913
54.1518	0.0806	0.0417	1.9320	58.0940	0.0594	0.0651	0.9120	49.8260	0.0871	0.0676	1.2882
55.8126	0.0889	0.0326	2.7290	59.7911	0.0650	0.0538	1.2078	51.4211	0.1159	0.0571	2.0324
57.3547	0.1011	0.0272	3.7154	61.2272	0.0839	0.0492	1.7061	52.7262	0.1231	0.0479	2.5704
59.0154	0.1140	0.0190	5.9979	62.4021	0.0943	0.0392	2.4044	53.7413	0.1436	0.0435	3.3037
60.4982	0.1214	0.0133	9.0991	63.4465	0.1003	0.0321	3.1189	54.4664	0.1631	0.0362	4.5082
61.6845	0.1340	0.0109	12.3027	64.4386	0.1104	0.0274	4.0365	55.4234	0.1727	0.0289	5.9704
63.1673	0.1531	0.0079	19.2752	65.3003	0.1215	0.0201	6.0534	56.6705	0.1859	0.0178	10.4472
65.2432	0.1815	0.0054	33.5738	66.2141	0.1317	0.0152	8.6497	57.6856	0.2073	0.0139	14.8936
67.6157	0.2062	0.0027	76.5597	67.2063	0.1398	0.0137	10.2329	58.5557	0.2176	0.0099	21.8776
69.3950	0.2031	0.0013	154.8817	68.3290	0.1532	0.0114	13.4896	59.5708	0.2398	0.0071	33.5738
73.3096	0.2735	0.0000	-	69.6345	0.1664	0.0094	17.7828	60.8759	0.2629	0.0040	65.1628
				70.5483	0.1760	0.0065	26.9153	62.1810	0.2772	0.0022	124.7384
				71.9321	0.1807	0.0011	158.4893	64.5012	0.3173	0.0000	-
				73.2115	0.1815	0.0000	-				

Table E.3. (Cont.)

Sample 142				Sample 156				Sample 161			
X-5				X-5				X-5			
Sw %	*krw*	*kro*	*krw/kro*	*Sw %*	*krw*	*kro*	*krw/kro*	*Sw %*	*krw*	*kro*	*krw/kro*
18.7994	0.0000	1.0000	0.0000	13.0855	0.0000	1.0000	0.0000	15.3887	0.0000	1.0000	0.0000
27.5244	0.0026	0.5429	0.0048	17.8416	0.0018	0.5880	0.0031	22.6071	0.0017	0.4941	0.0034
32.1080	0.0082	0.3735	0.0219	23.3704	0.0044	0.2529	0.0174	30.6187	0.0072	0.2063	0.0347
34.4812	0.0122	0.2441	0.0501	28.7301	0.0094	0.1420	0.0661	35.1137	0.0218	0.1543	0.1413
36.5286	0.0231	0.2210	0.1047	32.5930	0.0214	0.1025	0.2089	37.7578	0.0440	0.1525	0.2884
38.5761	0.0369	0.2142	0.1721	35.2487	0.0413	0.0924	0.4467	40.1375	0.0623	0.1075	0.5794
40.6003	0.0462	0.1785	0.2587	37.1801	0.0618	0.0784	0.7889	42.7816	0.0826	0.0916	0.9016
42.9037	0.0695	0.1555	0.4467	39.0633	0.0738	0.0627	1.1776	45.5579	0.1038	0.0707	1.4689
45.5095	0.0830	0.1181	0.7031	40.9464	0.0878	0.0516	1.7022	48.0698	0.1422	0.0631	2.2542
48.1852	0.1113	0.1120	0.9931	42.2743	0.1028	0.0365	2.8184	50.0529	0.1670	0.0505	3.3037
50.8609	0.1341	0.0958	1.3996	43.4814	0.1145	0.0301	3.8019	51.9038	0.1918	0.0384	5.0003
53.3039	0.1535	0.0768	1.9999	44.8093	0.1255	0.0207	6.0534	53.8340	0.2231	0.0274	8.1283
55.3979	0.1755	0.0637	2.7542	46.2096	0.1335	0.0135	9.8628	55.4997	0.2451	0.0197	12.4738
57.4919	0.1960	0.0440	4.4566	47.1994	0.1455	0.0101	14.4544	57.0862	0.2715	0.0130	20.9411
59.5859	0.2166	0.0294	7.3790	48.2376	0.1672	0.0066	25.5270	59.0693	0.3098	0.0073	42.4620
61.4472	0.2546	0.0199	12.8233	49.4447	0.1706	0.0020	85.3100	60.9201	0.3486	0.0032	107.6465
63.0758	0.2690	0.0121	22.2844	50.0000	0.1721	0.0011	158.4893	63.0354	0.3783	0.0000	-
65.2862	0.3099	0.0062	50.0000	50.8933	0.2163	0.0000	-				
70.0326	0.3666	0.0000	-								

Table E.3. (Cont.)

Sample 173				Sample 62				Sample 72			
X-5				X-6				X-6			
Sw %	*krw*	*kro*	*krw/kro*	*Sw %*	*krw*	*kro*	*krw/kro*	*Sw %*	*krw*	*kro*	*krw/kro*
13.0855	0.0000	1.0000	0.0000	13.6095	0.0000	1.0000	0.0000	15.2449	0.0000	1.0000	0.0000
14.1026	0.0000	1.0000	0.0000	22.6036	0.0041	0.4934	0.0083	51.5410	0.0322	0.0645	0.5000
43.2692	0.0044	0.1267	0.0348	28.8166	0.0100	0.1914	0.0522	52.9169	0.0589	0.0578	1.0186
46.3675	0.0106	0.0965	0.1097	36.8047	0.0380	0.1625	0.2339	54.2928	0.0619	0.0395	1.5668
48.7179	0.0206	0.0772	0.2666	41.8343	0.0480	0.0947	0.5070	55.8063	0.0733	0.0295	2.4831
51.0684	0.0320	0.0610	0.5248	44.3491	0.0498	0.0678	0.7345	57.3198	0.0854	0.0163	5.2360
53.8462	0.0529	0.0533	0.9931	46.7160	0.1417	0.1225	1.1561	58.3654	0.1000	0.0129	7.7625
56.4103	0.0671	0.0439	1.5276	48.7870	0.1797	0.1088	1.6520	58.9433	0.1051	0.0116	9.0782
58.4402	0.0763	0.0358	2.1281	50.9467	0.1270	0.0539	2.3550	59.7138	0.1137	0.0094	12.0781
60.1068	0.0909	0.0299	3.0409	52.8107	0.1642	0.0524	3.1333	61.2273	0.1314	0.0056	23.3346
61.4530	0.1000	0.0257	3.8905	54.3787	0.1796	0.0379	4.7424	63.0160	0.1526	0.0024	64.8634
62.8419	0.1078	0.0209	5.1642	55.7396	0.1945	0.0310	6.2661	66.8685	0.2035	0.0000	-
64.3376	0.1211	0.0155	7.8343	57.3964	0.2166	0.0228	9.4842				
65.7265	0.1320	0.0119	11.0662	59.8521	0.2328	0.0123	18.9234				
67.2222	0.1175	0.0068	17.2187	62.0710	0.2712	0.0057	47.2063				
69.0385	0.1731	0.0047	36.4754	63.5503	0.2886	0.0034	85.3100				
70.8547	0.1857	0.0019	97.4990	66.8047	0.3321	0.0000	-				
72.9915	0.2405	0.0000	-								

Table E.3. (Cont.)

Sample 75				Sample 83				Sample 88			
X-6				X-6				X-6			
Sw %	*krw*	*kro*	*krw/kro*	*Sw %*	*krw*	*kro*	*krw/kro*	*Sw %*	*krw*	*kro*	*krw/kro*
47.6334	0.0000	1.0000	0.0000	8.2426	0.0000	1.0000	0.0000	41.9971	0.0000	1.0000	0.0000
56.6969	0.0620	0.1961	0.3162	34.8367	0.0032	0.2000	0.0162	46.0352	0.0632	0.3832	0.1650
58.9627	0.0952	0.1485	0.6412	44.2457	0.0320	0.0923	0.3467	48.2379	0.0820	0.2529	0.3243
61.1279	0.1111	0.1132	0.9817	50.2722	0.0507	0.0338	1.4997	50.3671	0.1001	0.1744	0.5741
62.9406	0.1074	0.0785	1.3677	52.3328	0.0783	0.0316	2.4774	52.1292	0.1013	0.1290	0.7852
64.9547	0.1409	0.0740	1.9055	53.8880	0.0886	0.0233	3.8019	53.8913	0.1196	0.1144	1.0447
66.7170	0.1495	0.0575	2.6002	55.3655	0.1025	0.0192	5.3333	55.9471	0.1306	0.0912	1.4322
68.4794	0.1575	0.0443	3.5563	56.4541	0.1139	0.0147	7.7625	57.8928	0.1505	0.0802	1.8750
70.2417	0.1684	0.0340	4.9545	57.4261	0.1157	0.0096	12.0226	59.5448	0.1576	0.0650	2.4266
71.7523	0.1778	0.0247	7.1945	58.2037	0.1248	0.0063	19.8153	61.0132	0.1674	0.0520	3.2211
73.1621	0.1866	0.0187	10.0000	58.5925	0.1271	0.0048	26.3027	62.4816	0.1799	0.0435	4.1400
74.9245	0.2040	0.0128	15.9588	59.1757	0.1344	0.0033	40.7380	63.7665	0.1909	0.0371	5.1404
77.2407	0.2352	0.0079	29.6483	59.9533	0.1452	0.0025	58.8844	64.8678	0.1985	0.0317	6.2517
79.8087	0.2750	0.0041	66.3743	60.9253	0.1530	0.0016	97.2747	65.9692	0.2103	0.0279	7.5336
81.6717	0.3348	0.0023	144.2115	63.8414	0.1705	0.0000	-	67.6211	0.2298	0.0223	10.3276
85.1964	0.3916	0.0000	-					70.4846	0.2640	0.0128	20.5589
								73.5316	0.3026	0.0050	60.5341
								79.3686	0.3493	0.0000	-

Table E.3. (Cont.)

Sample 99				Sample 101			
X-6				X-6			
Sw %	*krw*	*kro*	*krw/kro*	*Sw %*	*krw*	*kro*	*krw/kro*
15.7706	0.0000	1.0000	0.0000	12.4183	0.0000	1.0000	0.0000
20.9229	0.0500	0.5902	0.0847	31.7320	0.0144	0.2137	0.0674
22.1774	0.0600	0.3637	0.1650	34.7386	0.0466	0.1941	0.2399
23.5215	0.0650	0.2301	0.2825	37.0261	0.0615	0.1410	0.4365
25.1792	0.0920	0.1990	0.4624	39.3137	0.0794	0.1288	0.6166
27.4194	0.1638	0.1965	0.8337	41.2745	0.0963	0.1058	0.9099
29.8835	0.1596	0.1409	1.1324	43.3987	0.1116	0.0959	1.1641
32.3477	0.1969	0.1149	1.7140	45.6863	0.1274	0.0806	1.5812
35.0358	0.1537	0.0642	2.3933	47.5817	0.1372	0.0654	2.0989
37.5000	0.1942	0.0525	3.6983	49.4771	0.1439	0.0499	2.8840
39.7401	0.2055	0.0351	5.8479	51.2745	0.1552	0.0360	4.3053
41.4427	0.2600	0.0294	8.8512	52.9085	0.1653	0.0249	6.6374
42.6075	0.2429	0.0201	12.1060	54.2157	0.1763	0.0181	9.7275
43.9964	0.2683	0.0153	17.5792	55.5229	0.1943	0.0132	14.7231
45.9229	0.2972	0.0090	33.0370	57.2549	0.2172	0.0068	31.9890
47.9391	0.3208	0.0037	85.7038	58.9869	0.2377	0.0030	79.4328
49.2832	0.3234	0.0017	186.2087	62.7451	0.2867	0.0000	-
51.5233	0.3881	0.0000	-				

Table E.4. X-Field capillary pressure data

Pc	Pore Throat Size	Sample									
		2181		2187		2190		2201		2209	
		X-2		X-2		X-2		-2		X-2	
		Drainage	Imbibition	Drainage	Imbibition	Drainage	Imbibition	Drainage	Imbibition	Drainage	Imbibition
psia	µm	Sw, %	Sw, %	Sw, %	Sw, %	Sw, %	Sw, %	Sw, %	Sw, %	Sw, %	Sw, %
3	71.09	100.00	49.15	100.00	56.52	100.00	66.80	100.00	68.92	100.00	61.27
6	35.54	100.00	49.15	100.00	56.01	100.00	66.79	100.00	68.90	100.00	61.27
9	23.70	100.00	49.15	100.00	55.79	100.00	66.55	100.00	68.75	100.00	61.29
12	17.77	100.00	49.10	100.00	55.79	100.00	66.18	100.00	68.74	100.00	61.18
15	14.22	100.00	49.10	100.00	55.75	100.00	61.44	100.00	65.89	100.00	61.14
18	11.85	100.00	49.10	100.00	55.75	100.00	54.67	100.00	63.45	100.00	58.09
21	10.16	100.00	49.09	100.00	55.66	100.00	45.74	100.00	57.80	100.00	52.52
24	8.89	100.00	49.07	100.00	55.62	100.00	39.36	100.00	49.59	100.00	46.30
27	7.90	100.00	48.97	100.00	55.62	100.00	35.70	100.00	43.49	100.00	42.65
30	7.11	100.00	48.78	100.00	55.62	100.00	31.46	100.00	39.43	100.00	39.26
40	5.33	100.00	48.70	100.00	55.47	99.60	22.30	100.00	27.63	100.00	28.35
55	3.88	100.00	47.28	100.00	54.78	91.11	16.51	93.70	17.37	99.85	18.85
75	2.84	100.00	42.86	100.00	51.94	66.49	12.86	58.25	12.54	79.00	14.01
95	2.24	100.00	39.14	100.00	46.90	42.03	11.22	35.91	10.73	47.55	11.31
115	1.85	100.00	35.94	100.00	42.23	29.27	9.82	24.43	9.39	35.72	10.05
165	1.29	96.27	29.67	95.33	31.13	18.00	8.93	14.45	8.73	19.64	8.17
315	0.68	57.03	20.66	63.52	16.98	11.64	7.13	8.74	6.73	10.13	6.44
615	0.35	30.68	16.41	22.37	11.91	7.72	6.19	6.58	6.03	7.64	5.42
915	0.23	19.24	15.03	13.37	10.66	6.51	5.94	5.85	5.75	5.76	5.27
1215	0.18	14.14	14.14	9.84	9.84	5.79	5.79	5.56	5.56	4.95	4.95

Table E.4. (Cont.)

Pc	Pore Throat Size	Sample									
		2213		2221		2225		2230		2233	
		X-2		X-2		X-2		X-2		X-2	
		Drainage	Imbibition	Drainage	Imbibition	Drainage	Imbibition	Drainage	Imbibition	Drainage	Imbibition
psia	µm	Sw, %	Sw, %	Sw, %	Sw, %	Sw, %	Sw, %	Sw, %	Sw, %	Sw, %	Sw, %
3	71.09	100.00	55.71	100.00	57.24	100.00	42.59	100.00	40.29	100.00	49.30
6	35.54	100.00	55.64	100.00	57.01	100.00	42.37	100.00	40.04	100.00	49.30
9	23.70	100.00	55.59	100.00	57.16	100.00	42.00	100.00	39.91	100.00	49.09
12	17.77	100.00	55.59	100.00	56.86	100.00	40.72	100.00	39.71	100.00	48.50
15	14.22	100.00	55.48	100.00	56.87	100.00	38.10	100.00	39.43	100.00	45.62
18	11.85	100.00	55.43	100.00	56.85	100.00	36.74	100.00	39.03	100.00	43.22
21	10.16	100.00	55.43	100.00	56.81	100.00	34.34	100.00	38.32	100.00	39.89
24	8.89	100.00	55.43	100.00	56.77	100.00	31.71	100.00	37.45	100.00	36.23
27	7.90	100.00	55.39	100.00	56.73	100.00	29.41	100.00	35.31	100.00	33.97
30	7.11	100.00	55.37	100.00	56.64	99.46	27.91	100.00	34.23	99.43	31.65
40	5.33	100.00	53.96	100.00	55.79	95.70	21.13	99.47	30.49	93.90	24.95
55	3.88	100.00	49.38	100.00	52.33	63.90	15.32	97.47	24.45	74.27	18.92
75	2.84	99.21	37.48	100.00	43.92	40.64	11.28	90.76	18.52	54.12	14.39
95	2.24	97.03	30.63	99.67	36.20	30.69	9.89	77.05	15.57	42.06	12.17
115	1.85	88.76	27.03	98.03	30.39	23.51	8.44	61.92	13.15	34.48	10.96
165	1.29	61.03	20.34	74.02	22.51	14.98	6.91	41.28	10.20	23.83	9.09
315	0.68	34.35	12.11	33.89	13.64	8.15	5.68	18.31	7.09	14.10	7.38
615	0.35	15.83	9.26	17.46	11.52	5.86	5.11	8.86	5.90	8.34	6.54
915	0.23	10.48	8.49	12.47	10.55	5.23	5.04	6.38	5.58	6.76	6.27
1215	0.18	8.01	8.01	10.28	10.28	4.95	4.95	5.55	5.55	6.27	6.27

Table E.4. (Cont.)

Pc	Pore Throat Size	Sample									
		2234		2239		2		4		8	
		X-2		X-2		X-3		X-4		X-4	
		Drainage	Imbibition	Drainage	Imbibition	Drainage	Imbibition	Drainage	Imbibition	Drainage	Imbibition
psia	µm	Sw, %	Sw, %	Sw, %	Sw, %	Sw, %	Sw, %	Sw, %	Sw, %	Sw, %	Sw, %
3	71.09	100.00	60.62	100.00	60.33	100.00	63.04	100.00	64.35	100.00	56.26
6	35.54	100.00	60.62	100.00	60.16	98.42	62.14	100.00	64.35	100.00	56.01
9	23.70	100.00	60.62	100.00	59.70	97.81	61.23	100.00	64.10	100.00	55.84
12	17.77	100.00	60.60	100.00	52.75	96.61	60.48	100.00	63.01	100.00	55.73
15	14.22	100.00	60.54	100.00	42.83	94.23	58.78	100.00	58.14	100.00	55.65
18	11.85	100.00	59.71	100.00	38.32	93.63	57.42	100.00	54.60	100.00	55.55
21	10.16	100.00	58.44	100.00	33.46	92.57	55.87	100.00	47.61	100.00	55.46
24	8.89	100.00	55.79	100.00	29.80	92.12	54.55	100.00	42.16	100.00	55.42
27	7.90	100.00	53.80	100.00	26.34	90.91	53.01	100.00	39.92	100.00	55.04
30	7.11	100.00	51.54	100.00	24.41	90.16	51.20	100.00	34.61	100.00	54.71
40	5.33	100.00	38.84	99.65	20.01	86.99	47.95	100.00	25.64	100.00	52.37
55	3.88	100.00	28.58	90.08	16.11	81.14	45.09	99.92	18.35	100.00	45.86
75	2.84	98.55	21.27	65.07	13.89	75.79	42.94	97.31	14.47	97.87	35.17
95	2.24	87.23	16.94	45.94	12.94	71.90	41.35	80.82	12.59	93.20	29.21
115	1.85	69.75	15.03	34.93	12.35	67.64	40.49	62.59	11.62	86.00	26.03
165	1.29	38.79	11.93	22.56	11.10	60.25	39.20	34.52	9.71	59.58	20.26
315	0.68	18.19	8.80	14.42	9.87	49.05	36.94	16.22	7.92	31.68	12.85
615	0.35	10.41	7.10	10.76	9.19	40.37	35.66	9.53	6.93	16.01	9.82
915	0.23	7.96	6.76	9.58	9.07	36.94	35.40	7.49	6.81	10.95	8.96
1215	0.18	6.50	6.50	9.02	9.02	35.40	35.40	6.68	6.68	8.62	8.62

Table E.4. (Cont.)

Pc	Pore Throat Size	Sample									
		9		10		11		97		103	
		X-4		X-4		X-4		X-5		X-5	
		Drainage	Imbibition	Drainage	Imbibition	Drainage	Imbibition	Drainage	Imbibition	Drainage	Imbibition
psia	µm	Sw, %	Sw, %	Sw, %	Sw, %	Sw, %	Sw, %	Sw, %	Sw, %	Sw, %	Sw, %
3	71.09	100.00	51.38	100.00	61.89	100.00	71.65	100.00	66.80	100.00	75.20
6	35.54	100.00	44.17	100.00	61.80	100.00	70.40	100.00	66.68	100.00	75.19
9	23.70	100.00	36.92	100.00	61.75	100.00	68.24	100.00	66.68	100.00	74.08
12	17.77	99.62	32.77	100.00	61.14	100.00	63.17	100.00	66.68	100.00	73.41
15	14.22	98.58	28.92	100.00	60.30	100.00	57.60	100.00	66.00	100.00	73.30
18	11.85	97.90	26.96	100.00	60.12	100.00	55.41	100.00	65.89	100.00	72.86
21	10.16	95.57	25.42	100.00	59.71	100.00	49.04	100.00	65.09	100.00	71.97
24	8.89	93.03	23.94	100.00	59.32	100.00	47.68	100.00	64.63	100.00	71.75
27	7.90	89.80	23.16	100.00	58.69	100.00	44.96	100.00	64.17	100.00	71.19
30	7.11	86.14	22.38	100.00	57.73	99.72	43.52	100.00	63.26	100.00	70.86
40	5.33	72.00	20.98	100.00	56.49	97.61	39.21	100.00	60.75	100.00	69.63
55	3.88	57.98	18.55	100.00	50.23	89.86	36.65	98.52	58.81	99.56	65.29
75	2.84	48.44	16.98	99.77	42.10	70.56	34.73	93.38	55.96	98.44	57.51
95	2.24	42.14	16.44	98.71	34.59	53.19	33.99	86.42	54.93	97.44	51.61
115	1.85	37.15	16.03	96.30	30.10	46.18	33.51	81.52	54.82	95.88	47.50
165	1.29	29.63	15.40	80.51	23.02	39.37	32.75	72.05	52.54	84.76	40.93
315	0.68	20.81	15.19	38.34	14.49	34.33	31.89	59.95	50.37	51.95	33.59
615	0.35	16.54	15.19	16.65	11.52	32.12	31.58	52.42	49.23	33.70	29.37
915	0.23	15.69	15.19	12.07	10.46	31.55	31.58	50.03	48.77	28.70	26.92
1215	0.18	15.19	15.19	10.18	10.18	31.08	31.08	48.66	48.66	26.47	26.47

Table E.4. (Cont.)

Pc	Pore Throat Size	Sample									
		116		127		135		137		140	
		X-5		X-5		X-5		X-5		X-5	
		Drainage	Imbibition	Drainage	Imbibition	Drainage	Imbibition	Drainage	Imbibition	Drainage	Imbibition
psia	µm	Sw, %	Sw, %	Sw, %	Sw, %	Sw, %	Sw, %	Sw, %	Sw, %	Sw, %	Sw, %
3	71.09	100.00	66.53	100.00	46.74	100.00	61.94	100.00	72.96	100.00	60.13
6	35.54	100.00	63.79	98.42	44.68	100.00	59.74	100.00	72.96	100.00	59.86
9	23.70	100.00	63.64	97.30	37.97	100.00	58.10	100.00	72.96	100.00	59.31
12	17.77	100.00	63.48	95.94	32.71	100.00	53.77	100.00	73.25	100.00	58.98
15	14.22	100.00	63.18	94.01	29.24	100.00	50.97	100.00	73.25	100.00	58.65
18	11.85	100.00	62.42	92.94	27.32	100.00	49.54	100.00	72.68	100.00	58.33
21	10.16	100.00	61.96	91.66	24.75	100.00	46.58	100.00	70.02	100.00	57.73
24	8.89	100.00	61.81	89.78	23.00	100.00	45.38	100.00	67.55	100.00	57.18
27	7.90	100.00	61.35	88.02	20.64	100.00	43.46	100.00	60.53	99.67	56.47
30	7.11	100.00	61.05	86.44	19.79	100.00	43.35	100.00	53.80	99.40	55.70
40	5.33	100.00	60.59	78.40	16.45	100.00	39.40	100.00	39.38	98.36	51.61
55	3.88	100.00	56.49	50.80	13.58	100.00	36.55	100.00	31.98	96.83	41.28
75	2.84	100.00	51.01	33.82	11.10	100.00	34.79	100.00	28.56	94.05	33.31
95	2.24	100.00	46.29	26.59	10.37	94.08	33.91	97.53	26.19	90.28	28.50
115	1.85	99.24	41.73	22.14	9.78	85.74	32.98	77.04	25.05	85.96	26.97
165	1.29	87.98	35.79	16.11	8.88	67.53	31.77	44.40	23.34	71.65	23.15
315	0.68	52.38	28.80	12.17	7.47	44.61	30.18	27.52	21.54	36.92	18.45
615	0.35	30.93	24.20	8.79	7.42	33.31	28.92	22.01	20.02	22.11	16.60
915	0.23	24.38	22.41	7.34	7.29	29.80	28.37	20.12	20.02	17.58	15.45
1215	0.18	22.41	22.41	6.82	6.82	27.88	27.88	20.02	20.02	15.18	15.18

Table E.4. (Cont.)

Pc	Pore Throat Size	Sample									
		142		147		150		157		161	
		X-5		X-5		X-5		X-5		X-5	
		Drainage	Imbibition	Drainage	Imbibition	Drainage	Imbibition	Drainage	Imbibition	Drainage	Imbibition
psia	µm	Sw, %	Sw, %	Sw, %	Sw, %	Sw, %	Sw, %	Sw, %	Sw, %	Sw, %	Sw, %
3	71.09	100.00	65.34	100.00	52.52	100.00	71.13	100.00	66.43	100.00	47.61
6	35.54	100.00	63.76	100.00	52.42	100.00	70.50	100.00	66.43	99.18	45.79
9	23.70	100.00	53.46	99.36	51.36	100.00	70.65	100.00	66.43	98.77	41.84
12	17.77	100.00	39.72	98.94	50.40	100.00	65.86	100.00	66.43	98.27	37.94
15	14.22	100.00	31.46	98.41	49.02	100.00	48.63	100.00	66.43	97.87	35.13
18	11.85	100.00	27.93	98.30	47.96	100.00	43.04	100.00	66.43	97.37	31.90
21	10.16	100.00	25.80	97.66	47.64	100.00	38.08	100.00	66.34	96.46	28.50
24	8.89	100.00	23.71	97.34	43.82	100.00	31.16	100.00	66.07	94.87	27.00
27	7.90	100.00	22.64	97.24	42.12	100.00	28.41	100.00	65.63	91.60	26.45
30	7.11	100.00	22.41	97.24	40.63	100.00	26.20	100.00	65.18	88.51	25.50
40	5.33	99.35	20.04	96.07	34.79	100.00	22.11	100.00	63.92	76.67	22.91
55	3.88	94.25	18.74	93.52	29.37	99.21	18.73	100.00	56.56	64.32	20.05
75	2.84	69.79	17.68	91.72	25.44	80.33	17.23	99.55	44.89	55.69	18.33
95	2.24	52.76	16.80	89.27	22.26	52.80	16.37	99.28	39.15	49.56	17.51
115	1.85	45.29	16.56	85.45	21.51	40.21	15.98	98.12	34.57	43.84	17.24
165	1.29	35.87	15.73	67.50	18.64	26.20	15.35	86.63	28.47	34.63	16.19
315	0.68	24.31	15.08	34.68	16.31	17.86	14.17	45.25	22.46	22.69	14.74
615	0.35	18.23	14.66	20.34	14.61	15.03	13.77	26.77	19.94	17.19	14.20
915	0.23	15.45	14.29	15.03	13.55	13.69	13.30	19.94	19.05	14.79	13.52
1215	0.18	13.83	13.83	12.91	12.91	12.43	12.43	19.05	19.05	13.47	13.47

Table E.4. (Cont.)

Pc	Pore Throat Size	Sample									
		165		167		58		60		64	
		X-5		X-5		X-6		X-6		X-6	
		Drainage	Imbibition	Drainage	Imbibition	Drainage	Imbibition	Drainage	Imbibition	Drainage	Imbibition
psia	µm	Sw, %	Sw, %	Sw, %	Sw, %	Sw, %	Sw, %	Sw, %	Sw, %	Sw, %	Sw, %
3	71.09	100.00	72.90	100.00	52.17	100.00	66.06	100.00	59.64	100.00	59.76
6	35.54	100.00	72.89	97.92	51.77	100.00	66.06	100.00	59.51	100.00	59.30
9	23.70	100.00	71.32	95.31	48.68	100.00	66.06	100.00	59.12	100.00	52.60
12	17.77	100.00	70.79	93.50	46.47	100.00	66.06	100.00	59.38	100.00	44.19
15	14.22	100.00	69.22	90.41	44.03	100.00	65.66	100.00	59.12	100.00	36.52
18	11.85	100.00	69.10	88.95	42.00	100.00	61.87	100.00	58.99	100.00	33.98
21	10.16	100.00	69.04	87.58	40.06	100.00	55.33	100.00	58.86	100.00	31.30
24	8.89	100.00	68.87	86.30	39.08	100.00	49.04	100.00	58.47	100.00	28.44
27	7.90	100.00	68.17	85.01	38.42	100.00	47.34	100.00	57.81	100.00	27.23
30	7.11	100.00	67.64	83.78	36.30	100.00	42.10	100.00	57.81	100.00	26.59
40	5.33	100.00	65.90	79.97	33.42	100.00	35.41	100.00	56.51	100.00	23.49
55	3.88	100.00	61.87	75.82	27.72	100.00	30.97	100.00	54.50	98.84	21.64
75	2.84	100.00	55.75	71.00	24.49	100.00	26.53	100.00	51.68	93.16	20.26
95	2.24	100.00	52.25	67.02	22.37	98.00	24.38	100.00	47.63	75.56	19.56
115	1.85	100.00	48.93	63.04	20.91	91.42	23.09	100.00	44.49	56.99	18.96
165	1.29	98.43	43.51	55.53	18.66	60.92	21.49	97.26	40.31	34.81	18.41
315	0.68	71.14	37.74	36.87	16.18	30.37	19.49	76.23	33.78	22.15	17.67
615	0.35	42.81	32.14	21.84	14.95	21.19	18.34	42.79	31.56	17.76	16.70
915	0.23	31.44	29.52	16.76	14.90	18.39	17.50	32.74	30.26	16.61	16.42
1215	0.18	28.47	28.47	14.90	14.90	17.40	17.40	28.69	28.69	16.33	16.33

Table E.4. (Cont.)

Pc	Pore Throat Size	Sample									
		66		72		79		87		90	
		X-6		X-6		X-6		X-6		X-6	
		Drainage	Imbibition	Drainage	Imbibition	Drainage	Imbibition	Drainage	Imbibition	Drainage	Imbibition
psia	µm	Sw, %	Sw, %	Sw, %	Sw, %	Sw, %	Sw, %	Sw, %	Sw, %	Sw, %	Sw, %
3	71.09	100.00	61.55	100.00	72.31	100.00	54.23	100.00	50.72	100.00	55.94
6	35.54	100.00	60.42	100.00	70.30	100.00	54.23	100.00	50.72	100.00	55.89
9	23.70	100.00	60.70	100.00	69.17	100.00	54.23	100.00	50.72	100.00	53.16
12	17.77	100.00	60.30	100.00	66.80	100.00	54.23	100.00	50.42	100.00	50.93
15	14.22	100.00	60.53	100.00	53.83	100.00	54.23	100.00	49.31	100.00	42.65
18	11.85	100.00	60.53	100.00	46.37	100.00	54.23	100.00	48.41	100.00	36.61
21	10.16	100.00	59.05	100.00	38.24	100.00	54.23	100.00	46.90	100.00	33.30
24	8.89	100.00	59.05	100.00	33.65	100.00	54.23	100.00	45.89	100.00	29.41
27	7.90	100.00	58.94	100.00	30.36	100.00	54.04	100.00	44.79	100.00	26.95
30	7.11	100.00	58.94	100.00	28.15	100.00	53.55	100.00	44.58	100.00	25.79
40	5.33	100.00	57.81	100.00	22.64	100.00	50.16	100.00	43.09	96.82	21.49
55	3.88	100.00	55.88	100.00	19.04	100.00	45.99	100.00	41.26	83.14	18.32
75	2.84	100.00	54.52	96.65	16.98	100.00	41.82	100.00	37.44	68.15	15.09
95	2.24	100.00	51.12	79.88	16.10	100.00	39.30	100.00	35.03	52.89	13.84
115	1.85	100.00	49.75	53.57	15.00	98.64	37.36	100.00	32.01	41.09	13.26
165	1.29	94.56	47.15	29.64	13.12	89.14	33.48	90.45	28.39	28.11	12.23
315	0.68	72.44	43.40	16.62	11.83	60.82	27.08	47.80	22.76	16.30	10.98
615	0.35	52.48	40.91	11.73	10.34	32.80	23.88	28.29	21.75	11.78	10.31
915	0.23	42.49	39.66	10.21	10.00	24.66	22.80	22.96	21.15	10.35	10.13
1215	0.18	38.98	38.98	9.77	9.77	21.55	21.55	21.15	21.15	9.64	9.64

Table E.4. (Cont.)

Pc	Pore Throat Size	Sample			
		96		98	
		X-6		X-6	
		Drainage	Imbibition	Drainage	Imbibition
psia	µm	Sw, %	Sw, %	Sw, %	Sw, %
3	71.09	100.00	61.48	100.00	63.67
6	35.54	100.00	61.48	100.00	63.45
9	23.70	100.00	61.29	100.00	59.00
12	17.77	100.00	60.61	100.00	51.40
15	14.22	100.00	59.17	100.00	39.57
18	11.85	100.00	56.66	100.00	36.15
21	10.16	100.00	54.84	100.00	30.54
24	8.89	100.00	54.26	100.00	26.10
27	7.90	100.00	52.04	100.00	24.59
30	7.11	100.00	51.95	100.00	22.27
40	5.33	100.00	48.67	98.40	18.54
55	3.88	100.00	45.11	90.26	15.92
75	2.84	100.00	41.06	70.25	13.87
95	2.24	100.00	39.14	50.11	12.76
115	1.85	99.52	38.18	38.06	12.27
165	1.29	86.13	33.36	24.28	11.56
315	0.68	50.50	28.16	14.67	10.62
615	0.35	32.69	24.50	11.34	10.22
915	0.23	26.62	23.73	9.69	9.73
1215	0.18	23.63	23.63	9.56	9.56

Table E.5. X-Field pore throat size data

Pore Throat Size	Injected Volume / Total Pore Volume, %			
(μm)	X-2	X-2	X-2	X-2
	2181	**2187**	**2190**	**2201**
< 0.5	47.23	48.22	10.18	7.94
0.5 - 1.0	36.41	36.87	5.77	4.67
1.0 - 1.5	14.33	12.37	7.19	6.40
1.5 - 2.0	2.03	2.54	11.46	10.23
2.0 - 2.5	0.00	0.00	19.28	17.50
2.5 - 3.0	0.00	0.00	17.42	18.44
3.0 - 3.5	0.00	0.00	12.50	18.00
3.5 - 4.0	0.00	0.00	8.26	11.22
4.0 - 4.5	0.00	0.00	3.35	2.49
4.5 - 5.0	0.00	0.00	2.68	1.99
5.0 - 5.5	0.00	0.00	1.55	1.11
5.5 - 6.0	0.00	0.00	0.13	0.00
6.0 - 6.5	0.00	0.00	0.11	0.00
6.5 - 7.0	0.00	0.00	0.09	0.00
7.0 - 7.5	0.00	0.00	0.02	0.00
7.5 - 8.0	0.00	0.00	0.00	0.00
8.0 - 8.5	0.00	0.00	0.00	0.00
8.5 - 9.0	0.00	0.00	0.00	0.00
9.0 <	0.00	0.00	0.00	0.00
TOTAL	*100.00*	*100.00*	*100.00*	*100.00*

Pore Throat Size	Injected Volume / Total Pore Volume, %			
(μm)	X-2	X-2	X-2	X-2
	2209	**2213**	**2221**	**2225**
< 0.5	9.20	27.47	27.79	7.30
0.5 - 1.0	7.38	24.98	33.32	5.48
1.0 - 1.5	10.40	21.24	23.87	6.09
1.5 - 2.0	13.69	18.53	13.73	7.64
2.0 - 2.5	22.13	5.87	1.11	9.00
2.5 - 3.0	20.28	1.28	0.17	9.68
3.0 - 3.5	10.59	0.40	0.00	11.81
3.5 - 4.0	6.20	0.24	0.00	10.47
4.0 - 4.5	0.06	0.00	0.00	12.56
4.5 - 5.0	0.05	0.00	0.00	10.05
5.0 - 5.5	0.03	0.00	0.00	6.08
5.5 - 6.0	0.00	0.00	0.00	1.21
6.0 - 6.5	0.00	0.00	0.00	1.03
6.5 - 7.0	0.00	0.00	0.00	0.88
7.0 - 7.5	0.00	0.00	0.00	0.46
7.5 - 8.0	0.00	0.00	0.00	0.26
8.0 - 8.5	0.00	0.00	0.00	0.00
8.5 - 9.0	0.00	0.00	0.00	0.00
9.0 <	0.00	0.00	0.00	0.00
TOTAL	*100.00*	*100.00*	*100.00*	*100.00*

Table E.5. (Cont.)

Pore Throat Size	Injected Volume / Total Pore Volume, %			
(μm)	X-2	X-2	X-2	X-2
	2230	2233	2234	2239
< 0.5	14.79	11.96	15.30	13.06
0.5 - 1.0	19.10	8.74	16.86	6.89
1.0 - 1.5	16.81	7.99	20.76	8.27
1.5 - 2.0	17.55	8.96	24.14	11.33
2.0 - 2.5	15.45	10.25	15.65	15.68
2.5 - 3.0	8.38	10.15	6.11	14.75
3.0 - 3.5	3.40	10.23	0.74	12.70
3.5 - 4.0	2.21	8.18	0.43	8.49
4.0 - 4.5	0.79	7.75	0.00	3.78
4.5 - 5.0	0.63	6.20	0.00	3.02
5.0 - 5.5	0.42	4.15	0.00	1.74
5.5 - 6.0	0.17	1.79	0.00	0.11
6.0 - 6.5	0.14	1.51	0.00	0.10
6.5 - 7.0	0.12	1.30	0.00	0.08
7.0 - 7.5	0.02	0.55	0.00	0.02
7.5 - 8.0	0.00	0.27	0.00	0.00
8.0 - 8.5	0.00	0.00	0.00	0.00
8.5 - 9.0	0.00	0.00	0.00	0.00
9.0 <	0.00	0.00	0.00	0.00
TOTAL	*100.00*	*100.00*	*100.00*	*100.00*

Pore Throat Size	Injected Volume / Total Pore Volume, %			
(μm)	X-3	X-3	X-4	X-4
	2	4	8	9
< 0.5	45.82	13.73	25.85	19.23
0.5 - 1.0	10.82	14.90	24.75	7.57
1.0 - 1.5	6.98	18.70	21.04	6.27
1.5 - 2.0	5.80	22.88	17.37	6.17
2.0 - 2.5	4.36	18.60	6.45	5.96
2.5 - 3.0	3.05	9.01	2.82	5.12
3.0 - 3.5	2.72	1.33	1.08	4.84
3.5 - 4.0	2.24	0.78	0.63	4.40
4.0 - 4.5	2.31	0.03	0.00	5.54
4.5 - 5.0	1.85	0.02	0.00	4.43
5.0 - 5.5	1.42	0.01	0.00	4.21
5.5 - 6.0	1.02	0.00	0.00	4.57
6.0 - 6.5	0.87	0.00	0.00	3.87
6.5 - 7.0	0.74	0.00	0.00	3.31
7.0 - 7.5	0.54	0.00	0.00	2.57
7.5 - 8.0	0.50	0.00	0.00	2.12
8.0 - 8.5	0.63	0.00	0.00	1.69
8.5 - 9.0	0.48	0.00	0.00	1.43
9.0 <	7.84	0.00	0.00	6.71
TOTAL	*100.00*	*100.00*	*100.00*	*100.00*

Table E.5. (Cont.)

Pore Throat Size	Injected Volume / Total Pore Volume, %			
(μm)	X-4	X-4	X-5	X-5
	10	11	97	103
< 0.5	30.27	33.51	57.15	45.16
0.5 - 1.0	36.67	4.24	11.00	29.04
1.0 - 1.5	20.78	4.73	8.21	15.64
1.5 - 2.0	9.59	6.64	7.20	6.70
2.0 - 2.5	1.92	12.49	6.23	1.39
2.5 - 3.0	0.59	12.73	4.59	0.73
3.0 - 3.5	0.12	9.80	2.61	0.56
3.5 - 4.0	0.07	6.59	1.69	0.38
4.0 - 4.5	0.00	3.06	0.59	0.18
4.5 - 5.0	0.00	2.45	0.47	0.14
5.0 - 5.5	0.00	1.63	0.26	0.08
5.5 - 6.0	0.00	0.68	0.00	0.00
6.0 - 6.5	0.00	0.58	0.00	0.00
6.5 - 7.0	0.00	0.50	0.00	0.00
7.0 - 7.5	0.00	0.24	0.00	0.00
7.5 - 8.0	0.00	0.13	0.00	0.00
8.0 - 8.5	0.00	0.00	0.00	0.00
8.5 - 9.0	0.00	0.00	0.00	0.00
9.0 <	0.00	0.00	0.00	0.00
TOTAL	*100.00*	*100.00*	*100.00*	*100.00*

Pore Throat Size	Injected Volume / Total Pore Volume, %			
(μm)	X-5	X-5	X-5	X-5
	116	127	135	137
< 0.5	44.40	10.92	40.41	25.47
0.5 - 1.0	32.12	3.93	19.75	13.50
1.0 - 1.5	16.60	4.02	15.69	20.33
1.5 - 2.0	6.44	5.14	13.38	26.31
2.0 - 2.5	0.44	6.09	7.72	13.12
2.5 - 3.0	0.00	7.05	3.05	1.27
3.0 - 3.5	0.00	8.62	0.00	0.00
3.5 - 4.0	0.00	8.14	0.00	0.00
4.0 - 4.5	0.00	10.90	0.00	0.00
4.5 - 5.0	0.00	8.72	0.00	0.00
5.0 - 5.5	0.00	5.87	0.00	0.00
5.5 - 6.0	0.00	2.60	0.00	0.00
6.0 - 6.5	0.00	2.20	0.00	0.00
6.5 - 7.0	0.00	1.88	0.00	0.00
7.0 - 7.5	0.00	1.20	0.00	0.00
7.5 - 8.0	0.00	0.96	0.00	0.00
8.0 - 8.5	0.00	0.92	0.00	0.00
8.5 - 9.0	0.00	0.83	0.00	0.00
9.0 <	0.00	10.03	0.00	0.00
TOTAL	*100.00*	*100.00*	*100.00*	*100.00*

Table E.5. (Cont.)

Pore Throat Size	Injected Volume / Total Pore Volume, %			
(μm)	X-5	X-5	X-5	X-5
	140	142	147	150
< 0.5	31.41	22.05	29.35	16.81
0.5 - 1.0	29.06	10.10	27.59	6.71
1.0 - 1.5	17.71	8.02	18.75	9.08
1.5 - 2.0	9.58	8.25	11.36	12.88
2.0 - 2.5	4.34	12.60	3.41	20.67
2.5 - 3.0	2.49	13.56	1.61	17.88
3.0 - 3.5	1.41	12.42	0.92	9.59
3.5 - 4.0	1.00	7.83	0.82	5.69
4.0 - 4.5	0.60	2.02	1.01	0.31
4.5 - 5.0	0.48	1.61	0.81	0.25
5.0 - 5.5	0.40	0.98	0.59	0.14
5.5 - 6.0	0.34	0.21	0.38	0.00
6.0 - 6.5	0.28	0.18	0.32	0.00
6.5 - 7.0	0.24	0.15	0.27	0.00
7.0 - 7.5	0.19	0.03	0.05	0.00
7.5 - 8.0	0.17	0.00	0.01	0.00
8.0 - 8.5	0.17	0.00	0.06	0.00
8.5 - 9.0	0.12	0.00	0.07	0.00
9.0 <	0.00	0.00	2.62	0.00
TOTAL	*100.00*	*100.00*	*100.00*	*100.00*

Pore Throat Size	Injected Volume / Total Pore Volume, %			
(μm)	X-5	X-5	X-6	X-6
	157	161	58	60
< 0.5	38.38	20.64	26.96	63.80
0.5 - 1.0	34.93	10.14	24.13	26.69
1.0 - 1.5	18.56	8.05	23.75	8.02
1.5 - 2.0	6.73	7.40	19.33	1.49
2.0 - 2.5	0.81	6.30	4.80	0.00
2.5 - 3.0	0.23	4.85	1.03	0.00
3.0 - 3.5	0.23	4.38	0.00	0.00
3.5 - 4.0	0.13	3.94	0.00	0.00
4.0 - 4.5	0.00	4.88	0.00	0.00
4.5 - 5.0	0.00	3.90	0.00	0.00
5.0 - 5.5	0.00	3.63	0.00	0.00
5.5 - 6.0	0.00	3.83	0.00	0.00
6.0 - 6.5	0.00	3.24	0.00	0.00
6.5 - 7.0	0.00	2.78	0.00	0.00
7.0 - 7.5	0.00	2.16	0.00	0.00
7.5 - 8.0	0.00	1.85	0.00	0.00
8.0 - 8.5	0.00	1.71	0.00	0.00
8.5 - 9.0	0.00	1.35	0.00	0.00
9.0 <	0.00	4.97	0.00	0.00
TOTAL	*100.00*	*100.00*	*100.00*	*100.00*

Table E.5. (Cont.)

Pore Throat Size	Injected Volume / Total Pore Volume, %			
(μm)	X-6	X-6	X-6	X-6
	64	66	72	79
< 0.5	20.52	65.02	14.80	50.41
0.5 - 1.0	10.22	22.42	10.65	29.62
1.0 - 1.5	14.20	9.60	15.11	13.45
1.5 - 2.0	19.82	2.96	24.01	5.73
2.0 - 2.5	19.33	0.00	23.43	0.79
2.5 - 3.0	10.18	0.00	9.30	0.00
3.0 - 3.5	2.89	0.00	1.70	0.00
3.5 - 4.0	1.82	0.00	0.99	0.00
4.0 - 4.5	0.46	0.00	0.00	0.00
4.5 - 5.0	0.36	0.00	0.00	0.00
5.0 - 5.5	0.20	0.00	0.00	0.00
5.5 - 6.0	0.00	0.00	0.00	0.00
6.0 - 6.5	0.00	0.00	0.00	0.00
6.5 - 7.0	0.00	0.00	0.00	0.00
7.0 - 7.5	0.00	0.00	0.00	0.00
7.5 - 8.0	0.00	0.00	0.00	0.00
8.0 - 8.5	0.00	0.00	0.00	0.00
8.5 - 9.0	0.00	0.00	0.00	0.00
9.0 <	0.00	0.00	0.00	0.00
TOTAL	*100.00*	*100.00*	*100.00*	*100.00*

Pore Throat Size	Injected Volume / Total Pore Volume, %			
(μm)	X-6	X-6	X-6	X-6
	87	90	96	98
< 0.5	40.55	14.62	43.88	13.43
0.5 - 1.0	36.18	9.69	30.79	7.75
1.0 - 1.5	18.08	9.72	17.58	9.38
1.5 - 2.0	5.19	11.99	7.48	12.53
2.0 - 2.5	0.00	14.26	0.28	16.77
2.5 - 3.0	0.00	10.79	0.00	14.29
3.0 - 3.5	0.00	7.61	0.00	10.16
3.5 - 4.0	0.00	5.98	0.00	6.85
4.0 - 4.5	0.00	5.41	0.00	3.21
4.5 - 5.0	0.00	4.32	0.00	2.57
5.0 - 5.5	0.00	2.81	0.00	1.64
5.5 - 6.0	0.00	1.03	0.00	0.52
6.0 - 6.5	0.00	0.87	0.00	0.44
6.5 - 7.0	0.00	0.74	0.00	0.38
7.0 - 7.5	0.00	0.15	0.00	0.07
7.5 - 8.0	0.00	0.00	0.00	0.00
8.0 - 8.5	0.00	0.00	0.00	0.00
8.5 - 9.0	0.00	0.00	0.00	0.00
9.0 <	0.00	0.00	0.00	0.00
TOTAL	*100.00*	*100.00*	*100.00*	*100.00*

Table E.6. X-Field J-Function data

X-2		X-2		X-2		X-2		X-2		X-2	
2181		2187		2190		2201		2209		2213	
J	Sw*	J	Sw*	J	Sw*	J	Sw*	J	Sw*	J	Sw*
0.014	1.000	0.010	1.000	0.014	1.000	0.017	1.000	0.013	1.000	0.008	1.000
0.020	0.957	0.014	0.948	0.018	0.996	0.023	0.933	0.018	0.998	0.012	0.991
0.037	0.500	0.027	0.595	0.025	0.906	0.032	0.558	0.025	0.779	0.015	0.968
0.073	0.193	0.052	0.139	0.035	0.644	0.040	0.321	0.031	0.448	0.018	0.878
0.109	0.059	0.077	0.039	0.044	0.385	0.048	0.200	0.038	0.324	0.025	0.576
0.144	0.000	0.103	0.000	0.053	0.249	0.070	0.094	0.054	0.155	0.049	0.286
				0.076	0.130	0.133	0.034	0.103	0.055	0.095	0.085
				0.145	0.062	0.259	0.011	0.201	0.028	0.141	0.027
				0.283	0.021	0.386	0.003	0.299	0.009	0.188	0.000
				0.422	0.008	0.512	0.000	0.397	0.000		
				0.560	0.000						

X-2		X-2		X-2		X-2		X-2		X-2	
2221		2225		2230		2233		2234		2239	
J	Sw*	J	Sw*	J	Sw*	J	Sw*	J	Sw*	J	Sw*
0.010	1.000	0.012	1.000	0.006	1.000	0.011	1.000	0.012	1.000	0.011	1.000
0.013	0.996	0.014	0.994	0.008	0.994	0.012	0.994	0.016	0.984	0.015	0.996
0.015	0.978	0.018	0.955	0.010	0.973	0.016	0.935	0.020	0.863	0.020	0.891
0.022	0.710	0.025	0.620	0.014	0.902	0.022	0.726	0.024	0.676	0.027	0.616
0.042	0.263	0.034	0.375	0.018	0.757	0.030	0.511	0.035	0.345	0.035	0.406
0.081	0.080	0.044	0.271	0.022	0.597	0.038	0.382	0.067	0.125	0.042	0.285
0.121	0.024	0.053	0.195	0.031	0.378	0.046	0.301	0.130	0.042	0.060	0.149
0.161	0.000	0.076	0.106	0.060	0.135	0.066	0.187	0.194	0.016	0.115	0.059
		0.145	0.034	0.117	0.035	0.125	0.083	0.258	0.000	0.224	0.019
		0.283	0.010	0.174	0.009	0.244	0.022			0.334	0.006
		0.421	0.003	0.230	0.000	0.364	0.005			0.443	0.000
		0.559	0.000			0.483	0.000				

Table E.6. (Cont.)

X-3		X-3		X-4		X-4		X-4		X-4	
2		4		8		9		10		11	
J	Sw*	J	Sw*	J	Sw*	J	Sw*	J	Sw*	J	Sw*
0.001	1.000	0.009	1.000	0.007	1.000	0.005	1.000	0.007	1.000	0.009	1.000
0.001	0.975	0.013	0.999	0.010	0.977	0.006	0.995	0.009	0.997	0.010	0.996
0.002	0.966	0.018	0.971	0.013	0.926	0.008	0.983	0.012	0.986	0.014	0.965
0.002	0.947	0.023	0.795	0.015	0.847	0.009	0.975	0.014	0.959	0.019	0.853
0.003	0.911	0.027	0.599	0.022	0.558	0.011	0.948	0.021	0.783	0.026	0.573
0.003	0.901	0.039	0.298	0.042	0.252	0.012	0.918	0.039	0.313	0.033	0.321
0.004	0.885	0.075	0.102	0.083	0.081	0.014	0.880	0.076	0.072	0.039	0.219
0.004	0.878	0.146	0.031	0.123	0.025	0.015	0.837	0.114	0.021	0.057	0.120
0.005	0.859	0.217	0.009	0.164	0.000	0.020	0.670	0.151	0.000	0.108	0.047
0.005	0.848	0.288	0.000			0.028	0.505			0.211	0.015
0.007	0.799					0.038	0.392			0.314	0.007
0.009	0.708					0.048	0.318			0.417	0.000
0.013	0.625					0.058	0.259				
0.016	0.565					0.083	0.170				
0.020	0.499					0.159	0.066				
0.028	0.385					0.311	0.016				
0.054	0.211					0.462	0.006				
0.105	0.077					0.614	0.000				
0.156	0.024										
0.207	0.000										

Table E.6. (Cont.)

X-5		X-5		X-5		X-5		X-5		X-5	
97		102		116		127		135		137	
J	Sw*	J	Sw*	J	Sw*	J	Sw*	J	Sw*	J	Sw*
0.005	1.000	0.007	1.000	0.011	1.000	0.002	1.000	0.012	1.000	0.019	1.000
0.007	0.971	0.009	0.994	0.013	0.990	0.003	0.983	0.016	0.918	0.024	0.969
0.009	0.871	0.012	0.979	0.018	0.845	0.005	0.971	0.019	0.802	0.029	0.713
0.012	0.736	0.016	0.965	0.035	0.386	0.006	0.956	0.027	0.550	0.042	0.305
0.014	0.640	0.019	0.944	0.069	0.110	0.008	0.936	0.052	0.232	0.080	0.094
0.021	0.456	0.027	0.793	0.103	0.025	0.009	0.924	0.101	0.075	0.157	0.025
0.039	0.220	0.052	0.346	0.136	0.000	0.011	0.910	0.150	0.027	0.234	0.001
0.077	0.073	0.102	0.098			0.012	0.890	0.199	0.000	0.310	0.000
0.114	0.027	0.151	0.030			0.014	0.871				
0.152	0.000	0.201	0.000			0.015	0.854				
						0.021	0.768				
						0.028	0.472				
						0.039	0.290				
						0.049	0.212				
						0.059	0.164				
						0.085	0.100				
						0.162	0.057				
						0.317	0.021				
						0.472	0.006				
						0.626	0.000				

Table E.6. (Cont.)

X-5		X-5		X-5		X-5		X-5		X-5	
140		142		147		150		157		161	
J	Sw*	J	Sw*	J	Sw*	J	Sw*	J	Sw*	J	Sw*
0.005	1.000	0.013	1.000	0.001	1.000	0.016	1.000	0.008	1.000	0.001	1.000
0.006	0.996	0.018	0.992	0.002	0.993	0.022	0.991	0.012	0.994	0.003	0.991
0.006	0.993	0.024	0.933	0.003	0.988	0.030	0.775	0.015	0.991	0.004	0.986
0.009	0.981	0.033	0.649	0.003	0.982	0.038	0.461	0.018	0.977	0.006	0.980
0.012	0.963	0.042	0.452	0.004	0.980	0.046	0.317	0.025	0.835	0.007	0.975
0.016	0.930	0.051	0.365	0.005	0.973	0.066	0.157	0.048	0.324	0.009	0.970
0.020	0.885	0.073	0.256	0.006	0.970	0.127	0.062	0.094	0.095	0.010	0.959
0.024	0.835	0.140	0.122	0.006	0.968	0.248	0.030	0.140	0.011	0.011	0.941
0.035	0.666	0.273	0.051	0.007	0.968	0.369	0.014	0.186	0.000	0.013	0.903
0.067	0.256	0.406	0.019	0.009	0.955	0.490	0.000			0.014	0.867
0.131	0.082	0.539	0.000	0.013	0.926					0.019	0.730
0.195	0.028			0.017	0.905					0.026	0.588
0.258	0.000			0.022	0.877					0.035	0.488
				0.027	0.833					0.045	0.417
				0.038	0.627					0.054	0.351
				0.073	0.250					0.078	0.244
				0.142	0.085					0.149	0.107
				0.211	0.024					0.291	0.043
				0.281	0.000					0.432	0.015
										0.574	0.000

Table E.6. (Cont.)

X-5		X-5		X-6		X-6		X-6		X-6	
165		167		58		60		64		66	
J	Sw*	J	Sw*	J	Sw*	J	Sw*	J	Sw*	J	Sw*
0.010	1.000	0.002	1.000	0.017	1.000	0.011	1.000	0.011	1.000	0.010	1.000
0.014	0.978	0.004	0.976	0.022	0.976	0.015	0.962	0.015	0.986	0.014	0.911
0.027	0.597	0.006	0.945	0.026	0.896	0.029	0.667	0.021	0.918	0.026	0.548
0.052	0.200	0.008	0.924	0.038	0.527	0.057	0.198	0.026	0.708	0.051	0.221
0.077	0.042	0.010	0.887	0.072	0.157	0.085	0.057	0.032	0.486	0.076	0.058
0.102	0.000	0.012	0.870	0.141	0.046	0.113	0.000	0.046	0.221	0.101	0.000
		0.014	0.854	0.210	0.012			0.087	0.070		
		0.016	0.839	0.279	0.000			0.170	0.017		
		0.018	0.824					0.253	0.003		
		0.020	0.809					0.337	0.000		
		0.027	0.765								
		0.037	0.716								
		0.050	0.659								
		0.063	0.612								
		0.077	0.566								
		0.110	0.477								
		0.210	0.258								
		0.411	0.082								
		0.611	0.022								
		0.811	0.000								

Table E.6. (Cont.)

X-6		X-6		X-6		X-6		X-6		X-6	
Tapa No : 72		Tapa No : 79		Tapa No : 87		Tapa No : 90		Tapa No : 96		Tapa No : 98	
J	Sw*	J	Sw*	J	Sw*	J	Sw*	J	Sw*	J	Sw*
0.017	1.000	0.014	1.000	0.014	1.000	0.013	1.000	0.012	1.000	0.012	1.000
0.023	0.963	0.017	0.983	0.021	0.879	0.017	0.965	0.014	0.994	0.017	0.982
0.029	0.777	0.024	0.862	0.040	0.338	0.024	0.813	0.020	0.818	0.023	0.892
0.035	0.485	0.046	0.501	0.077	0.091	0.032	0.648	0.039	0.352	0.031	0.671
0.051	0.220	0.090	0.143	0.115	0.023	0.041	0.479	0.076	0.119	0.040	0.448
0.097	0.076	0.134	0.040	0.153	0.000	0.049	0.348	0.112	0.039	0.048	0.315
0.189	0.022	0.178	0.000			0.071	0.204	0.149	0.000	0.069	0.163
0.281	0.005					0.135	0.074			0.131	0.057
0.373	0.000					0.263	0.024			0.256	0.020
						0.392	0.008			0.381	0.001
						0.520	0.000			0.506	0.000

APPENDIX F

PVT DATA

Table F.1. Constant Mass Expansion Test Results

Pressure (psig)	Relative Volume	Oil Density (gr/cc)
3000	0.9854	0.9374
2000	0.9900	0.9327
1000	0.9938	0.9295
750	0.9952	0.9281
500	0.9968	0.9267
400	0.9975	0.9261
300	0.9982	0.9254
200	0.9992	0.9245
150	0.9997	0.9241
105	1.0000	0.9237
93	1.0047	

Table F.2. Viscosity Test Results

Pressure (psig)	Viscosity (cp)
3000	207.4
2500	198.4
2000	183.4
1500	172.2
1000	161.9
500	151.6
250	144.0
150	138.2
105	138.0
60	141.0
0	184.4

Table F.3. Zero-Flash Separator Test Results

Pressure (psig)	Gas / Oil Ratio (scf / STB)
3000	1.0199
2000	1.0251
1000	1.0286
750	1.0301
500	1.0318
400	1.0324
300	1.0332
200	1.0342
150	1.0347
105	1.0351
0	1.0231

Table F.4. Compositional Analysis Results

Components	Separator Gas Mol %	Separator Oil Mol %	Reservoir Oil Mol %
N_2	8.834	0.000	0.120
C_1	87.923	0.000	3.770
C_2	1.421	0.220	0.300
C_3	0.465	0.280	0.300
iC_4	0.290	0.230	0.240
nC_4	0.177	0.570	0.560
iC_5	0.231	1.180	1.140
nC_5	0.273	1.300	1.260
nC_6	0.0381	5.770	5.550
nC_7		9.220	8.860
C_8		10.630	10.220
C_9		11.210	10.770
C_{10}		13.360	12.840
C_{11}		7.760	7.460
C_{12}		7.240	6.960
C_{13}		3.930	3.780
C_{14}		2.110	2.030
C_{15}		2.320	2.230
C_{16}		1.810	1.740
C_{17}		0.990	0.950
C_{18}		1.400	1.350
C_{19}		1.360	1.310
C_{20}		1.710	1.640

C_{21}		0.950	0.910
C_{22}		0.870	0.840
C_{23}		0.860	0.830
C_{24}		0.950	0.910
C_{25}		0.590	0.570
C_{26}		2.270	2.180
C_{27}		4.480	4.300
C_{28}		3.220	3.090
C_{29}		0.230	0.220
C_{30}		0.350	0.340
C_{31}		0.180	0.170
C_{32}		0.300	0.290
C_{33}		0.000	0.000
C_{34}		0.000	0.000
C_{35}		0.000	0.000
C_{36}		0.000	0.000
C_{36+}		0.000	0.000
	100.000	100.000	100.000

Table F.5. Relative volume - EOS results for Riazi and Daubert's method.

Vr							
PR		SRK-Peneloux		SRK		PR-Peneloux	
P-psi	Vr	P-psi	Vr	P-psi	Vr	P-psi	Vr
3000	0.9873	3000	0.9821	3000	0.9848	3000	0.9867
2000	0.9914	2000	0.9878	2000	0.9896	2000	0.9909
1000	0.9959	1000	0.9942	1000	0.9950	1000	0.9957
750	0.9971	750	0.9959	750	0.9965	750	0.9969
500	0.9983	500	0.9977	500	0.9980	500	0.9983
400	0.9989	400	0.9984	400	0.9987	400	0.9988
300	0.9994	300	0.9992	300	0.9993	300	0.9993
200	0.9999	200	0.9999	200	1.0000	200	0.9999
181	1.0000	193	1.0000	193	1.0000	181	1.0000
150	1.0847	150	1.1176	150	1.1001	150	1.0890
105	1.3184	105	1.3650	105	1.3108	105	1.3345
100	1.3587	100	1.4075	100	1.3470	100	1.3768
93	1.4229	93	1.4751	93	1.4046	93	1.4443

Table F.6. Viscosity - EOS results for Riazi and Daubert's method.

Viscosity							
PR		SRK-Peneloux		SRK		PR-Peneloux	
P-psi	μ_o, cp	P-psi	μ_o, cp	P-psi	μ_o, cp	P-psi	μ_o, cp
3000	239.29	3000	260.31	3000	261.71	3000	260.73
2500	214.48	2500	233.32	2500	234.58	2500	233.70
2000	189.67	2000	206.33	2000	207.45	2000	206.66
1500	164.86	1500	179.34	1500	180.31	1500	179.63
1000	140.05	1000	152.35	1000	153.18	1000	152.60
500	115.24	500	125.36	500	126.04	500	125.57
250	102.84	250	111.87	250	112.47	250	112.05
181	99.39	193	108.78	193	109.37	181	108.30
150	102.07	150	112.64	150	113.25	150	111.27
105	106.68	105	117.39	105	118.03	105	116.38
60	112.12	60	122.98	60	123.66	60	122.43
0	174.63	0	191.47	0	192.60	0	191.75

Table F.7. Relative volume - EOS results for Behrens and Sandler's lumping method.

Vr							
PR		**SRK-Peneloux**		**SRK**		**PR-Peneloux**	
P-psi	Vr	P-psi	Vr	P-psi	Vr	P-psi	Vr
3000	0.9801	3000	0.9738	3000	0.9765	3000	0.9794
2000	0.9860	2000	0.9814	2000	0.9833	2000	0.9855
1000	0.9929	1000	0.9905	1000	0.9915	1000	0.9926
750	0.9948	750	0.9931	750	0.9938	750	0.9946
500	0.9968	500	0.9958	500	0.9962	500	0.9967
400	0.9976	400	0.9969	400	0.9972	400	0.9976
300	0.9985	300	0.9980	300	0.9982	300	0.9984
200	0.9994	200	0.9992	200	0.9993	200	0.9993
150	0.9998	150	0.9998	150	0.9998	150	0.9998
127	1.0000	130	1.0000	130	1.0000	127	1.0000
105	1.1040	105	1.1178	105	1.1059	105	1.1075
100	1.1355	100	1.1492	100	1.1341	100	1.1401
93	1.1860	93	1.1994	93	1.1793	93	1.1923

Table F.8. Viscosity - EOS results for Behrens and Sandler's lumping method.

Viscosity							
PR		SRK-Peneloux		SRK		PR-Peneloux	
P-psi	μ_o, cp	P-psi	μ_o, cp	P-psi	μ_o, cp	P-psi	μ_o, cp
3000	259.64	3000	259.58	3000	259.58	3000	259.64
2500	232.72	2500	232.66	2500	232.66	2500	232.72
2000	205.80	2000	205.75	2000	205.75	2000	205.80
1500	178.88	1500	178.84	1500	178.84	1500	178.88
1000	151.96	1000	151.92	1000	151.92	1000	151.96
500	125.04	500	125.01	500	125.01	500	125.04
250	111.58	250	111.55	250	111.55	250	111.58
150	106.20	150	106.17	150	106.17	150	106.20
127	104.94	130	105.11	130	105.11	127	104.94
105	108.57	105	109.24	105	109.24	105	108.58
60	117.45	60	117.85	60	117.85	60	117.45
0	2636.02	0	2013.76	0	2013.76	0	2637.25

Table F.9. Relative volume - EOS results for Lee's lumping method.

Vr							
PR		SRK-Peneloux		SRK		PR-Peneloux	
P-psi	Vr	P-psi	Vr	P-psi	Vr	P-psi	Vr
3000	0.9797	3000	0.9732	3000	0.9761	3000	0.9787
2000	0.9857	2000	0.9810	2000	0.9831	2000	0.9850
1000	0.9928	1000	0.9903	1000	0.9914	1000	0.9924
750	0.9947	750	0.9929	750	0.9937	750	0.9944
500	0.9968	500	0.9957	500	0.9961	500	0.9966
400	0.9976	400	0.9968	400	0.9972	400	0.9975
300	0.9985	300	0.9980	300	0.9982	300	0.9984
200	0.9993	200	0.9992	200	0.9993	200	0.9993
150	0.9998	150	0.9998	150	0.9998	150	0.9998
127	1.0000	131	1.0000	131	1.0000	127	1.0000
105	1.1073	105	1.1227	105	1.1094	105	1.1130
100	1.1394	100	1.1551	100	1.1382	100	1.1468
93	1.1910	93	1.2068	93	1.1843	93	1.2011

Table F.10. Viscosity - EOS results for Lee's lumping method.

Viscosity							
PR		SRK-Peneloux		SRK		PR-Peneloux	
P-psi	μ_o, cp	P-psi	μ_o, cp	P-psi	μ_o, cp	P-psi	μ_o, cp
3000	259.65	3000	264.17	3000	264.17	3000	259.65
2500	232.73	2500	236.78	2500	236.78	2500	232.73
2000	205.81	2000	209.39	2000	209.39	2000	205.81
1500	178.89	1500	182.00	1500	182.00	1500	178.89
1000	151.96	1000	154.61	1000	154.61	1000	151.97
500	125.04	500	127.22	500	127.22	500	125.05
250	111.58	250	113.53	250	113.53	250	111.59
150	106.20	150	108.05	150	108.05	150	106.20
127	104.96	131	107.00	131	107.00	127	104.96
105	108.61	105	111.24	105	111.24	105	108.61
60	117.40	60	119.94	60	119.94	60	117.40
0	2561.36	0	2208.75	0	2208.75	0	2561.38

Table F.11. Relative volume - EOS results for reservoir fluid composition.

Vr							
PR		SRK-Peneloux		SRK		PR-Peneloux	
P-psi	Vr	P-psi	Vr	P-psi	Vr	P-psi	Vr
3000	0.9839	3000	0.9771	3000	0.9789	3000	0.9837
2000	0.9889	2000	0.9840	2000	0.9852	2000	0.9887
1000	0.9945	1000	0.9920	1000	0.9927	1000	0.9944
750	0.9961	750	0.9943	750	0.9947	750	0.9960
500	0.9977	500	0.9966	500	0.9969	500	0.9976
400	0.9983	400	0.9976	400	0.9978	400	0.9983
300	0.9990	300	0.9985	300	0.9987	300	0.9990
200	0.9997	200	0.9995	200	0.9996	200	0.9997
152	1.0000	155	1.0000	155	1.0000	152	1.0000
150	1.0065	150	1.0150	150	1.0138	150	1.0066
105	1.2163	105	1.2283	105	1.2107	105	1.2192
100	1.2530	100	1.2655	100	1.2450	100	1.2564
93	1.3117	93	1.3249	93	1.2998	93	1.3158

Table F.12. Viscosity - EOS results for reservoir fluid composition.

Viscosity							
PR		SRK-Peneloux		SRK		PR-Peneloux	
P-psi	μ_o, cp	P-psi	μ_o, cp	P-psi	μ_o, cp	P-psi	μ_o, cp
3000	259.183	3000	259.085	3000	259.085	3000	259.183
2500	232.311	2500	232.223	2500	232.223	2500	232.311
2000	205.438	2000	205.361	2000	205.361	2000	205.438
1500	178.566	1500	178.499	1500	178.499	1500	178.566
1000	151.694	1000	151.637	1000	151.637	1000	151.694
500	124.822	500	124.775	500	124.775	500	124.822
250	111.385	250	111.343	250	111.343	250	111.385
152	106.13	155	106.243	155	106.243	152	106.13
150	106.393	150	106.839	150	106.839	150	106.393
105	112.572	105	112.934	105	112.934	105	112.572
60	119.991	60	120.215	60	120.215	60	119.991
0	1967.828	0	3395.332	0	3395.332	0	1967.828